INVESTIGATING THE ROLE OF THE E3 UBIQUITIN LIGASE HUWE1 IN DNA REPAIR: IMPLICATIONS IN CANCER THERAPY

Daniel Martinho

A Thesis Submitted to the Faculty of Graduate Studies in Partial Fulfillment of the Requirements for the Degree of Master of Science

Graduate Program in Biology
York University
Toronto, Ontario
November 2023

Abstract

The ubiquitin E3 ligase HUWE1 (HECT, UBA, and WWE containing protein 1) plays a crucial role in various cellular processes including DNA damage repair and has been implicated in ovarian cancer. This study therefore used cell-based assays to characterize the impact of HUWE1 depletion on DNA damage repair outcomes in response to different stressors. Since combinations of DNA-damaging agents with poly(ADP-ribose) polymerase inhibitors are being explored to improve ovarian cancer treatment, the impact of HUWE1 on DNA damage and survival following these combination treatments was also investigated. It was demonstrated that HUWE1 depletion increased cellular DNA damage and delayed DNA repair in response to treatment with various DNA damaging agents. HUWE1 depletion increased the synergistic effect of combination treatments with poly(ADP-ribose) polymerase inhibitors and DNA damaging agents on DNA damage and cell survival. The WWE domain of HUWE1 is known to interact with poly(ADP-ribose), so a potential interaction between HUWE1 and the important DNA repair protein poly(ADP-ribose) polymerase 1 was studied as a possible mechanism underlying the effects on DNA damage and cell survival. This study identified that HUWE1 is an important regulator of multiple DNA repair pathways, and a modulator of cell responsiveness to treatments with poly(ADP-ribose) polymerase inhibitors and DNA damaging agents. This suggests that HUWE1 is a possible target for improving ovarian cancer therapies.

Acknowledgements

I would like to express my deepest gratitude to the following people who have supported me throughout my MSc. First and foremost, I would like to thank my supervisor **Dr. Yi Sheng**, without whom this project would not have been possible. Dr. Sheng, thank you for your guidance and support both in and out of the lab. You have allowed me the opportunity to take my own direction with this project, and your door has always been open when I have had questions. Thank you for your trust in me. I have enjoyed our scientific discussions, and I am extremely grateful for the encouragement and expertise you have shared with me throughout my studies.

I would also like to thank my advisor, **Dr. Emanuel Rosonina**, for helping to improve my project with thoughtful questions and excellent feedback. I am truly grateful for your input and guidance.

I also extend my sincere gratitude to all the amazing members of the Sheng Lab I have had the opportunity to work with over the past years. To **Gaby** and **Song**, thank you for helping to prepare me for my project and for always being willing to answer my many questions during my first few months. To **Angelo**, **Nour**, and **Rufei**, it has been my pleasure to train with and work alongside you. Thank you as well to the undergraduate students that I have worked with, **Nour**, **Vanessa**, **Sanjay**, and **Nikita**. Mentoring you was an enriching experience, and I have enjoyed learning alongside you. Thank you all for your contributions. To everyone in the Sheng Lab group, thank you for the all the conversations, laughs, science talk and friendship. This experience would not have been the same without you.

There are many people in the Life Sciences Building who I would also like to thank, including **David**, **Joyce**, **Suki**, **Krstina**, **Jennifer**, **Connor, Nick**, **Aneesah**, **Kyra**, **Farnaz**, **Sehaj**, **Sihat**, **Britney and Yanan**, for their friendship and generosity with their time and expertise.

To my family, I could never put into words how grateful I am for everything you have done for me. **Mom**, **Dad**, **Sofia**, **Avó**, and **Avô**, none of this would have been possible without you. Thank you for your never-ending support and patience, and for always believing in me.

Finally, to **Sarah**, I am incredibly lucky to have you by my side. I appreciate your love and belief in me more than I could begin to say, and I am truly grateful that we got to share in this experience together. You have made the last few years truly special. Thank you for your constant support throughout my thesis project and beyond.

Table of Contents

List of Tables

Chapter 2:

List of Figures

Chapter 1: Introduction

1.1 An Overview of DNA Damage

Cellular DNA, which encodes the genetic information required for cells to carry out their functions, is constantly exposed to various stressors which can alter its structure or composition (Chatterjee & Walker, 2017; Jackson & Bartek, 2009). These stressors can be of endogenous or exogenous origin, arising from either natural cellular processes or from external influences, and lead to the formation of DNA lesions (Chatterjee & Walker, 2017; Hakem, 2008; Mikolaskova et al., 2018). Some common sources of endogenous DNA damage include errors in DNA replication during cell division, and reactive oxygen species that arise from cellular processes such as electron transport in mitochondria (Chatterjee & Walker, 2017; Ciccia & Elledge, 2010; Jackson & Bartek, 2009). Exogenous stressors can include environmental factors, such as UV radiation, and chemical agents (Jackson & Bartek, 2009).

These stressors can cause various kinds of DNA damage which can threaten genomic integrity. Apurinic and apyrimidinic sites (AP sites) are thought to be the most common kind of DNA lesion, arising spontaneously from hydrolysis of the N-glycosidic bonds in DNA and other processes an estimated ten thousand times per human cell per day (Ciccia & Elledge, 2010; Ignatov et al., 2017). Examples of DNA lesions induced by exogenous stressors include pyrimidine dimers, the primary result of ultraviolet (UV) radiation, alkylation of bases, induced by alkylating agents such as methyl methanesulfonate (MMS), and bulky intrastrand crosslinks that distort the structure of DNA, which can be caused by chemotherapeutics like cisplatin (Ciccia & Elledge, 2010; Ignatov et al., 2017; Kciuk et al., 2020; Kiss et al., 2021). Double strand breaks (DSB) are generally considered to be the most deleterious form of DNA damage (Huang & Zhou, 2021; Jackson & Bartek, 2009; Kciuk et al., 2020).

Regardless of the source or the type of lesion, quick and efficient repair is essential to avoid adverse effects for the cell and organism. If not adequately repaired, these lesions can accumulate and lead to mutation, replication cessation, and cell death (Chatterjee & Walker, 2017; Ignatov et al., 2017; Jackson & Bartek, 2009). Genome instability is also associated with the development of human diseases ranging from vascular conditions such as atherosclerosis to neurodegenerative disorders like Alzheimer's disease (Czarny et al., 2020; Uryga et al., 2016). In particular, genomic instability is closely linked to cancer development and progression (Huang & Zhou, 2021; Jackson & Bartek, 2010; Moon et al., 2023). Therefore, cells have evolved various complex and interconnected pathways to repair the constantly occurring DNA damage and preserve genome integrity (Ciccia & Elledge, 2010; Jackson & Bartek, 2010; Mikolaskova et al., 2018). The common DNA damage repair pathways are summarized in the following section.

1.2 DNA Damage Repair

DNA damage repair is a term for the set of pathways that make up a cell's response to DNA damage. While much remains to be understood regarding DNA damage repair and the true extent of pathways employed by the cell to address DNA lesions, there are five main pathways that have received particular attention: base excision repair (BER), nucleotide excision repair (NER), mismatch repair (MMR), and the two DSB repair pathways homologous recombination (HR) and non-homologous end joining (NHEJ) (Chatterjee & Walker, 2017; Jackson & Bartek, 2009). It is important to note that these pathways may have different sub-pathways, crosstalk, and other intricacies that are responsible for addressing specific lesions in specific cellular contexts, though only general mechanisms will be presented here.

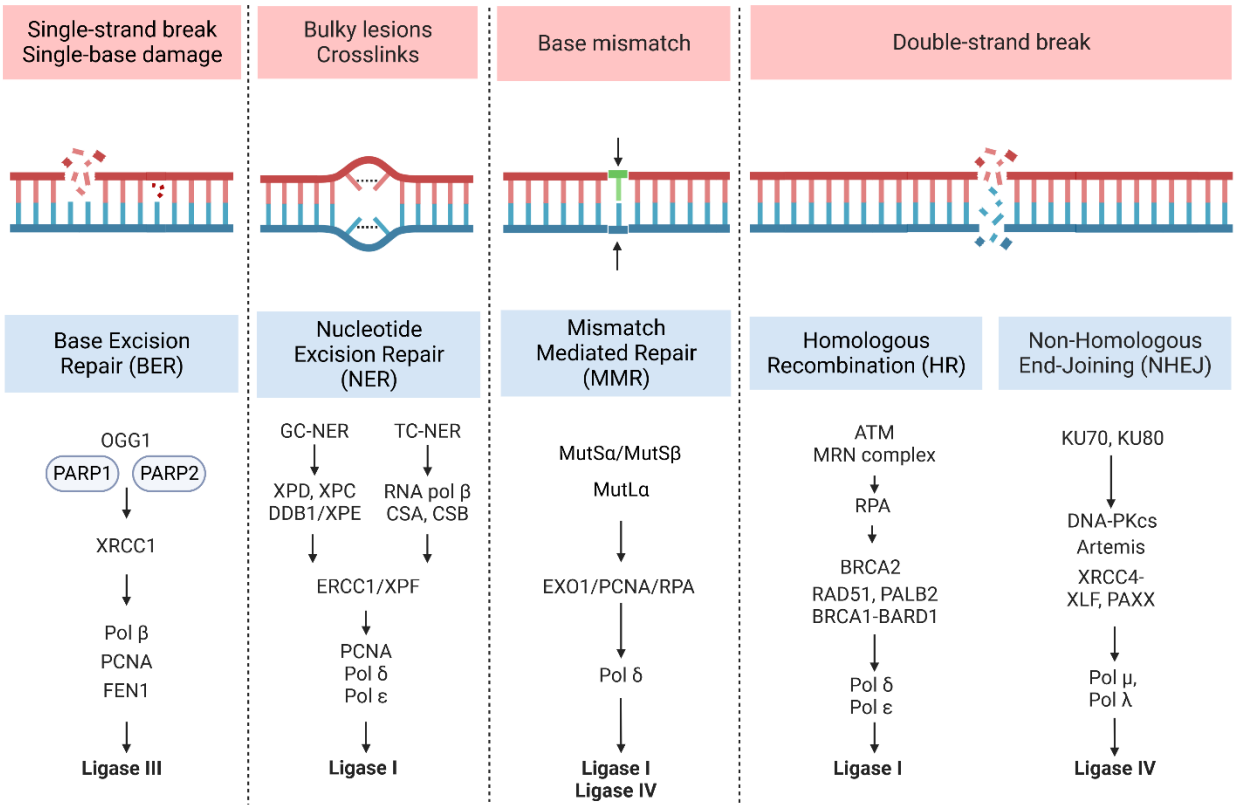

Figure 1-1: An Overview of DNA Damage and Common Repair Pathways
Graphical representation of different DNA lesions and key components of the five common repair pathways involved in their repair. Adapted from "DNA Repair Mechanisms", by BioRender.com (2023). Retrieved from https://app.biorender.com/biorender-templates.

1.2.1 Base Excision Repair

BER is primarily used for repair of single nucleotide lesions that arise from oxidative stressors, spontaneous deamination of bases, AP sites, or alkylation of bases (Almeida & Sobol, 2007; Chatterjee & Walker, 2017). This pathway overlaps significantly with another DNA damage repair pathway, single strand break repair (SSBR), because the process of BER results in the formation of temporary single strand breaks (SSBs) when the damaged base is removed (Almeida & Sobol, 2007; Dianov & Hübscher, 2013). There are two main pathways in BER; the short-patch pathway replaces a single nucleotide, while the long-patch pathway can replace roughly 2-13 nucleotides (Almeida & Sobol, 2007; Dianov & Hübscher, 2013). In general, the lesion is recognized by DNA glycosylases which excise the damaged base, creating a nick in the

DNA (Chatterjee & Walker, 2017; Odell et al., 2013). The type of glycosylase that carries out the removal of the base determines whether the short-patch or long-patch is required, as bifunctional glycosylases with β-lyase activity create different DNA ends (Chatterjee & Walker, 2017). In short-patch repair, the endonuclease APE1 cleaves the DNA upstream of the nick, creating an SSB (Chatterjee & Walker, 2017; Odell et al., 2013). Polymerase β (Pol β) subsequently synthesizes the missing base, and the final ligation is carried out by either DNA Ligase 1 (LIG1) or LIG3 in complex with the scaffolding protein XRCC1 (Almeida & Sobol, 2007; Chatterjee & Walker, 2017; Odell et al., 2013). In the long-patch pathway the broken DNA ends are additionally processed by APE1 before Pol β, ε, or δ, in cooperation with other factors like PARP1, displace roughly 2-13 nucleotides of the broken strand and synthesize new nucleotides to fill in both the break and the displaced nucleotides (Almeida & Sobol, 2007; Chatterjee & Walker, 2017). The displaced set of nucleotides are excised by the endonuclease FEN1, and the new DNA is ligated by LIG1 or LIG3 (Almeida & Sobol, 2007; Chatterjee & Walker, 2017).

1.2.2 Nucleotide Excision Repair

NER is also subdivided into two main pathways, the global genome (GG) and transcription-coupled (TC) pathways of NER. These pathways primarily repair bulkier lesions than BER, including pyrimidine dimers produced by UV radiation, and intrastrand adducts (Chatterjee & Walker, 2017; Huang & Zhou, 2021; Marteijn et al., 2014). In GG-NER, the protein XPC cooperates with other factors to detect bulky DNA lesions (Marteijn et al., 2014; Spivak, 2015). XPC cannot readily identify pyrimidine dimers, so these lesions are first bound by a complex of DDB2 and DDB1 which facilitates binding of XPC (Chatterjee & Walker, 2017; Marteijn et al., 2014; Spivak, 2015). The XPC-DNA lesion is then recognized by the multi-subunit TFIIH complex, which confirms the presence of damage and unwinds the double-

stranded DNA helix around the lesion (Chatterjee & Walker, 2017; Huang & Zhou, 2021; Marteijn et al., 2014 Zhang X et al., 2022). In TC-NER, transcription stalls when RNA polymerase II encounters a bulky lesion (Marteijn et al., 2014; Spivak, 2015). This results in the recruitment of TC-NER specific proteins CSA and CSB and associated complexes that include some GG-NER factors, which likely help move or backtrack the stalled RNAPII out of the way and recruit the TFIIH complex for the DNA to be unwound (Chatterjee & Walker, 2017; Marteijn et al., 2014). Both pathways then recruit various factors including RPA to protect the unwound single strand DNA (ssDNA), and the endonucleases XPG and ERCC1-XPF which are responsible for cutting away the damaged DNA (Huang & Zhou, 2021; Marteijn et al., 2014; Spivak, 2015). Various replication-associated proteins together with Pol δ, Pol ε or Pol κ then synthesize the missing nucleotides, and the final nick is ligated by either LIG1 or XRCC1-LIG3 (Chatterjee & Walker, 2017; Marteijn et al., 2014; Spivak, 2015; Zhang X et al., 2022).

1.2.3 Mismatch Repair

While less well understood than other repair pathways in mammalian cells, the MMR pathway is primarily responsible for correcting base mismatches that arise endogenously as a result of errors during DNA replication, as well as small insertions or deletions (indels) up to 13 nucleotides (Chatterjee & Walker, 2017; Huang & Zhou, 2021; Liu D et al., 2017). Human homologs of MutSα bind to mismatches or small indels of up to 3 nucleotides, and MutSβ homologs binds the larger indels up to 13 nucleotides for initiation of the MMR pathway (Chatterjee & Walker, 2017; Liu D et al., 2017). These proteins then recruit and form a complex with MutLα (Liu D et al., 2017; Olave & Graham, 2021). It is then believed that interaction with PCNA stimulates endonuclease activity in a subunit of MutLα, which moves along the DNA to create a nick upstream of the lesion (Chatterjee & Walker, 2017; Liu D et al., 2017). Exonuclease

1 (EXO1) is also recruited to excise the patch of DNA that contained the lesion, leaving a section of ssDNA that is bound by RPA (Chatterjee & Walker, 2017; Huang & Zhou, 2021; Liu D et al., 2017). The above processes may be repeated until the damaged section of DNA is successfully removed (Fishel, 2015). Pol δ fills in the missing nucleotides and the newly repaired DNA is ligated by LIG1 (Chatterjee & Walker, 2017; Huang & Zhou, 2021; Liu D et al., 2017). Many questions remain regarding MMR, including whether it can respond to additional lesions besides mismatches and small indels, how the initial sensors of the damage can differentiate between the template and newly synthesized strand to ensure the mismatched base is the one removed, and how the pathway is able to function independently of EXO1 (Chatterjee & Walker, 2017; Huang & Zhou, 2021; Liu D et al., 2017). Despite the lack of clarity regarding the specific mechanisms of MMR in eukaryotic cells, defects in MMR have been linked to human diseases including cancer, similarly to defects in other DNA repair pathways (Huang & Zhou, 2021; Liu D et al., 2017; Olave & Graham, 2021).

1.2.4 Double Strand Break Repair

HR and NHEJ are the two main pathways of double strand break repair. NHEJ is a repair mechanism that functions throughout the cell cycle, while HR is limited to the S and G2 phases due to its requirement for a sister chromatid to serve as a template for repair (Li et al., 2019; Scully et al., 2019). Given that it is not temporally restricted, NHEJ is believed to be the primary repair pathway (Li et al., 2019; Scully et al., 2019; Yang et al., 2016). In NHEJ, the DSB is detected and bound by the proteins Ku70 and Ku80, typically one dimer at each end of the break, which protect the DNA from resection and recruit other repair factors including DNA PKcs (DNA-dependent protein kinase catalytic subunit), DNA ligase 4 (LIG4), and the scaffolding proteins XRCC4, XLF, and PAXX (Chatterjee & Walker, 2017; Li et al., 2019; Scully et al.,

2019; Yang et al., 2016). Ku70/80 and DNA-PKcs carry out a long range alignment of the two DNA ends, after which the kinase activity of DNA-PKcs together with XLF and a non-catalytic function of the LIG4-XRCC4 complex bring the ends into closer alignment (Graham et al., 2016; Scully et al., 2019). These long and short range alignments are dynamic, suggesting that the process may repeat until the broken ends are appropriately aligned (Graham et al., 2016; Scully et al., 2019). Several other factors, such as Artemis and PNKP, process the broken ends to ensure compatibility before Pol λ and Pol μ fill in any gaps and the break is ligated by LIG4 (Chatterjee & Walker, 2017; Scully et al., 2019; Yang et al., 2016).

Cells may employ an alternative end joining (aEJ) pathway when critical NHEJ factors are absent, or to address repair blockages and collapsed replication forks (Chang et al., 2017; Ramsden et al., 2022; Scully et al., 2019). While not as well understood, in this pathway DSBs are recognized by a complex of MRE11, RAD50, and NBS1 called the MRN complex (Chang et al., 2017). The complex is stimulated by CtIP and processes the broken DNA ends, cutting away 15 to 100 nucleotides at the 5' end to generate 3' overhangs of ssDNA (Chang et al., 2017). The repair steps rely on Pol θ to expose microhomologies in the ssDNA which can direct repair by Pol θ and other polymerases (Chang et al., 2017; Scully et al., 2019). LIG3 is the main ligase involved in joining the broken ends, though LIG1 has also been shown to play a role (Ramsden et al., 2022).

For HR, DSBs are also recognized and bound by the MRN complex (Chatterjee & Walker, 2017; Li et al., 2019; Scully et al., 2019). The MRN complex recruits and activates the multifunctional kinase ATM, which stimulates the endonuclease activity of MRE11 together with CtIP (Bakr et al., 2015; Chatterjee & Walker, 2017; Scully et al., 2019). The endonuclease activity of MRE11 creates a nick up to 300 nucleotides away from the free 5' end of the DNA

break, which is followed by digestion of DNA towards the break by the 3'-5' exonuclease activity of MRE11 (Chatterjee & Walker, 2017; Li et al., 2019; Scully et al., 2019). This step is believed to displace Ku70/80, and additional enzymes may be recruited to clear other factors from blocking access to the DNA ends (Li et al., 2019; Scully et al., 2019). EXO1, or the endonuclease DNA2 with the helicase BLM, carry out long range resection which results in long 3' overhangs of ssDNA (Li et al., 2019; Scully et al., 2019). RPA binds the ssDNA to protect it from degradation and is eventually displaced by BRCA2, which loads RAD51 onto ssDNA together with BRCA1-BARD1 and PALB2 (Li et al., 2019; Scully et al., 2019). RAD51 promotes strand invasion into the sister chromatid and the formation of a D-loop structure, which requires a minimum of 8 consecutive base pairs between the invading strand and the sister chromatid. The invading strand is extended in a template-directed manner by several polymerases including Pol δ (Chatterjee & Walker, 2017; Li et al., 2019; Scully et al., 2019). Resolution of this structure and completion of HR can proceed by a number of sub-pathways, including double Holliday junction, synthesis-dependent strand annealing, break-induced replication, and single strand annealing (Ceccaldi et al., 2016; Li et al., 2019; Scully et al., 2019). HR has traditionally been considered the less error-prone of the two major DSB repair pathways, though some sub-pathways such as break-induced replication and single strand annealing have been found to be error-prone (Ceccaldi et al., 2016; Guirouilh-Barbat et al., 2014; Li et al., 2019; Scully et al., 2019). The choice of repair pathway to address DSBs is tightly regulated at various stages and depends on the nature of the break and surrounding microenvironment, and thus continues to be the subject of much study (Ceccaldi et al., 2016; Scully et al., 2019; Yang et al., 2016).

1.3 Post-Translational Modifications in DNA Damage Repair

Fine regulation of the various DNA damage response pathways is key for a coordinated and effective cellular response to DNA lesions. Post-translational modification of proteins is an important aspect of this regulatory network underlying DNA damage repair. There are various kinds of chemical modifications that can impact both the activity and interactions that proteins can have (Bradley, 2022). Two post-translational modifications that play critical roles in coordinating DNA damage repair are described here.

1.3.1 The Role of PARylation in DNA Damage Repair

PARylation is a crucial protein post-translational modification in DNA damage repair that involves the covalent attachment of linear or branching PAR chains on serine, glutamate, aspartate, and other less frequent residues of target proteins (Groslambert et al., 2021; Kamaletdinova et al., 2019; Kang et al., 2022; Wei & Yu, 2016). Cellular levels of PAR are typically low, with PAR synthesis being primarily stimulated by DNA damage (Liu C et al., 2017; Shieh et al., 1998). PAR is synthesized by proteins of the poly(ADP-ribose) polymerase (PARP) family, with PARP1 being responsible for up to 90% of DNA damage induced PARylation (Kamaletdinova et al., 2019; Kang et al., 2022; Liu C et al., 2017). PARP1 is composed of an N-terminal DNA binding domain containing three zinc fingers (ZF1-3), an automodification domain, and a C-terminal catalytic domain (Alemasova & Lavrik, 2019; Liu C et al., 2017; Kamaletdinova et al., 2019; Kang et al., 2022). The DNA binding ZF motifs of PARP1 are believed to allow the protein to swing along DNA, where it can undergo a conformational change to an active state upon recognition of SSBs, DSBs, or stalled replication forks (Alemasova & Lavrik, 2019; Huang & Kraus, 2022; Liu C et al., 2017; Rudolph et al., 2018). In this way, PARP1 acts as an initial sensor of DNA damage (Groslambert et al., 2021;

Kang et al., 2022; Wei & Yu, 2016). The donor site of the catalytic (ADP-ribosyl)transferase domain then binds NAD^+ and transfers an ADP-ribose to the target at the acceptor site (Alemasova & Lavrik, 2019; Wei & Yu, 2016). Self-PARylation of PARP1, or its PARylation through dimerization with other PARP1 or PARP2 molecules, alters its function by reducing its affinity for intact DNA (Alemasova & Lavrik, 2019; Kamaletdinova et al., 2019; Muthurajan et al., 2014). AutoPARylation of PARP1 leads to an accumulation of PAR chains, which bear negative charges and promote dissociation of PARP1 from DNA via electrostatic repulsion (Hopkins et al., 2015; Murai et al., 2012; Rudolph et al., 2021; Satoh & Lindahl, 1992).

DNA damage induced activation of PARP1 and PARylation is key for the early recruitment of repair factors to the sites of DNA lesions (Chaudhuri & Nussenzweig, 2017; Kang et al., 2022). PARP1 has been implicated in BER and SSBR, which overlap significantly. PARP1 and PARylation are important for recruitment of XRCC1 and PNKP to sites of SSBs and interact with other BER proteins including Pol β and LIG3 (Chaudhuri & Nussenzweig, 2017; Dantzer et al., 2000; Hanzlikova et al., 2017; Schreiber et al., 2002; Wei & Yu, 2016). In NER, PAR mediates the recruitment of XPC, while DDB2 interacts with and stimulates PARP1 activation and subsequent histone modification to promote repair (Chaudhuri & Nussenzweig, 2017; Kang et al., 2022; Pines et al., 2012). PARP1 also has known interactions with EXO1, which is involved in MMR as well as HR (Kamaletdinova et al., 2019; Zhang et al., 2015).

PARP1 and its PARylation activity also play important roles in DSB repair. PARP1 interacts with and mediates recruitment of MRE11, the exonuclease component of the MRN complex that is crucial for initiation of HR repair (Haince et al., 2008). Additionally, PARP1 has been shown to compete with Ku proteins for binding of broken DNA ends, interfering with the early stages of NHEJ (Hochegger et al., 2006; Wang et al., 2006). This suggests an important

role for PARP1 in DSB repair pathway choice, as it favors HR or aEJ pathways over NHEJ (Chaudhuri & Nussenzweig, 2017; Liu C et al., 2017; Wang et al., 2006). In addition, PARP1 mediated PARylation is important for recruitment of BRCA1 via its interacting partner BARD1 (Chaudhuri & Nussenzweig, 2017; Li & Yu, 2013). Interestingly, subsequent PARylation of BRCA1 attenuates its activity to prevent hyperactivation of HR, exemplifying the intricate regulatory effects of PARylation in DNA damage repair (Chaudhuri & Nussenzweig, 2017; Hu et al., 2014).

This complexity is further highlighted by the fact that PARP1 and PARylation also have NHEJ promoting activity. For example, PARP1 activation and subsequent decondensation of chromatin allow for recruitment of ZNF384 at damaged sites, which in turn promotes recruitment of Ku70/80 (Singh et al., 2021). Furthermore, PARylation of DNA-PKcs can stimulate its catalytic activity (Ruscetti et al., 1998). PARP1 is thus an evidently crucial player in regulation and fine tuning of DSB repair. Taken together, these examples demonstrate the crucial and central role of PARP1 in recruiting early DNA repair factors, as well as regulating important components of various DNA repair pathways. PARP1 and PARylation are thus key factors in the complex regulatory landscape of DNA repair.

1.3.2 Ubiquitination in DNA Damage Repair

Ubiquitination is another post-translational modification that plays an essential role in the regulation of DNA damage repair and other biological processes (Bachiller et al., 2020; Huang & D'Andrea, 2006; Kao et al., 2018). An E1 ubiquitin-activating enzyme transfers ubiquitin to an E2 ubiquitin-conjugating enzyme, after which an E3 ubiquitin ligase transfers ubiquitin from the E2 to the target protein (Bachiller et al., 2020, Koo et al., 2023; Sekiguchi & Matsushita, 2022). Ubiquitination typically takes place on the ε-amine group of lysine residues, and ubiquitin itself

can undergo ubiquitination at any of its seven lysine residues or the amine group of the first methionine to form polyubiquitin chains (Kwon & Ciechanover, 2017; Sekiguchi & Matsushita, 2022). Different ubiquitin linkages offer an array of signals that differentially regulate protein function and recruitment (Kwon & Ciechanover, 2017; Schwertman et al., 2016). Polyubiquitination, such as K48-linked polyubiquitination, is associated with proteasomal degradation, while K63-linked polyubiquitin plays an important role in DSB repair signaling (Dantuma & van Attikum, 2016; Kao et al., 2018; Lee et al., 2017; Schwertman et al., 2016).

Ubiquitination plays a crucial role in the regulation of DNA damage repair, as the variability of polyubiquitin chains allows for intricate modulation of protein recruitment and stability (Kao et al., 2018). In fact, several critical DNA damage repair proteins are ubiquitin E3 ligases. For example, a complex that includes DDB1 and DDB2 polyubiquitinates XPC in BER, which enhances the DNA binding affinity of XPC (Huang & D'Andrea, 2006; Sugasawa et al., 2005). K63-linked ubiquitination of XPC by RNF111 is also crucial for removal of XPC from damaged sites and continuation of the repair process (Cuijk et al., 2015; Dantuma & van Attikum, 2016). Furthermore, self-polyubiquitination of DDB2 by the DDB1-DDB2 complex decreases its DNA binding and promotes dissociation from DNA lesions, and eventual degradation of DDB2 (Huang & D'Andrea, 2006; Sugasawa et al., 2005).

Another well characterized example of the importance of ubiquitin in coordinating the DNA damage response is the function of the E3 ligases RNF8 and RNF168. As part of DSB recognition and repair, RNF8 is recruited to the sites of DNA damage and mediates K63-linked ubiquitination of histone H1 surrounding the lesion (Lee et al., 2017; Schwertman et al., 2016; Smeenk & Mailand, 2016). This ubiquitination serves to recruit RNF168, which in turn promotes K27- and K63-linked polyubiquitination of histone H2A and H2AX to promote recruitment of

DNA repair factors, including 53BP1 and BRCA1 (Gatti et al., 2015; Schwertman et al., 2016; Sekiguchi & Matsushita, 2022; Smeenk & Mailand, 2016). These examples demonstrate the versatile functions of ubiquitination and E3 ligases in DNA repair regulation and signaling.

1.4 Functions of HUWE1 in DNA Damage Repair

HECT, UBA, and WWE domain containing protein 1, or HUWE1, is a large and conserved HECT E3 ligase that plays important roles in a variety of cellular pathways, including DNA damage repair (Choe et al., 2016; Hunkeler et al., 2021; Kao et al., 2018; Kunz et al., 2020; Wang et al., 2014; Zhong et al., 2005). The protein folds into a ring-like structure that contains multiple interaction domains, including ubiquitin binding domains, a poly(ADP-ribose) (PAR) binding WWE domain, and a BH3 domain that is known to interact with the anti-apoptotic factor Mcl-1 (Hunkeler et al., 2021; Kao et al., 2018; Qi et al., 2022). The binding domains and ring structure are believed to contribute to HUWE1's wide range of substrates that underlie its involvement in different cellular pathways (Gong et al., 2020; Hunkeler et al., 2021; Kao et al., 2018; Zhong et al., 2005). The N-terminal portion of the protein, which includes these domains, was also found to be important for transfer of ubiquitin from E2 ligases to HUWE1, and thus contributes to the protein's catalytic activity (Hunkeler et al., 2021). The catalytic HECT domain is found at the C-terminal end of the protein and sits above the ring structure. (Hunkeler et al., 2021; Kao et al., 2018).

HUWE1 is able to promote various kinds of ubiquitination, including monoubiquitination, K48 polyubiquitination, and non-proteolytic K63 polyubiquitination among others (Kao et al., 2018; Wang G et al., 2012). This further diversifies the functional impact of HUWE1, and thus helps explain how it can carry out its diverse modulatory effects (Kao et al., 2018). Among the substrates of HUWE1 are various oncogenic and tumor suppressor proteins,

including p53, BRCA1 and Myc, and there is evidence linking both over and under expression of HUWE1 to cancer progression (Crawford et al., 2020; Gong et al., 2020; Myant et al., 2017; Su et al., 2019; Yang et al., 2017). HUWE1 may therefore act as a tumor suppressor or an oncogene, depending on its regulation or preferred substrates in different cellular contexts (Gong et al., 2020; Kao et al., 2018).

HUWE1 plays diverse roles in cellular responses to DNA damage, including in multiple DNA repair pathways, via interaction with and ubiquitination of a variety of substrates. For example, in BER, knockdown of HUWE1 resulted in increased cellular levels of Pol β, decreased the amount of ubiquitinated Pol β and improved the repair of H_2O_2 induced damaged (Parsons et al., 2009). Ultimately, HUWE1 was implicated in monoubiquitination of Pol β, which in turn primed the polymerase for polyubiquitination and degradation mediated by another E3 ligase (Parsons et al., 2009). Additionally, HUWE1 similarly interacts with and mediates degradation of Pol λ, which is potentially involved in BER as well as in NHEJ (Braithwaite et al., 2005; Kao et al., 2018; Markkanen et al., 2012).

HUWE1 also contributes to DSB repair by ubiquitination of histones. In response to DNA damage, HUWE1 mediates modification of histone H1 with monoubiquitin or short ubiquitin chains (Mandemaker et al., 2017). These modifications are believed to serve as a primer for recruitment and activation of RNF8 mediated H1 ubiquitination (Mandemaker et al., 2017). As a result, HUWE1 becomes implicated in the RNF8/RNF168 cascade which promotes recruitment of DNA damage repair factors like 53BP1 to the site of DNA lesions (Mandemaker et al., 2017). Furthermore, HUWE1 also plays a role in ubiquitination and proteasomal degradation of histone H2AX, which is a histone H2A variant important for promoting DSB repair signaling (Atsumi et al., 2015; Kao et al., 2018; Qi et al., 2022).

HUWE1 also regulates many HR and NHEJ proteins, including regulation of the stability of the HR protein BRCA1 and neddylation of DNA-PKcs to promote NHEJ efficiency (Guo et al., 2020; Huang & Zhou, 2021; Wang et al., 2014). Taken together, these examples demonstrate a complex landscape of DNA damage repair regulation by HUWE1. The involvement of HUWE1 in direct and indirect regulation of DNA repair proteins in multiple pathways, as well as modulation of the histone environment, suggest that HUWE1 plays an important role in coordinating efficient repair of DNA damage, though its detailed mechanisms are not yet fully understood.

1.5 Connections Between DNA Damage and Cancer

The incidence of mutations in the human genome can interfere with the proper function and regulation of proteins (Moon et al., 2023). These mutations may interfere with regulation of processes such as cell growth and replication, increasing the risk of cancer development (Huang & Zhou, 2021). Most carcinogens owe their cancer-causing properties to their ability to induce DNA damage and mutations (Jackson & Bartek, 2009). Indeed, defects in DNA damage repair are a common feature of cancer biology, as the resultant genomic instability can lead to an accumulation of mutations (Huang & Zhou, 2021; Moon et al., 2023; O'Connor, 2015). For example, mutations in the HR proteins BRCA1 and BRCA2 are known to be associated with the development of breast and ovarian cancers (Jackson & Bartek, 2009; Moon et al., 2023). The loss of function of a repair pathway must be compensated for by other mechanisms of repair, thus increasing a cell's reliance on the remaining pathways (O'Connor, 2015). For example, cancer cells deficient in BRCA1/2 may need to rely on the more error-prone NHEJ or aEJ pathways to prevent cell death (Li et al., 2021). These defects in DNA damage repair can result

in a greater vulnerability of cancer cells to DNA-damaging chemotherapeutics (de Almeida, 2021; Hosoya & Miyagawa, 2014; Moon et al., 2023).

The standard treatments for cancer include surgical removal and induction of DNA damage via radiation or chemotherapeutic drugs (de Almeida et al., 2021; Moon et al., 2023; O'Connor, 2015). Cancer cells can exhibit increased sensitivity to DNA damaging therapies due to their characteristic genomic instability, as they experience greater accumulation of DNA damage that can promote the activation of cell death pathways (Huang & Zhou, 2021; Li et al., 2021; Moon et al., 2023). However, there is a need for treatments that more specifically target cancer cells, as DNA-damage inducing chemotherapies are also cytotoxic to healthy cells and can have severe adverse effects on patients (Moon et al., 2023). Furthermore, mutations in DNA damage repair pathways can also give rise to resistance to therapeutics (Li et al., 2021). Specific defects in repair pathways can therefore be predictive of patient responsiveness to different therapeutic approaches (Moon et al., 2023). For example, mutations in BRCA1/2 are indicative of susceptibility to platinum based chemotherapy, while overexpression of Ku70/80 has been linked to resistance to both chemotherapy and radiation therapies (Huang & Zhou, 2021; Moon et al., 2023).

More recently, cancer therapies have developed to target components of DNA damage repair, to enhance the efficacy of existing chemotherapies and overcome resistance (de Almeida, 2021; Hosoya & Miyagawa, 2014; Moon et al., 2023). These therapies aim to interfere with DNA damage repair and induce synthetic lethality (Moon et al., 2023; Reuvers et al., 2020). Synthetic lethality refers to when perturbation of two genes or proteins, which do not reduce viability on their own, results in significant cell death (Chaudhuri & Nussenzweig, 2017; O'Connor, 2015). As mentioned, cancer cells often have DNA damage repair defects which

render them reliant on alternative mechanisms of repair to adequately address DNA lesions (O'Connor, 2015). By targeting these alternative pathways, cancer cells would be unable to adequately repair DNA damage induced by damaging chemotherapeutics and undergo cell death (Moon et al., 2023; O'Connor, 2015; Reuvers et al., 2020). Importantly, these treatments specifically target cancer cells, as normal cells with intact DNA repair pathways would still have functional DNA damage repair (O'Connor, 2015; Reuvers et al., 2020). These DNA repair targeting therapies have already brought significant benefit to cancer patients, such as in the case of ovarian cancer.

1.6 Ovarian Cancer and PARP Inhibition

Ovarian cancer is the seventh most common cancer in women and is the most lethal cancer affecting the female reproductive system (Ferlay et al., 2014; Lheureux et al., 2019; Lisio et al., 2019). The disease is often asymptomatic in early stages, contributing to late detection and high mortality (Bowtell et al., 2015; Lheureux et al., 2019). Of the many subtypes of ovarian cancer, high grade serous ovarian cancer (HGSOC) is the most commonly identified and the deadliest, accounting for 75% of all ovarian cancers and up to 80% of all ovarian cancer mortality (Bowtell et al., 2015; Lheureux et al., 2019; Lisio et al., 2019). HGSOCs frequently exhibit p53 mutations and genomic instability, with roughly 16% of HGSOC patients having mutations in BRCA1 or BRCA2 and 50% having deficiencies in HR repair in total (Bowtell et al., 2015; Lheureux et al., 2019). HGSOC treatment has typically involved surgical intervention followed by cytotoxic treatment with carboplatin and paclitaxel (Lheureux et al., 2019; Lisio et al., 2019). While a majority of HGSOC patients respond to this chemotherapy, over 80% of them are likely to experience disease recurrence (Kim et al., 2018; Lisio et al., 2019; Matulonis et al., 2016; Wang et al., 2022). Though up to 50% of recurrent HGSOC may still respond to platinum-

based therapy, the development of resistance quickly becomes an issue, with recurrent HGSOC typically considered to be incurable (Bowtell et al., 2015; Lisio et al., 2019; Matulonis et al., 2016). Resistance can arise through various mechanisms, including reversion of mutations that render cells susceptible to chemotherapy or overexpression of efflux transporters (Christie & Bowtell, 2017). The optimization of existing therapies, as well as development of novel combination therapies that specifically target cancer cells and minimize the risk of resistance, are therefore crucial for ameliorating HGSOC patient outcomes (Bowtell et al., 2015; Lisio et al., 2019).

PARP inhibitors (PARPi), drugs inhibiting the catalytic activity of PARP1 and other DNA damage associated PARPs, are a relatively novel class of drugs that revolutionized the treatment of ovarian cancer and HGSOC (Miller et al., 2022; Mirza et al., 2020). Early reports showing that cells with depletions of BRCA1 and BRCA2 had increased sensitivity to PARP1 depletion and inhibition led to further investigation and eventual clinical approval of the first PARPi, olaparib, in 2014 (Bryant et al., 2005; D'Andrea, 2018; Farmer et al., 2005; Mirza et al., 2020). PARPi are believed to function through two main mechanisms. Firstly, since PARPi are particularly effective in cancers deficient in homologous recombination, they can exert their effect through synthetic lethality (D'Andrea, 2018; Zhou et al., 2020). Given the importance of PARP1 in DNA repair, especially BER/SSBR, inhibition of its function results in accumulation of DNA lesions that can be converted into DSBs during replication (Bryant et al., 2005; D'Andrea, 2018; Farmer et al., 2005; Lord & Ashworth, 2017; Zhou et al., 2020). HR defective cancer cells are unable to repair this damage by HR and must rely on lower fidelity repair mechanisms, leading to genomic instability and eventually cell death (Lord & Ashworth, 2017; Zhou et al., 2020). The second widely accepted mechanism is PARP trapping (Keung et al.,

2019; Zhou et al., 2020). Inhibition of the catalytic activity of PARP1 interferes with its dissociation, which is in part reliant on autoPARylation and electrostatic repulsion from the buildup of PAR, resulting in PARP1 remaining bound to DNA at the sites of DNA lesions (Keung et al., 2019; Murai et al., 2012; Zhou et al., 2020). This trapped PARP1 becomes a lesion itself, interfering with repair and requiring HR to be appropriately removed, which again results in synthetic lethality in HR deficient cancer cells (Keung et al., 2019; Murai et al., 2012; Zhou et al., 2020). It is important to note that trapping efficiency of different PARPi has been associated with efficacy, though some studies show a more complex relationship between trapping and efficacy depending on cellular context and treatment strategies (Hopkins et al., 2015; Keung et al., 2019; Zhou et al., 2020).

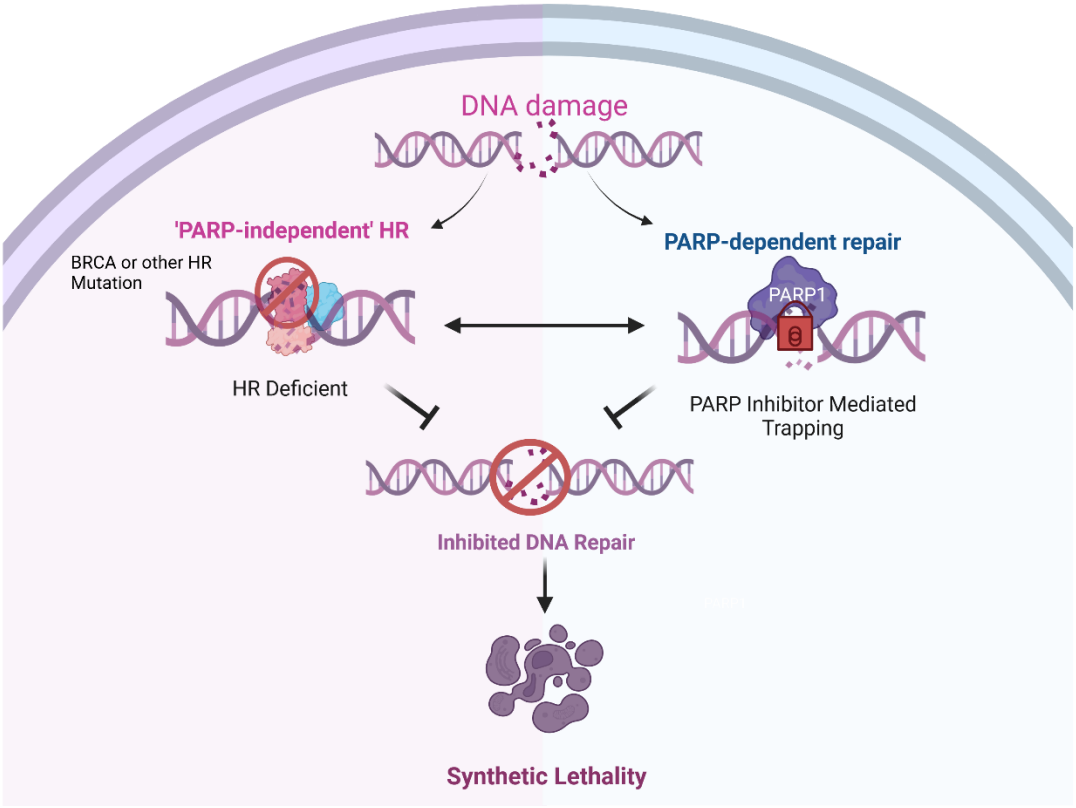

Figure 1-2: PARP inhibitors: accumulating damage and synthetic lethality
Simplified diagram of the two commonly accepted mechanisms underlying PARPi function. PARP inhibitors block PARP dependent BER/SSBR/NHEJ processes and trap PARP1 at DNA damage sites, resulting in accumulating lesions that HR-deficient cancer cells are unable to repair. Created with BioRender.com.

PARPi were originally approved as maintenance therapies for patients with recurrent and platinum sensitive ovarian cancer with HR deficiencies (Miller et al., 2022; Mirza et al., 2020). Interestingly, PARPi have also been shown to provide benefits to patients without HR deficiency, with subsequent approvals for olaparib, rucaparib, and niraparib for maintenance therapies regardless of HR status (Mirza et al., 2020). More recently, PARPi have also been studied as a first-line treatment, alone and in combination with existing chemotherapeutics (Foo et al., 2021; Mirza et al., 2020). Several clinical trials have indicated that PARPi significantly improve patient outcomes in the first-line setting, including slight benefits to patients without HR deficiencies (Foo et al., 2021; Mirza et al., 2020). However, various mechanisms can give rise to PARPi resistance, including upregulation of efflux pumps and mutations that restore HR (Keung et al., 2019; Zhou et al., 2020). Combination therapies are therefore being explored to overcome or limit the development of resistance, and to sensitize patients with poor responses to PARPi (Beniey et al., 2023; Boussios et al., 2019; D'Andrea, 2018; Foo et al., 2021; Miller et al., 2022; Mirza et al., 2020). The identification of novel targets that can cooperatively enhance PARPi therapies, and biomarkers predictive of PARPi responsiveness, are therefore crucial for the continued improvement of HGSOC treatment (Miller et al., 2022; Zhou et al., 2020).

1.7 Rationale

Much research has been dedicated to the understanding of the mechanisms underlying DNA damage repair. DNA damage repair pathways are crucial for preserving genomic integrity and preventing mutation and the development of disease states in human cells. Despite this, there is clearly much that remains to be discovered. Investigating new mechanisms in DDR, the "fine tuning" underlying their regulatory control, and their dysregulation in disease provide insight

into these complex and essential pathways, allowing for the development of novel interventions to improve outcomes in DDR associated diseases.

The E3 ligase HUWE1 is an important protein in DDR pathways and is associated with disease ranging from cancer to intellectual disability (Gong et al., 2020; Kao et al., 2018; Kunz et al., 2020; Qi et al., 2022; Wang et al., 2014). However, the extent of HUWE1's influence on DNA damage and the precise mechanisms of its participation in DDR are still not fully understood. Therefore, this project sought to investigate the impact of HUWE1 depletion on cellular genome stability in both the presence and absence of DNA damage.

Furthermore, given the recent advent and success of PARPi for ovarian cancer therapy, the influence of HUWE1 depletion on cellular DNA damage in response to PARPi was also examined. Characterizing the impact of HUWE1 on cellular responsiveness to PARPi could elucidate a new factor regulating PARPi effectiveness in cancer therapy.

Post-translational modifications, such as ubiquitination and PARylation, play crucial roles in DNA damage repair by recruiting and regulating various DNA repair factors (Huang & D'Andrea, 2006; Groslambert et al., 2021; Kang et al., 2022; Kao et al., 2018; Sugasawa et al., 2005; Wei & Yu, 2016). Interestingly, WWE domains such as the one found in HUWE1 are known to mediate binding to PAR chains, and consequently to PARylated proteins (Gatti et al., 2020; Hunkeler et al., 2021; Wang Z et al., 2012; Zhang et al., 2011). During DNA damage repair, PARP1 is the key enzyme responsible for PARylation of other proteins, as well as self-PARylation to regulate its association with DNA (Alemasova & Lavrik, 2019; Kamaletdinova et al., 2019; Kang et al., 2022; Liu C et al., 2017; Muthurajan et al., 2014). Therefore, it is hypothesized that HUWE1 can interact with PARP1 and regulate its stability, similarly to other WWE-containing E3 ligases (Gatti et al., 2020, Hunkeler et al., 2021, Wang Z et al., 2012, Zhang

et al., 2011). This thesis therefore aimed to provide experimental evidence of the regulation of PARP1 by HUWE1.

Thus, the main objectives underlying the project are:

1. **Characterization of HUWE1 depletion and its impact on DNA damage repair**

   Despite the known functions of HUWE1 in DNA damage repair, much remains to be investigated regarding its actual impact on cellular DNA damage in response to stressors and novel mechanisms underlying its effects. To begin to elucidate this, alkaline comet assays were utilized to assess the effect of HUWE1 depletion on the amount of DNA lesions following various DNA damage treatments. Additionally, histone profiling was conducted to begin to elucidate possible impacts of HUWE1 deletion on chromatin in response to DNA damage.

2. **Characterization of the effect of HUWE1 loss on cellular responsiveness to PARPi**

   An interaction between HUWE1 and PARP1 resulting in PARP1 degradation suggests that HUWE1 status could affect cellular responsiveness to PARP inhibitors, a relatively novel and revolutionary class of cancer therapeutics. Experiments were conducted to examine the impact of the absence of HUWE1 on DNA damage and cellular survival after treatment with PARP inhibitor, which can provide insight into HUWE1's therapeutic significance in ovarian cancer.

3. **Characterization of the interaction between HUWE1 and PARP1**

   Since the WWE domain is known to modulate binding to PARylated proteins, the impact of HUWE1 on PARP1, an important DDR protein that is responsible for the majority of cellular PAR, must be investigated. Co-immunoprecipitation and subcellular fractionation

experiments were conducted to investigate the nature of the interaction between HUWE1 and PARP1, and to observe the impact of HUWE1 depletion on PARP1 protein levels

Chapter 2: Materials and Methods

2.1 Cell Culture

Immortalized wild-type and HUWE1 knockout mouse embryonic fibroblast (MEF) cells were obtained from Dr. Tak Mak (University of Toronto). Human embryonic kidney cells (HEK293T), and HEK293T/ATCC cells selected for high transfection efficiency, were obtained from Dr. Samuel Benchimol (York University). OVCAR3 ovarian cancer cells were obtained from Dr. Chun Peng (York University). All cell lines were grown in a humidified incubator at 37°C and 5% CO_2. All cell lines were grown in Dulbecco's Modified Eagle Medium (DMEM) supplemented with 10% fetal bovine serum (FBS) and 1% penicillin/streptomycin (P/S). OVCAR3 shHUWE1 and empty vector (EV) cells were additionally cultured with 2µg/mL puromycin to maintain selective pressure for cells expressing their respective plasmids. Cells were passaged when between 80-90% confluency.

2.2 Cell Treatments

2.2.1 Drug Treatment

Solid stocks of etoposide (Millipore-Sigma #E1383), AZD2461 (Millipore-Sigma #SML1858), PJ34 (Millipore-Sigma #528150), and olaparib (Toronto Research Chemicals #O514500) were diluted in dimethyl sulfoxide (DMSO). Stock of cisplatin (Millipore-Sigma #232120) was diluted in PBS. These stock solutions were stored at -20°C in small aliquots. Cells were treated with each drug by diluting the concentrated stock solutions to the desired concentration and volume in complete culture media. For recovery periods, drug-containing media was removed and replaced with fresh media.

2.2.2 UV Irradiation

Prior to UV treatment, media was removed from cell culture plates, and cells were rinsed with PBS. Plates were placed on a thin layer of ice in a glass tray, and the lids were removed.

The tray was then placed into a SpectroLinker XL-1500 UV crosslinker, and cells were treated with 20 J/m^2, as indicated. Media was replenished, and the cell plates were placed back into a humidified incubator at 37° C with 5% CO_2 for the indicated times to allow DNA damage to form prior to experimental procedures.

2.3 Total Cell Lysis

RIPA lysis buffer was prepared from RIPA base (**Table 2.1**) by adding appropriate protease inhibitors (**Table 2.2**). Cell pellets collected by centrifugation and washed with PBS. Freshly collected or frozen cell pellets in 1.5mL microcentrifuge tubes were resuspended in 0.5mL of cold RIPA lysis buffer and vortexed at max speed for 15 seconds, followed by a 30 minute incubation on ice. Tubes were then vortexed at max speed for 15 seconds and sonicated at 10% amplitude for 20-30 pulses (pulse on 1 second, pulse off 3 seconds using Fischer Scientific Sonic Dismembrator Model 500), or sonicated at 20% amplitude for 5-10 pulses using a handheld sonicator. Samples were then centrifuged at 16 000g for 15 minutes at 4°C to pellet cell debris. Lysates were typically immediately prepared for western blotting and stored at -20°C, or occasionally stored at -80°C prior to preparation and use.

Table 2.1 Base RIPA Buffer Recipe

Reagent	Final Concentration
Tris pH 7.4	50mM
NaCl	150mM
Triton X-100	1%
Sodium deoxycholate	0.5%
Sodium dodecyl sulfate	0.1%
EDTA	1mM

Table 2.2 List of Protease Inhibitors

Reagent	Final Concentration
Benzamidine Hydrochloride	1mM
Phenylmethane Sulfonyl Fluoride (PMSF)	1mM
50X Protease Inhibitor Cocktail (Thermo #78425)	1X
ADP-HPD (PARGi) (Sigma-Aldrich #118415)	1mM

2.4 Western Blot

Concentration of protein samples was determined by use of a BCA assay (Thermo Scientific #23225) with bovine serum albumin (BSA) protein standards according to manufacturer instructions. Sample concentrations were normalized, between 0.75-1μg/μL with double distilled water and a final 1X SDS sample buffer, followed by boiling for 5-10 minutes to denature proteins. Equal amounts of protein were loaded in each well of 4-12% polyacrylamide gradient gels (Invitrogen #NP0321BOX) and run at 100V for approximately 1.5 hours or until the dye front reached the end of the gel. Transfer to PVDF membranes was conducted overnight for 19 hours, 30V at 4° C. Ponceau-S (Santa Cruz #sc-301558) staining was used to assess transfer success. Following transfer, membranes were blocked for 2 hours in 5% milk in Tris-buffered saline with Tween20 (TBST), and 1 hour in 5% BSA-TBST. After a brief water rinse, membranes were incubated with primary antibodies (**Table 2.3**) overnight at 4° C with gentle rocking. Membranes were then washed three times for 5 minutes with TBST before 1 hour incubation with the appropriate species-specific HRP-conjugated secondary antibodies at room temperature with gentle rocking. Following this, membranes were washed 4 times for 15 minutes with TBST prior to the addition of the chemiluminescent substrate (PerkinElmer #NEL105001, FisherSci #45-002-401) for 5 minutes. The immunoblots were imaged using the MicroChemi imager (DNR Bio Imaging Systems) or with a film developer.

Table 2.3 List of Primary Antibodies

Antibody	Catalog Number		Antibody	Catalog Number
HUWE1	Bethyl#A300-486A		H2AX	CST#2595
HUWE1	Bethyl#A303-836A		yH2AX	CST#80312
β-Actin	Sigma#5441		H3	CST#4499
Vinculin	CST#4650		H4	CST#13919
GAPDH	Proteintech#60004-1-Ig		Macro H2A	CST#8551
PARP	CST#9542		H3K4me3	CST#9751
PARP	Santa Cruz #sc-8007		H3K9me3	CST#13969
PAR/MAR	CST#83732		H3K36me3	CST#4909
γH2AX	CST#80312		H3K79me3	CST#4260
γH2AX	CST#2577		H3K9Ac	CST#9649
Acetyl-K	CST#9441		H4K8Ac	CST#2594
H1.2	Invitrogen #PA5-32009		H2BK5Ac	CST#12799
H2A	CST#12349		H2AK5Ac	CST#2576

2.5 Alkaline Comet Assay

Comet assays were performed according to manufacturer instructions (Trevigen #4250-050-K). In brief, cells were grown to 70-80% confluency and subjected to the indicated treatments. Meanwhile, 1% low melting agarose (LMA) was melted in boiling water and cooled at 37°C for a minimum of 20 minutes before aliquoting 450µL into 1.5mL microcentrifuge tubes prewarmed at 37°C. Lysis solution (R&D Systems #4250-050-01, or published recipe by Nandhakumar et al., 2011, 146.1g NaCl, 37.2g disodium EDTA, 1.2g Tris, 700mL of ddH_2O, 12g NaOH, 1g SDS, adjusted pH to 10 and final volume to 890mL. Working solution prepared by adding 1.6mL of 1% Triton X-100 to 108mL of this stock) was cooled at 4°C for a minimum of 20 minutes. Minimizing light exposure, cells were harvested and diluted to 200 000 cells/mL in PBS, and 50µL of each sample was taken and combined with the 450µL aliquots of LMA. After mixing, 50µL was spread on the sample area of the comet slides and stored for 10-30 minutes at 4°C in the dark to allow adhesion. Slides were then gently immersed in lysis solution and incubated overnight at 4°C. Slides were then incubated in alkaline unwinding solution for 1 hour at 4°C before electrophoresis was carried out at 21V for 30 minutes. This was followed by

successive 5 minute incubations in ddH2O (twice) and 70% ethanol, after which the slides were dried at 37°C for 15 minutes, stained with SYBR Gold, and allowed to dry completely prior to imaging. Slides were stored at 4°C. Comet analysis was conducted with OpenComet software (Gyori et al., 2014) through ImageJ, and data analysis performed with GraphPad Prism. Outliers detected by OpenComet were examined and removed manually where appropriate.

2.6 HUWE1 Knockdown and Knockout by Lentiviral Transduction

For HUWE1 knockdown, DH5α bacteria were separately transformed with PAX2 and VSVG packaging plasmids, and a pGIPZ empty vector (Horizon #RHS4349) or pGIPZ-shHUWE1 (Horizon #VGH5518-200172, clone ID V2LHS_110969) construct. The bacteria were grown in 200-500mL of LB broth with 100µg/mL of ampicillin to select for transformed bacteria. Plasmid DNA was purified using Qiagen Midi or Maxi prep kits (Qiagen 12143, 12162) according to manufacturer instructions. 293T/ATCC cells were transfected with a combination of PAX2, VSVG, and either the empty vector (EV) or shHUWE1 in a 1:1:2 ratio, with a 1:3 ratio of DNA to PolyJet (SignaGen #SL100688). 3µg of each packaging plasmid and 6µg of either EV or shHUWE1 were used to transfect each 10cm plate, in 10mL of media. Lentiviral media was harvested 24 hours and 48 hours post transfection and filtered through a .45µm syringe filter before being stored in 5mL aliquots at -80°C. 10cm plates of OVCAR3 wild-type cells were incubated with 5mL of lentiviral media and 5mL of complete media for 24 hours with 8µg/mL polybrene to enhance transduction efficiency. Following this, fresh media was added, and the cells were allowed to recover for another 24 hours. Selection of successfully transfected cells was performed by incubation with 2µg/mL puromycin. Success of transduction was assessed by fluorescence microscopy to observe GFP expression. Cells were selected for 48-72 hours in

puromycin prior to freezing at -80°C for later use. Efficiency of HUWE1 knockdown was assessed by western blot.

For HUWE1 knockout, a lentiCRISPR vector (addgene #49535) carrying a gRNA targeting HUWE1 was obtained from Dr. Yi Sheng (**Fig S-1**). Virus production and infection carried out as described above. The CRISP-Cas9 construct also encoded a puromycin resistance gene to allow for selection. Following infection and initial pooled selection, the cells were diluted to a single cell per well in 96 well plates for prolonged selection of single colonies. Successful knockout was confirmed by western blot.

2.7 Histone Extraction

Histones were isolated by acid extraction according to the simplified acid extraction protocol from the Bedford Lab (University of Texas). Wild-type and HUWE1 knockout MEF cells were harvested and washed with cold PBS. Cells were then lysed by incubating in RIPA lysis buffer with the addition of protease inhibitors for 30 minutes on ice, and vortexed on max speed for 15 seconds. Cells were then centrifuged at 16 000g at 4°C for 10 minutes. The supernatant was discarded. Histones were precipitated from the pellet by adding 150µL of 0.8M hydrochloric acid and sonicating at 10% amplitude (pulse on 1s, pulse off 3s using a Fischer Scientific Sonic Dismembrator Model 500) for 15 pulses, and incubating on ice for 1 hour. Samples were then centrifuged at 16 000g at 4°C for 10 minutes, and the histone-containing supernatant was transferred to a new tube. Samples were neutralized by adding 90µL of 1.5M Tris-HCl pH 8.5, with dropwise addition of additional buffer if required. Following protein quantification by BCA assay, samples were prepared for western blotting. Equal amounts of protein (20µg) were run on 15% SDS-PAGE gels to ensure appropriate separation of histones.

2.8 Co-Immunoprecipitation

Following treatment as indicated, 293T cells were harvested by trypsinization and centrifugation. Cells were then resuspended in and incubated with 1mL of IP Lysis Buffer (Thermo Scientific #87787) with the addition of protease inhibitors (**Table 2.2**) for 5 minutes on ice with periodic mixing by pipetting and inverting. Samples were centrifuged at 13 000g for 10 minutes at 4°C, and the supernatant was transferred to a new tube. A BCA assay was used to determine protein concentrations. 150µg of lysate from each sample was prepared separately as input at a concentration of 1µg/µL, by combining with SDS sample buffer and water and boiling for 10 minutes. For each sample, 0.5mg of protein in 500µL of lysis buffer was precleared with protein A/G Sepharose beads for 1 hour and incubated overnight at 4°C with 4µL of primary antibody targeting HUWE1 (Bethyl #A300-486A), or an equivalent amount of IgG of the same isotype, on a rotating mixer. Protein A/G magnetic beads (Thermo Scientific #88802) were blocked for 30 minutes with 5% BSA-TBST and washed twice with 500µL of IP lysis buffer. Equal amounts of beads (20µL) were added to each sample for an additional hour. Beads were then collected and washed 7 times for 10 minutes with 1mL of IP lysis buffer on an end over end rotator. A magnetic rack was used to remove wash buffer from beads. Equal volumes (60-100µL) of 4X SDS sample buffer were added to each sample, and samples were boiled for 10 minutes. Equal volumes from each sample were then loaded together with inputs on 4-12% polyacrylamide gradient gels for western blotting.

2.9 Subcellular Fractionation

2.9.1 Commercial Subcellular Fractionation Kit

Fractionation performed according to manufacturer instructions (Thermo Scientific #78840) with minor modifications. All buffers used for the extraction obtained from the kit were

supplemented with protease inhibitors, including 1μM PARG inhibitor (**Table 2.2**) to preserve poly(ADP-ribose) dependent interactions. In brief, after 2 hour treatment with 10μM etoposide and 1μM AZD2461, cells were harvested from 10cm plates and washed with cold PBS before being pelleted by centrifugation. Cell pellets were incubated with ice cold CEB buffer for 10 minutes at 4°C on a shaker at 500rpm, followed by centrifugation at 500g for 5 minutes. The supernatant (cytoplasmic fraction) was removed. Ice cold MEB buffer was then added for another 10 minutes at 4°C on a shaker at 500rpm, and samples were centrifuged at 3000g for 5 minutes. The supernatant (membrane fraction) was removed. Ice-cold NEB buffer was then added, and samples were pipetted 5-10 times to mix before incubating for 30 minutes at 4°C on a shaker at 500rpm. To collect the nuclear soluble fraction, samples were centrifuged at 5000g for 5 minutes and the supernatant was transferred to a new tube. Finally, room temperature NEB buffer with micrococcal nuclease and calcium chloride was added to the pellet, followed by a 30 second vortex at max speed and incubation for 15 minutes at room temperature. Samples were then vortexed at max speed for 15 seconds and centrifuged at 16 000g for 5 minutes before transferring the chromatin-associated protein supernatant to a new tube. Samples were then prepared for western blotting.

2.9.2 Modified Fractionation Method

Following treatment with 0.2mM MMS and 25μM olaparib for 4 hours, cells were washed 3 times with cold PBS and harvested by scraping in 1mL of Buffer A (10mM HEPES pH8, 10mM KCl, 1.5mM $MgCl_2$, 340mM sucrose, 10% glycerol, 1mM DTT, Khan et al., 2020) with protease inhibitors (**Table 2.2**). After transferring cells to 1.5mL microcentrifuge tubes, Triton-X 100 was added to a final concentration of 0.2% and samples were mixed and incubated for 5 minutes on ice. Samples were then centrifuged at 600g for 5 minutes at 4°C, and the

supernatant (cytoplasmic fraction) was transferred to a new tube. Remaining nuclear pellets were incubated with 250µL of Modified Wuarin-Schibler buffer (**Table 2.4**) with protease inhibitors for 20 minutes on ice. Samples were centrifuged at 10 000g for 10 minutes, and the pellet (chromatin) was transferred to a new tube. The remaining supernatant is the nuclear soluble fraction. 500µL of 2X SDS sample buffer without bromophenol blue was added to the chromatin, and 250µL was added to the nuclear soluble fraction. Samples were then boiled for 10 minutes to denature proteins prior to protein quantification and sample preparation for western blotting.

Table 2.4 Modified Wuarin-Schibler Buffer Recipe

Reagent	Final Concentration
Tris-HCl pH 7	10mM
NaCl	0.3M
Urea	1M
NP-40	1%

2.10 CellTiter-Glo Viability Assays

Cell viability assays were performed utilizing CellTiter-Glo 2.0, or CellTiter-Glo Luminescent Viability Assays (Promega #G7571 or #G9242). For the latter, substrate and buffer were combined and the resulting reagent was aliquoted and stored at -80°C. For the former, the already reconstituted reagent was aliquoted and stored at -80°C. All experimental procedures were conducted as follows. Cells were seeded at 15 000-30 000 cells/well in black 96-well plates with transparent well bottoms. CellTiter-Glo reagent was thawed and combined 1:1 with PBS. Following treatment, media was removed from each well and replaced with 100µL of reagent. Plates were then shaken at 500rpm for 30 minutes (CellTiter-Glo 2.0) or 10 minutes followed by another 10 minutes without shaking (CellTiter-Glo). Luminescence was measured at 528/20nm on a Synergy H4 Hybrid Microplate Reader (Agilent BioTek). Data analysis performed using GraphPad Prism.

2.11 Statistical Analysis

Statistical analysis performed using GraphPad Prism 9.5.1 for Windows software. Comet assay data analyzed by two-way ANOVA with multiple comparisons, and CellTiter-Glo survival assays analyzed by unpaired t-test.

Chapter 3: Influences of HUWE1 on DNA Repair and PARPi Sensitivity

Contributions to work:

Vanessa Giglio contributed to MEF timecourse comet assays (Fig 3-2).

Sanjay Amit Seegobin contributed to OVCAR3 shHUWE1 comet assays (Fig 3-6, 3-7)

Nour Nader and Sanjay Amit Seegobin assisted in generating CRISPR-Cas9 HUWE1 knockout OVCAR3 cells (Fig 3-9).

3.1 The Effect of HUWE1 Knockout on DNA Damage Repair in Mouse Embryonic Fibroblasts

HUWE1 has been shown to participate in the regulation of DNA damage repair pathways at multiple stages via interaction with its target proteins (Choe et al., 2016; Hunkeler et al., 2021; Kao et al., 2018; Kunz et al., 2020; Wang et al., 2014; Zhong et al., 2005). Previous research has also demonstrated that HUWE1 knockout results in increases in endogenous DNA damage (Kunz et al., 2020). To gain insight into the role of HUWE1 in DNA damage repair, the impact of HUWE1 deletion on cellular levels of DNA damage in response to exogenous stressors was investigated.

To examine this, DNA damage was induced in wild type (WT) and HUWE1 knockout (KO) immortalized mouse embryonic fibroblast (MEF) cells by treatment with etoposide (**Fig 3-1A)**. Etoposide is a topoisomerase II inhibitor that results in the formation of double strand breaks (Le et al., 2023; Tammaro et al., 2013). Levels of cellular DNA damage were assessed by use of an alkaline comet assay, a single cell gel electrophoresis experiment that allows visualization of DNA breaks in the cell via fluorescence microscopy (**Fig 3-1B**). Following treatment with 10μM etoposide for 2 hours, the extent of DNA damage present in the cell was quantitatively measured by calculating tail moments. Tail moments are a parameter that can represent the amount of DNA fragmentation, defined as the percentage of fluorescent signal present in the migrated DNA "tail" multiplied by the length of the tail and divided by 100.

In agreement with the previous observation by Kunz and colleagues (2020), untreated HUWE1 knockout MEFs exhibited slightly greater tail moments relative to WT cells with mean tail moments of 0.45 and 0.96, despite the lack of statistical significance (**Fig 3-1C**). Following a 2 hour treatment with 10μM etoposide, both WT and KO cells demonstrated a clear increase in

tail moments. HUWE1 KO cells demonstrated significantly greater tail moments compared to WT cells (mean tail moment, WT: 63.9, KO 100.2), indicating that HUWE1 knockout results in increased sensitivity to the induction of DNA double strand breaks by etoposide in MEF cells.

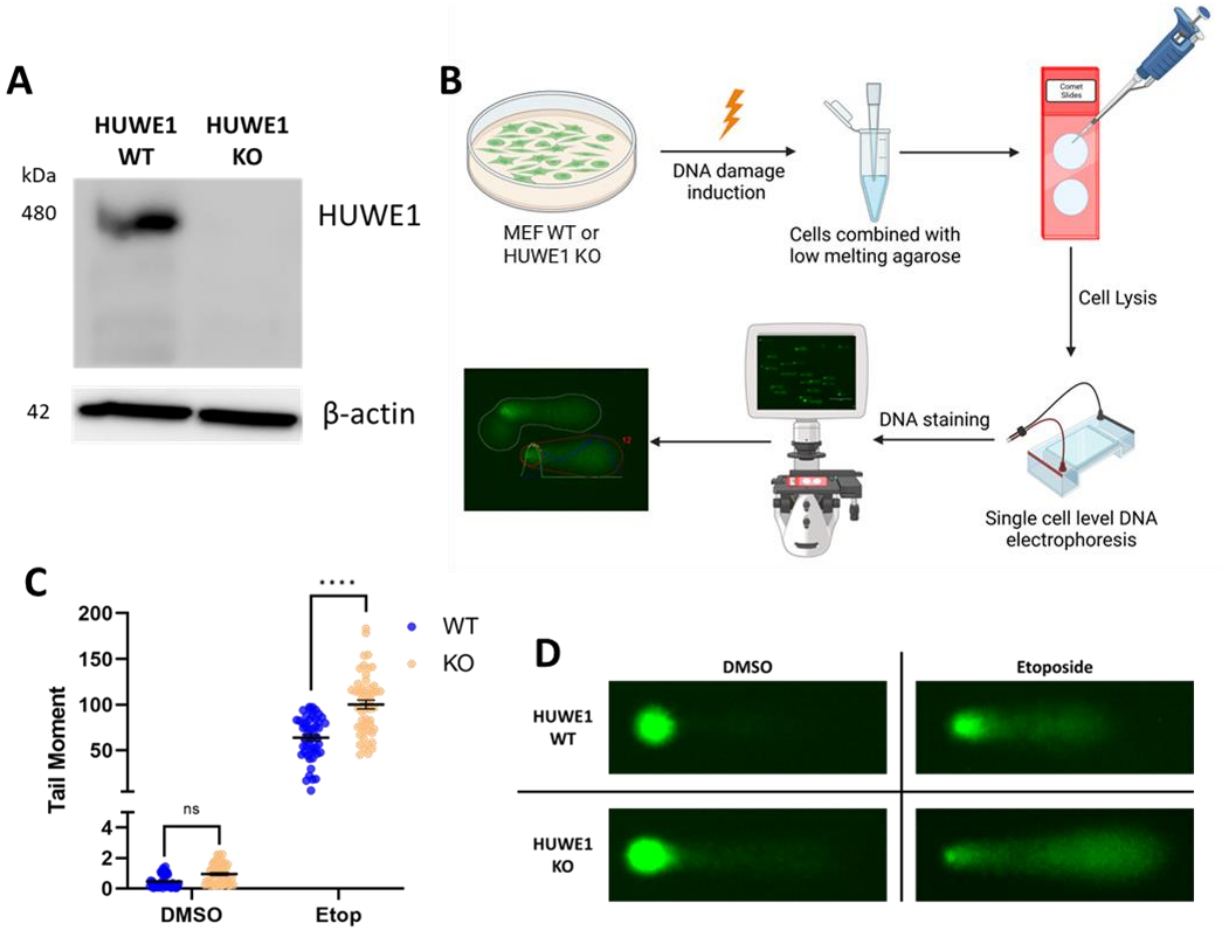

Figure 3-1: HUWE1 knockout results in increased DNA damage in MEF cells.
A) Western blot of nuclear fractions of wild type and HUWE1 knockout mouse embryonic fibroblasts. B) Graphical workflow of the comet assay procedure. C) WT and HUWE1 KO MEF cells were treated with 10μM etoposide or DMSO as a vehicle control for 2 hours before being harvested for comet assay procedures. >50 cells were quantified per treatment group, and the middle 50 values used for analysis. Comets analyzed with OpenComet, statistical analysis by two-way ANOVA with multiple comparisons using GraphPad Prism, ns = no significance, **** $p < 0.0001$. D) Representative comet images from each treatment group.

To examine DNA repair over time, DNA damage was further assessed at various recovery time points (1, 5, and 23 hours) after 1 hour treatment with 10μM etoposide. Consistent with previous observations, HUWE1 KO cells endogenously had a slightly elevated mean tail moment of 0.43 relative to WT MEF cells with a mean tail moment of 0.32 (**Fig 3-2A, B**). Etoposide treated HUWE1 KO cells had greater damage relative to WT cells throughout the course of the experiment. At 1 hour of recovery time, WT cells had a mean tail moment of 1.2, while HUWE1 KO cells peaked with a mean tail moment of 17.38. By 23 hours of recovery, KO cells still had a higher mean tail moment compared to that of the WT cells. Taken together, these results suggest that depletion of HUWE1 not only sensitizes MEF cells to double strand breaks, but also that this increased damage persists over time.

WT and HUWE1 KO cells were also treated with UV radiation. UV radiation predominantly induces pyrimidine dimers, which are mainly repaired by nucleotide excision repair (NER), though other lesions and repair pathways are also involved (Kciuk et al., 2020; Wang et al., 2022). UV-induced lesions can be converted to single strand breaks and double strand breaks via interference with transcription and replication associated processes over time (Rastogi et al., 2010; Yajima et al., 2009). Thus, assessing the impact of HUWE1 KO on DNA damage in response to UV radiation provides insight into the involvement of HUWE1 in not only DSB repair, but other DNA damage repair pathways as well.

The cells were irradiated with 20 J/m^2 U of UV radiation and then allowed to recover for different periods of time (2, 4, and 6, and 24 hours). DNA damage was again assessed by comet assay. Similar to the trend observed with etoposide treatment, HUWE1 KO cells demonstrated increased and persistent relative to WT cells throughout the course of the experiment (**Fig 3-2C, D**). Interestingly, WT cells exhibited peak levels of DNA damage at the 2 hour timepoint with a

mean tail moment of 7.44, while the amount of DNA damage in HUWE1 KO cells continued to increase until reaching peak levels at 6 hours post irradiation with a mean tail moment of 30.91. This suggests that knockout of HUWE1 not only sensitizes MEF cells to UV-induced DNA damage, but also impedes or slows DNA repair. These findings, together with the etoposide study, demonstrate a significant and complex role for HUWE1 in multiple DNA damage repair pathways.

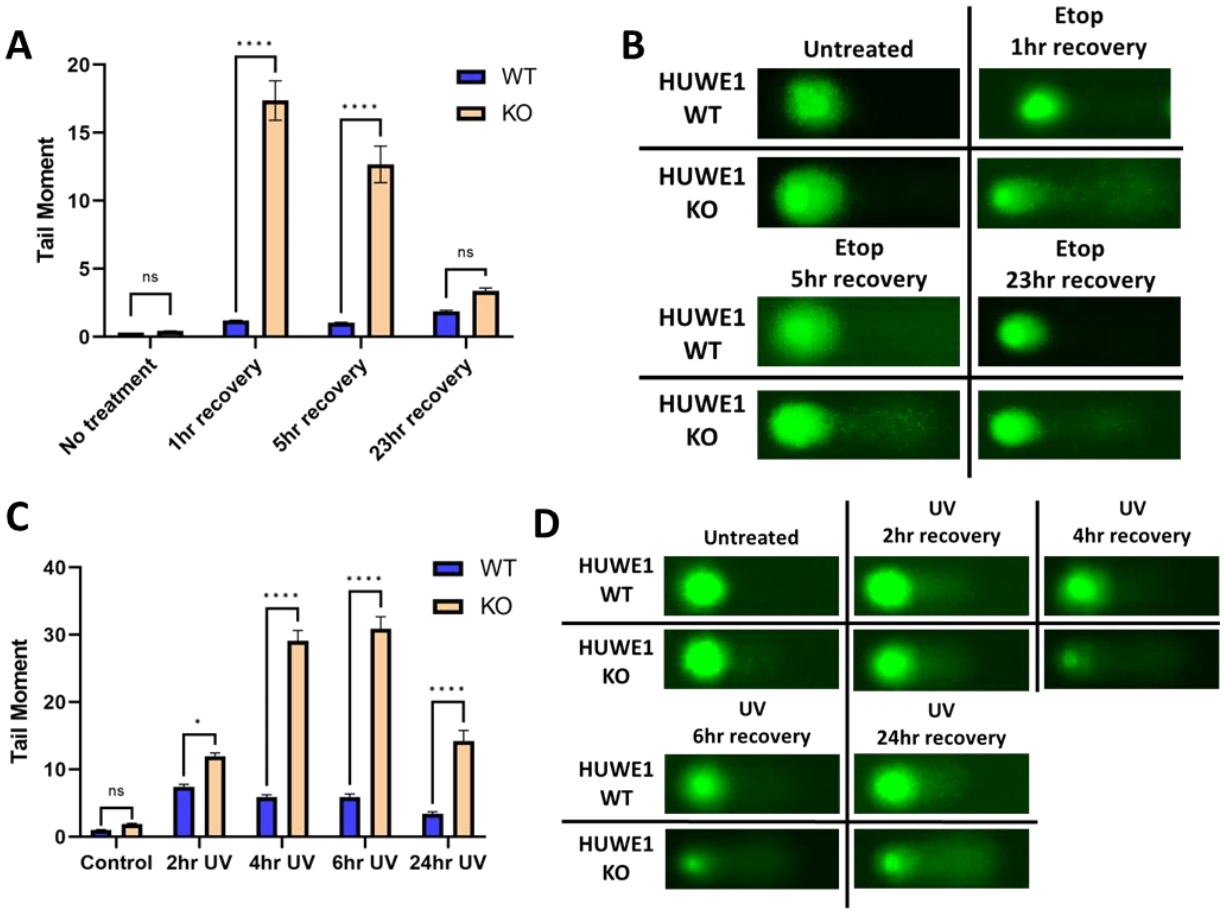

Figure 3-2: HUWE1 knockout MEFs experience increased and prolonged DNA damage.
A) Mean tail moments of MEF WT and HUWE1 KO cells treated with A) 10uM etoposide for 1 hour, or B) 20J/m^2 UV irradiation, and allowed to recover for the indicated times prior to harvest. >150 cells quantified per treatment group, and middle 150 values used for analysis. Comets analyzed with OpenComet, statistical analysis by two-way ANOVA with multiple comparisons using GraphPad Prism, ns = no significance, * $p<0.05$, **** $p< 0.0001$. B) D) Representative comet images from each treatment group.

3.2 The Effect of PARP Inhibition on DNA Damage in HUWE1 Knockout MEF Cells

PARP inhibitors are thought to work by trapping PARP1 at DNA lesions and blocking PARP-dependent DNA repair, resulting in an accumulation of DNA damage (Chaudhuri & Nussenzweig, 2017; D'Andrea, 2018; Zhou et al., 2020). While particularly effective in HR-deficient cancers, PARPi have also been investigated for their ability to potentiate other chemotherapeutic agents (Beniey et al., 2023, Boussios et al., 2019; Chaudhuri & Nussenzweig, 2017; D'Andrea, 2018; Onji & Murai, 2022; Sun et al., 2018, Zhou et al., 2020). Since HUWE1 knockout impaired DNA repair and resulted in increased DNA damage, the question of whether HUWE1 depletion could affect DNA damage in response to treatment with PARPi emerged.

AZD2461 is a new generation PARPi that inhibits PARP1 and PARP2 (Guibbal et al., 2020; O'Connor et al., 2016). To investigate whether HUWE1 status can affect DNA damage repair in response to PARPi treatment, WT and HUWE1 KO MEF cells were treated with etoposide in combination with AZD2461, and alkaline comet assays were again used to measure DNA damage.

Consistent with previous observations, HUWE1 knockout resulted in greater levels of DNA damage in control and etoposide treated cells (**Fig 3-3A, B**). Treatment with AZD2461 alone did not induce DNA damage beyond endogenous levels observed in the vehicle control for either WT or HUWE1 KO cells. Importantly, HUWE1 KO cells treated with etoposide and AZD2461 in combination exhibited greater tail moments compared to both WT cells and to single treatment with etoposide. Combination treatment of HUWE1 KO cells resulted in a mean tail moment of 141.86, compared to 91.37 in WT cells, while HUWE1 KO cells treated with etoposide alone had a mean tail moment of 128.58. Ultimately, these findings suggest that HUWE1 depletion can increase the susceptibility of cells to DNA lesions following treatment

with etoposide and PARPi, which in turn suggests that HUWE1 is an important factor modulating cellular responses to PARPi treatment.

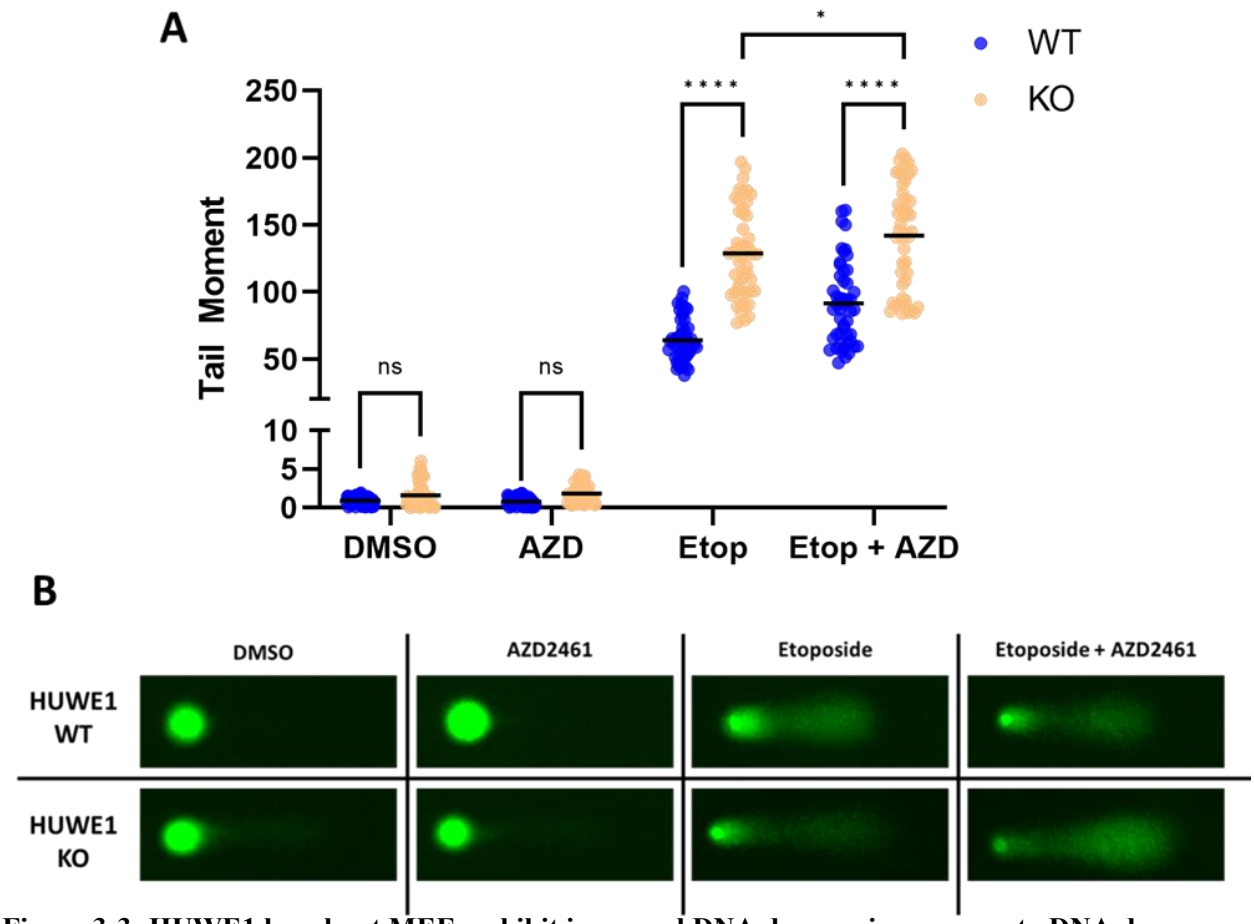

Figure 3-3: HUWE1 knockout MEFs exhibit increased DNA damage in response to DNA damage and PARP inhibition.

A) Mean tail moments of MEF WT and HUWE1 KO cells treated with 10μM etoposide and 1μM AZD2461 for 2 hours. >50 comets quantified with OpenComet per treatment group, and middle 50 values used for analysis. Representative of n=2 experiments. Statistical analysis by two-way ANOVA with multiple comparisons using GraphPad Prism, ns = no significance, * $p<0.05$, ** $p<0.01$, **** $p< 0.0001$. B) Representative comet images from each treatment group.

3.3 Survival of HUWE1 Knockout MEF Cells in Response to PARP Inhibition

The effect of HUWE1 KO on DNA damage in response to etoposide and AZD2461 suggests that there may also be an impact on cellular survival to these stressors. To investigate the impact of HUWE1 knockout on cell survival, WT and HUWE1 KO MEFs were treated with etoposide, AZD2461, or a combination of both drugs for 24 hours. The surviving percentage of cells was then assessed by a CellTiter-Glo® viability assay (**Fig 3-4A)**. Upon addition of the CellTiter-Glo® reagent, cells lyse and release ATP, which participates in a luciferase reaction that produces a chemiluminescent signal proportional to the amount of ATP present. This signal is therefore also proportional to the number of viable cells that were present.

HUWE1 KO cells exhibited similar responses to treatment with either etoposide or AZD2461 alone as WT cells (**Fig 3-4B, C)**. AZD2461 treatment did not induce significant cell death, with 97.7% of WT cells and 93.9% of HUWE1 KO cells surviving at the highest dose of 5μM (**Fig 3-4D)**. Treatment with etoposide resulted in a similar decrease in survival for both WT and KO cells, with 18.5% and 18.4% of cells surviving the 40μM treatment, respectively. However, combination treatment with both drugs resulted in significantly decreased survival of HUWE1 KO cells relative to WT, with 3% of cells surviving compared to 24% in WT cells (**Fig 3-4D, E).** Importantly, the combination treatment in HUWE1 KO cells resulted in survival rates that were also significantly lower than treatment with etoposide alone. Taken together, these results demonstrate that HUWE1 modulates cell sensitivity to PARPi treatment, and thus suggest that HUWE1 may modulate the effectiveness of PARPi therapies.

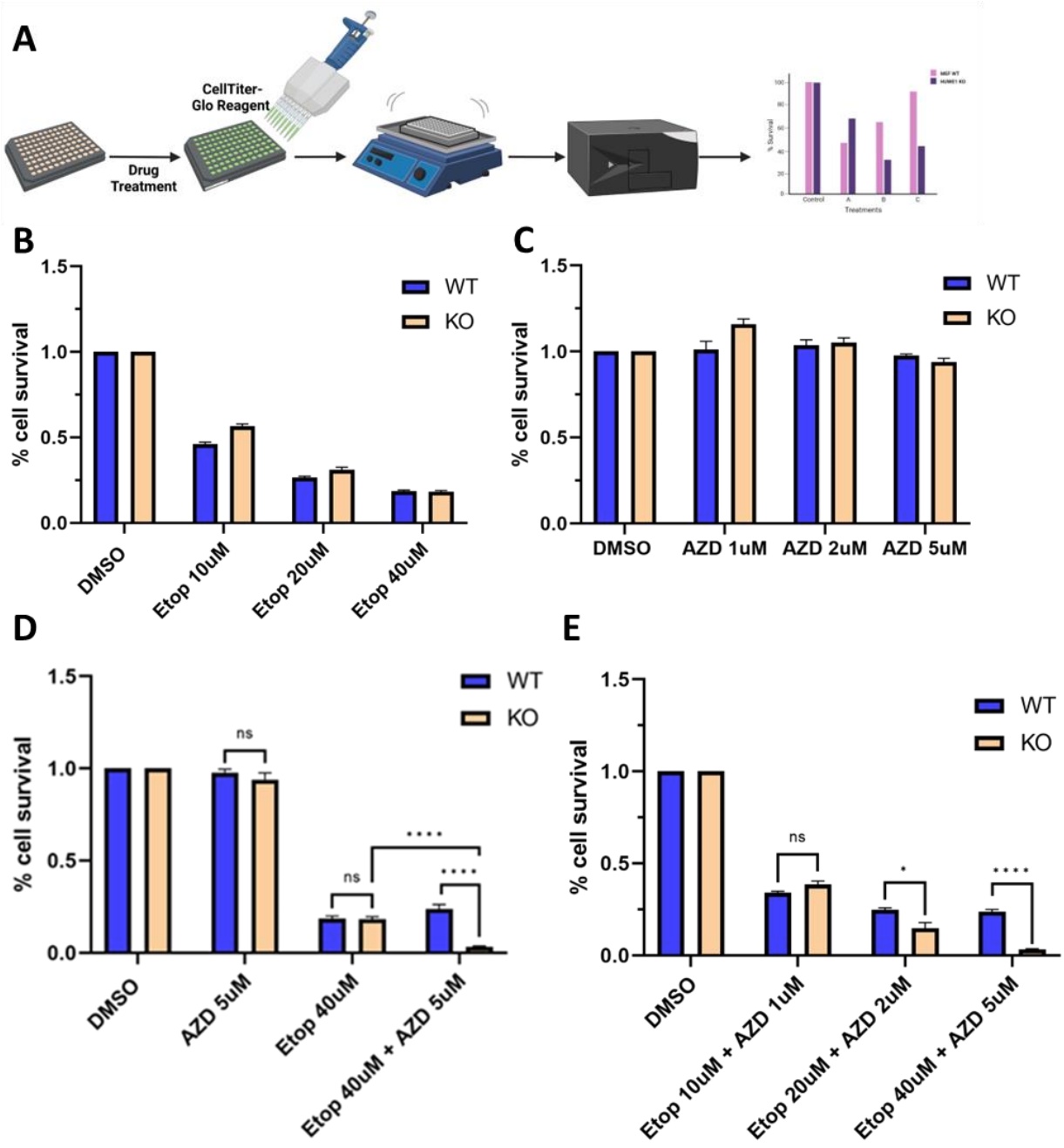

Figure 3-4: HUWE1 knockout sensitizes MEF cells to treatment with etoposide and AZD2461. A) Workflow of the CellTiter-Glo® viability assay. MEF WT and HUWE1 KO cells were treated with 10-40μM etoposide and 1-5μM AZD2461 for 24 hours in a 96 well plate. Graphs show cell survival in response to increasing concentrations of B) etoposide or C) AZD2461 alone. D) Bar graph showing the decrease in survival in KO cells following double treatment with etoposide and AZD2461. E) Survival of cells in response to different combinations of etoposide and AZD2461. Survival values displayed are the mean of 4 biological replicates per treatment group. Representative of n=3 experiments, statistical analysis by unpaired t-test using GraphPad Prism, ns = no significance, * $p<0.05$, **** $p< 0.0001$.

3.4 Modulation of DNA Damage Repair by HUWE1 in High Grade Serous Ovarian Cancer

Deficiencies in DNA damage repair are recurring features in cancer biology, as they lead to an accumulation of mutations that can lead to cancer development and progression (Li et al., 2021; Moon et al., 2023). These DNA repair defects can also result in cancer cells having a cancer-specific vulnerability that can be exploited by DNA damaging chemotherapies (Li et al., 2021; Moon et al., 2023; O'Connor 2015). However, genomic instability can also result in the development of resistance (Li et al., 2021). Elucidating the impact of HUWE1 on DNA damage in a more clinically relevant cell line is therefore an important first step towards characterizing its potential impact on cancer chemotherapies.

A high grade serous ovarian cancer (HGSOC) cell line, OVCAR3, was selected to further study the role of HUWE1 in DNA damage repair. These cells have been characterized as homologous recombination deficient (HRD), though the specific mechanisms underlying the impaired repair remain to be determined (Bradbury et al., 2020). A stable HUWE1 knockdown OVCAR3 cell line (shHUWE1) was established to investigate the impact of HUWE1 depletion in these cancer cells. To accomplish this, a lentiviral system was employed to deliver an shRNA construct targeting HUWE1 into OVCAR3 cells. The pGIPZ-shHUWE1 construct had been used previously to successfully knock down HUWE1 protein levels (Inoue et al., 2013). The pGIPZ backbone additionally encoded a puromycin resistance gene, to enable selection of cells expressing the plasmid, and a green fluorescent protein (GFP) tag, to allow detection of plasmid expression by fluorescence microscopy (**Fig 3-5A)**. Following viral infection and selection, transduction efficiency and expression of the construct was assessed by fluorescence microscopy (**Fig 3-5B).** Western blotting confirmed that HUWE1 protein levels were knocked down (**Fig 3-**

5C). These shHUWE1 and pGIPZ empty vector (EV) OVCAR3 cells were then used to investigate the impact of HUWE1 knockdown on DNA damage and repair.

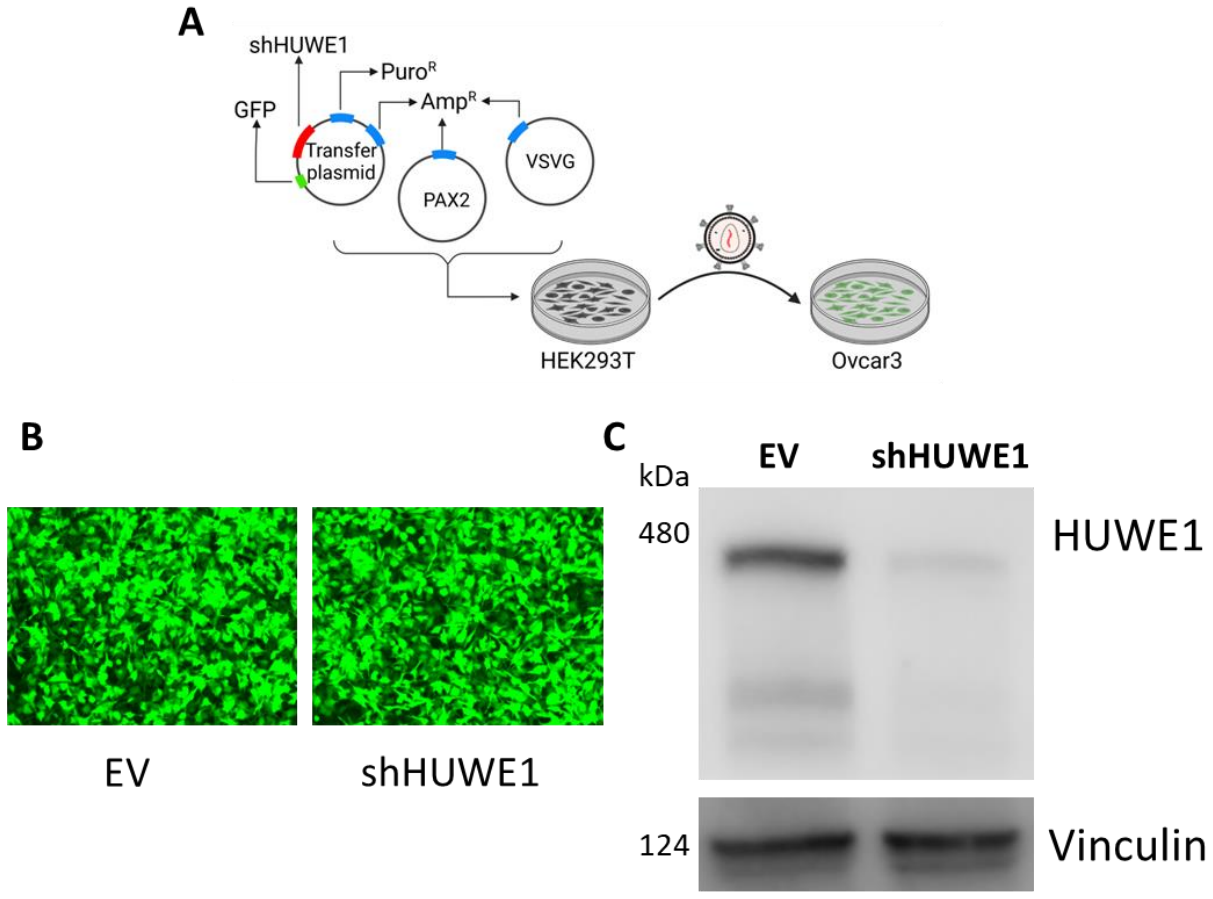

Figure 3-5: Generation of the shHUWE1 knockdown OVCAR3 cell line. A) Graphical workflow demonstrating the process of HUWE1 knockdown by viral transduction. OVCAR3 cells were transduced with a pGIPZ-shHUWE1 (CLONEID) construct, or an empty vector. B) Fluorescent imaging of OVCAR3 shHUWE1 and EV cell lines after the first 48 hours of selection for visual confirmation of transduction efficiency by GFP expression. C) Western blot confirming successful HUWE1 knockdown.

To study the role of HUWE1 in DNA damage repair in OVCAR3 cells, the levels of DNA damage in shHUWE1 or EV cells were examined by comet assay in the presence or absence of different exogenous stressors, etoposide and cisplatin. Similar to what was observed in MEF cells, untreated shHUWE1 cells had a very slight increase in basal DNA damage relative to EV cells (**Fig 3-6).** When treated with 10μM etoposide for 2 hours, both shHUWE1 and EV cells demonstrated the expected increase in DNA damage (**Fig 3-6A)**. The shHUWE1 cells exhibited significantly greater tail moments, with a mean tail moment of 33.62, compared to EV cells with a mean tail moment of 18.19.

Cells were additionally treated with cisplatin, a chemotherapeutic that primarily induces intrastrand adducts (Kiss et al., 2021). These lesions are mainly repaired by nucleotide excision repair, though other repair pathways and types of DNA lesions have been observed in response to cisplatin treatment (Kiss et al., 2021). Comet tails elicited by cisplatin treatment were mild compared to the other treatments, likely due to limited detection of bulky adducts by this method (Ngo et al., 2020). Nevertheless, shHUWE1 cells again demonstrated the trend of increased DNA damage, with a mean tail moment of 2.12, compared to 1.38 for EV cells (**Fig 3-6C)**.

Taken together these findings highlight that HUWE1 is a significant contributor to DNA damage susceptibility in response to a variety of DNA lesions, demonstrating that HUWE1 is an important modulator of diverse DNA repair pathways. The impact of HUWE1 depletion on cellular DNA damage levels is consistent with the observations in MEF cells and suggests that HUWE1 depletion may be a viable strategy for modulating cancer cell sensitivity to DNA damaging chemotherapeutics.

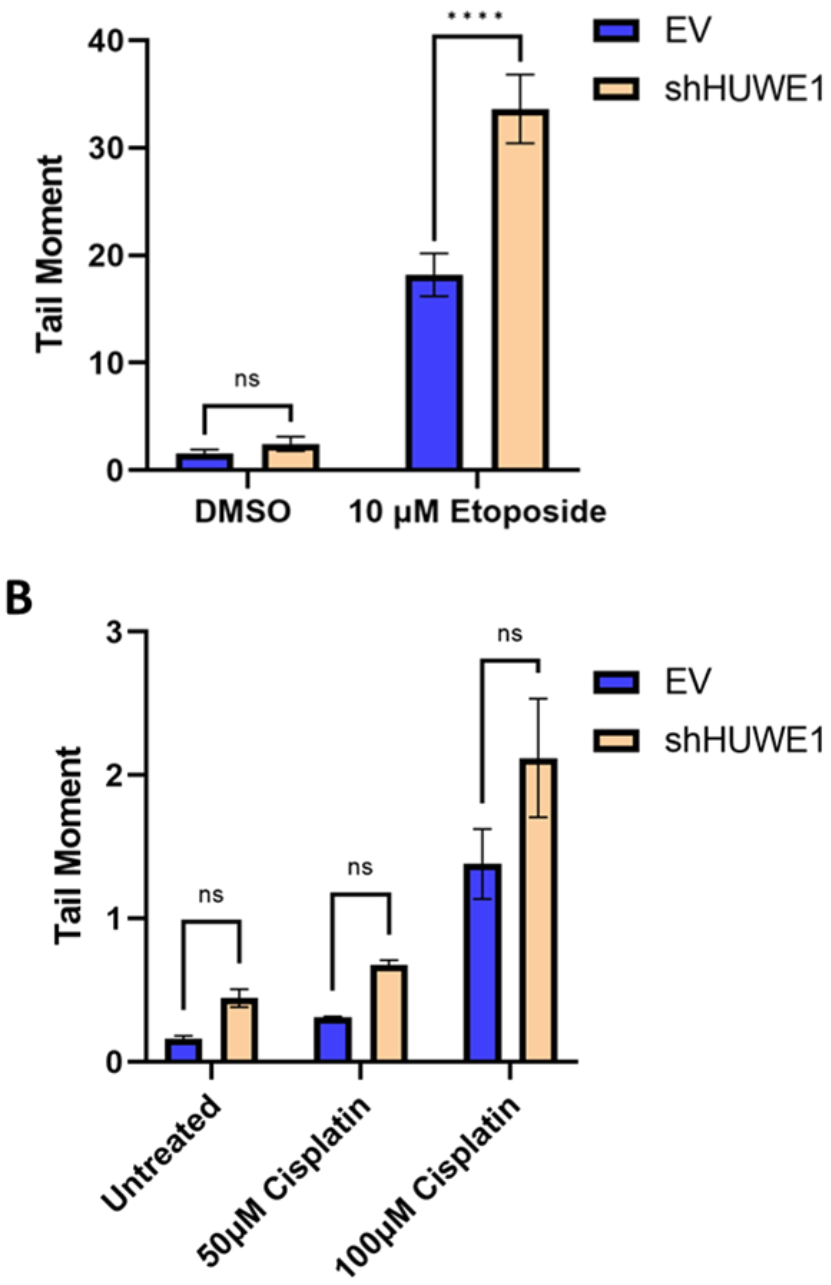

Figure 3-6: HUWE1 knockdown increased DNA damage in response to different damaging agents in OVCAR3 cells.
EV or shHUWE1 OVCAR3 cells were treated with A) 10μM etoposide for 2 hours, B) 50 and 100μM cisplatin for 24 hours. >80, and >100 comets quantified with OpenComet per treatment group, and analysis carried out on the middle 80 and 100 values, respectively. Statistical analysis by two-way ANOVA with multiple comparisons using GraphPad Prism, ns = no significance, **** $p < 0.0001$

3.5 HUWE1 Regulates DNA Damage in PARPi Treated Ovarian Cancer Cells

The discovery that HUWE1 modulates cellular responses to PARPi in MEF cells is an early indicator that HUWE1 could be an important factor in determining cellular response to PARPi therapies. Determining whether HUWE1 can similarly regulate DNA damage in PARPi-treated ovarian cancer cells is crucial for further characterizing its potential as a prognostic factor or therapeutic target.

To investigate this, OVCAR3 shHUWE1 and EV cells were treated with different DNA damaging agents in combination with PARPi. DNA damage was induced by treatment with etoposide, and also by treatment with MMS, which is primarily repaired by base excision repair with some evidence for additional contribution by homologous recombination repair (Lundin et al., 2005; Nikolova et al., 2010). The levels of DNA damage in the presence or absence of AZD2461 were then measured by the alkaline comet assay.

In agreement with previous observations, shHUWE1 cells demonstrated greater sensitivity to the DNA damaging agents tested, having greater mean tail moments compared to EV cells (**Fig 3-7**). Importantly, combination treatments of shHUWE1 cells with each DNA damaging agent in conjunction with AZD2461 resulted in a further increase in damage relative to EV cells and to treatment with the damaging agent alone, even though AZD2461 does not significantly increase damage on its own (**Fig 3-7A-B**). These results demonstrate that depletion of HUWE1 robustly increases DNA damage experienced by ovarian cancer cells in response to co-treatment with various DNA damage inducing agents and AZD2461. This provides further evidence that HUWE1 is a viable prognostic factor or therapeutic target for improving PARPi therapies in ovarian cancer.

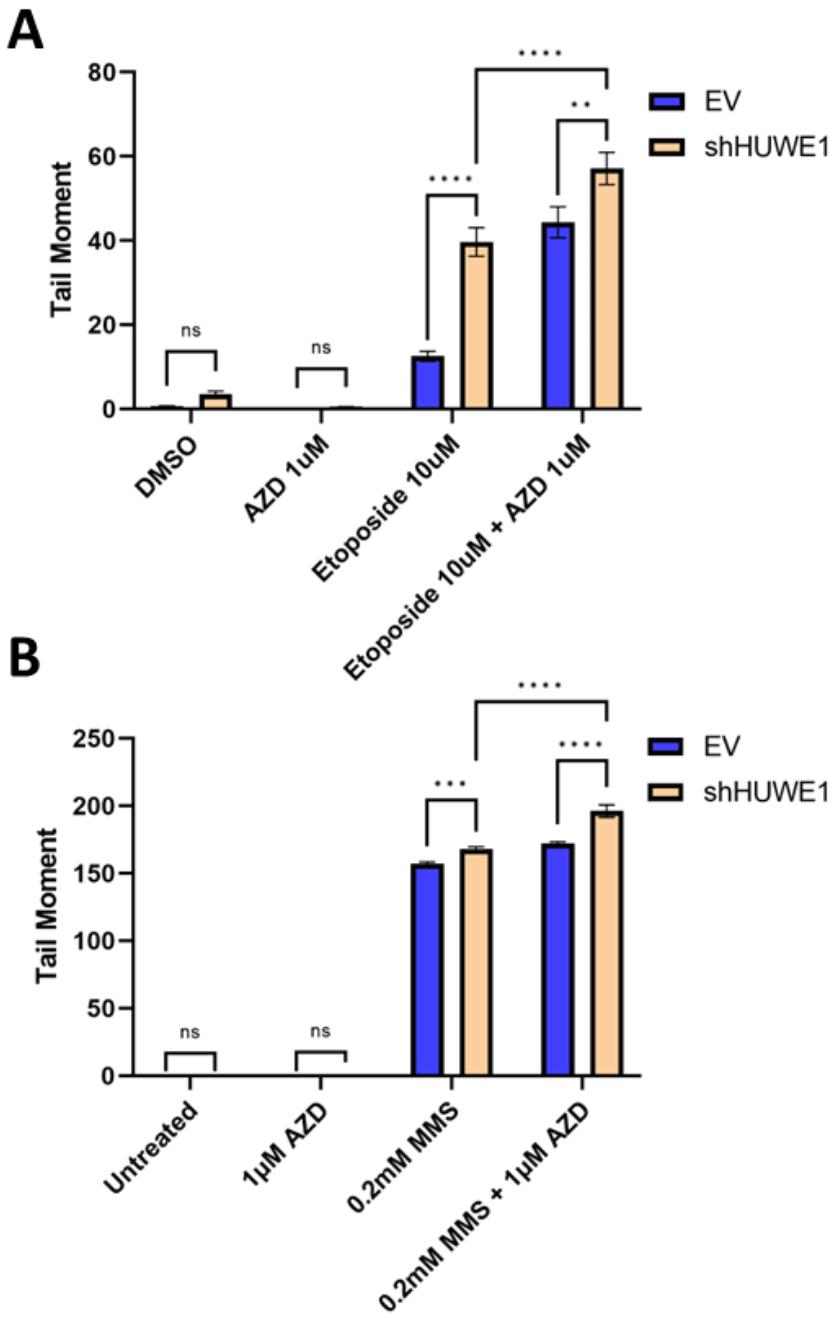

Figure 3-7: HUWE1 knockdown increased DNA lesions after treatment with damaging agents and AZD2461 in OVCAR3 cells

Mean tail moments of OVCAR3 EV or shHUWE1 treated with AZD2461 in combination with A) 10μM etoposide for 2 hours or B) 0.2mM MMS for 4 hours. OpenComet was used to quantify >100 comets per treatment group. The middle 100 values were then used for analysis. Representative of n=2 experiments. Statistical analysis by two-way ANOVA with multiple comparisons using GraphPad Prism, ns = no significance, ** $p<0.01$, *** $p<0.001$, **** $p< 0.0001$.

3.6 Knockdown of HUWE1 Sensitizes OVCAR3 Cells to PARPi and DNA Damage.

Since HUWE1 deletion results in higher levels of DNA damage in OVCAR3 cells, the logical next step was to test the effect of HUWE1 depletion on the survival of these cells. This is a crucial piece of insight into the importance of HUWE1 for therapeutic interventions in ovarian cancer. To examine this, OVCAR3 shHUWE1 and EV cells were treated with a range of concentrations of etoposide (0-80μM) and AZD2461 (0-20μM) for 24 hours. Cell survival was then assessed by CellTiter-Glo® viability assay.

The results showed that treatment with etoposide or AZD2461 alone resulted in a slight decrease in cell survival, with over 60% of cells surviving in both cases (**Fig 3-8A)**. For these single drug treatment groups, HUWE1 knockdown appeared to have mild to moderate effects on cell survival relative to EV cells (**Fig 3-8B, C**). Combination treatment induced visibly greater cell death in both EV and shHUWE1 cells, and shHUWE1 cells had decreased survival rates relative to EV (**Fig 3-8A, D**). These findings again suggest that HUWE1 is a factor in determining cellular responses to PARPi and DNA damaging treatments, and thus provide a foundation for continued research aimed at understanding the influence of HUWE1 on patient responses to PARPi.

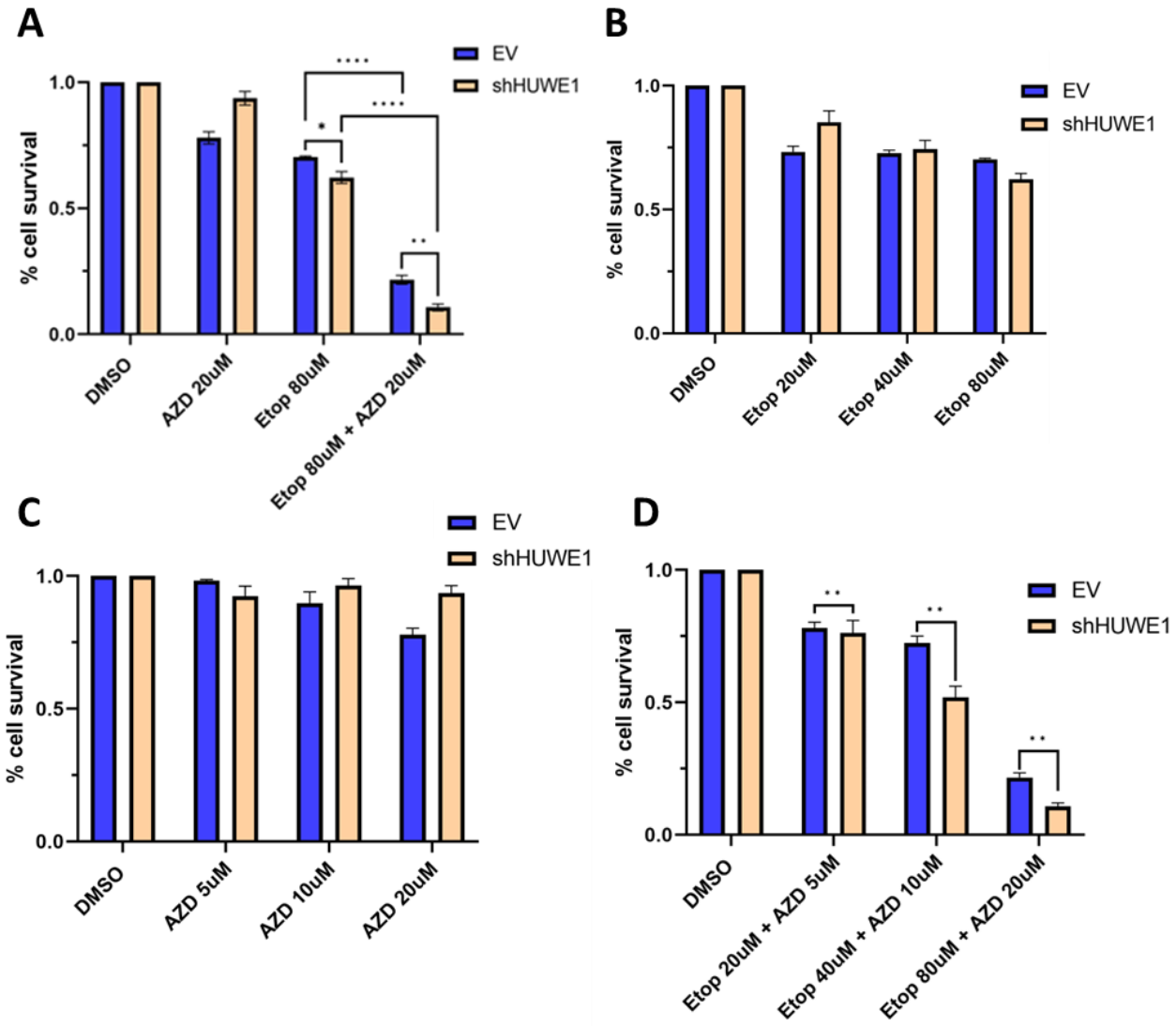

Figure 3-8: HUWE1 knockdown sensitizes OVCAR3 cells to treatment with etoposide and AZD2461.

A) Survival of OVCAR3 EV and shHUWE1 cells treated with 80µM etoposide, 20µM AZD2461, or a combination of the two drugs for 24 hours. B)-D) Cell survival in response to treatment with increasing concentrations of etoposide or AZD2461, alone and in combination. All survival values are means of 4 biological replicates, obtained with the CellTiter-Glo® viability assay. Representative of n=3 experiments, statistical analysis by unpaired t-test using GraphPad Prism, ns = no significance, * $p<0.05$, ** $p<0.01$, **** $p< 0.0001$.

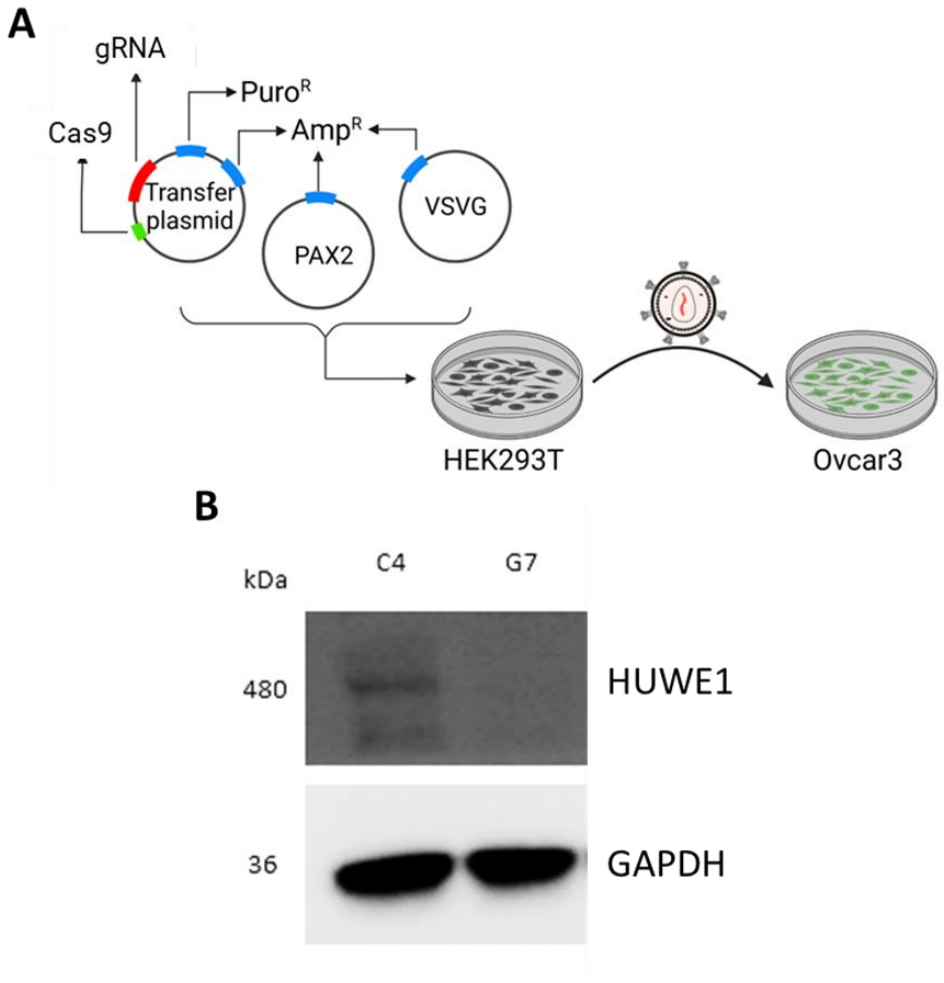

Figure 3-9: Generation of a stable HUWE1 knockout OVCAR3 cell line.
A) Graphical workflow demonstrating the process of HUWE1 knockout by viral transduction. OVCAR3 cells were transduced with a CRISPR-Cas9 construct targeting HUWE1, diluted to single cells in 96 well plates, and grown in selective media for a minimum of 3 weeks. B) Western blot confirming successful HUWE1 knockout in the G7 clone, compared to unsuccessful knockout in the C4 clone.

3.7 HUWE1 Knockout Modulates Synergism of PARPi and DNA Damage Treatment

While stable knockdown of HUWE1 in OVCAR3 cells provided a good model for examining the impact of HUWE1 depletion on cellular sensitivity to PARPi, shRNA knockdown does not completely eliminate protein expression. Furthermore, the transduced constructs could have off target effects that alter the cellular mechanisms underlying the observed experimental outcomes. It is therefore important to corroborate the effects of shHUWE1 by use of a different system. To this end, a stable HUWE1 knockout OVCAR3 cell line was established using CRISPR-Cas9 (**Fig 3-9A**). A lentiviral vector was used to deliver the CRISPR-Cas9 construct into OVCAR3 cells. Following initial pooled selection for 48 hours, the cells were diluted to a single cell per well in 96 well plates for selection of single colonies. After colonies were established, western blotting was used to determine whether HUWE1 was successfully knocked out. (**Fig 3-9B)**. The G7 clone was found to lack HUWE1 expression and was selected for use, being referred to hereafter as the HUWE1 KO OVCAR3 cell line.

To further explore the effect of HUWE1 KO on OVCAR3 cells in response to DNA damaging agents and PARPi treatment, WT and HUWE1 KO OVCAR3 cells were treated with etoposide and AZD2461 for 24 hours and subjected to CellTiter-Glo® survival assays. The results showed that HUWE1 KO OVCAR3 cells were more sensitive than WT cells when treated with etoposide or AZD2461 alone, with a decrease in survival of 10% and 9% respectively (**Fig 3-10A)**. Again, the combination treatment resulted in an evident drop in survival for both WT and KO cells. HUWE1 KO cells were significantly more sensitive to combination treatment, with only 9.2% of KO cells surviving compared to 27.1% of WT cells, a decrease in survival of 18%. Importantly, when etoposide concentrations are kept constant, increasing concentrations of AZD2461 are inversely correlated with cell survival (**Fig 3-10B)**. These results suggest that

HUWE1 deletion may promote a synergistic effect sensitizing OVCAR3 cells to treatment with etoposide and AZD2461

To assess the impact of HUWE1 on the combinatorial effects of etoposide and AZD2461, a matrix was constructed consisting of the mean percentage of cells surviving in response to treatment with each drug, alone and in combination, across the entire range of concentrations tested (**Fig 3-10C, D)**. Synergy analysis was performed using the SynergyFinder 2.0 software (Ianevski et al., 2020). Drugs that act synergistically have a greater effect when administered together than would be expected based on their individual effects (Cokol et al., 2011; Tallarida, 2011). The software utilizes the input data and the Zero Interaction Potency (ZIP) model as a reference for the expected effect if the two drugs do not interact and are additive, and then compares this to the input matrix to calculate a synergy score (Ianevski et al., 2017; Yadav et al., 2015). A synergy score of 10 or greater is indicative that the effect of the two drugs is synergistic. Etoposide and AZD2461 were found to be marginally synergistic in WT cells, with an overall synergy score of 10.95 and a peak synergy score of 12.36 (**Fig 3-10C)**. The drugs were found to act with greater synergism in HUWE1 KO cells, with an overall synergy score of 16.095 and a peak synergy score of 19.13 (**Fig 3-10D)**. When considered together, this data provides further evidence that a deficiency in HUWE1 provides an advantage for combination treatments of PARPi and DNA damaging agents, strengthening the conclusions that HUWE1 is a viable potential therapeutic target and prognostic factor for determining ovarian cancer responsiveness to PARPi therapies.

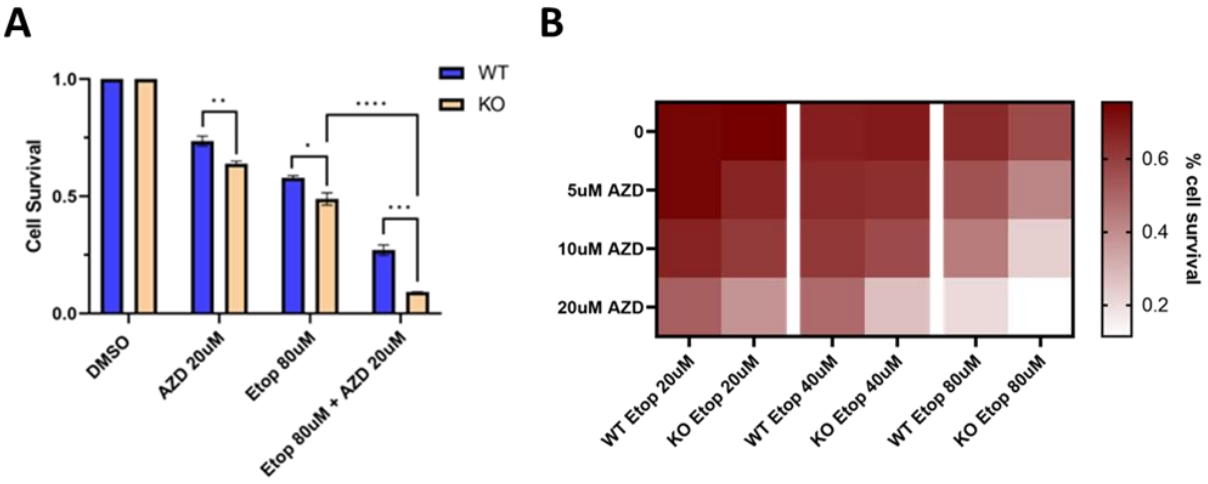

C

WT Survival

Etop \ AZD	0	5µM	10µM	20µM
80µM	65.0871	54.7319	44.2705	20.5368
40µM	67.6176	64.6971	61.2247	48.6055
20µM	73.8478	73.8053	66.4223	51.4496
0	100	98.4512	92.2835	80.023

Synergy score	Most synergistic area score	Method
10.95	12.36	ZIP

D

KO Survival

Etop \ AZD	0	5µM	10µM	20µM
80µM	56.56	41.8094	23.2259	11.4768
40µM	68.74	63.5309	56.596	27.3667
20µM	75.42	66.0454	60.4897	38.2417
0	100	71.21	65.96	70.42

Synergy score	Most synergistic area score	Method
16.09	19.13	ZIP

Figure 3-10: HUWE1 knockout in OVCAR3 cells results in increased sensitivity to etoposide and AZD2461 in a synergistic fashion.

A) Cell survival of WT and HUWE1 KO OVCAR3 cells treated with 80µM etoposide and 20µM AZD2461. Values are mean survival from 4 biological replicates per treatment group. Results representative of n=3 CellTiter-Glo® experiments. Statistical analysis by unpaired t-test, * $p<0.05$, ** $p<0.01$, *** $p<0.001$, **** $p< 0.0001$. B) Heatmap comparing survival of WT and HUWE1 KO OVCAR3 cells treated with constant etoposide concentrations as indicated and increasing AZD2461 concentrations from 5-20µM. C) D) The drug-drug interaction between etoposide and AZD2461 was analyzed through survival of WT and KO cells, respectively, using SynergyFinder 2.0 software. A synergy score greater than 10 is indicative that the drugs are likely acting synergistically. Overall and most synergistic area scores are indicated in the bottom panel.

Chapter 4: Characterizing a Novel Interaction Between HUWE1 and PARP1

Contributions to work:

Dr. Yi Sheng assisted with the final optimizations of the immunoprecipitation experiment (Fig 4-1A).

4.1 HUWE1 interacts with and regulates endogenous PARP1 protein levels

The WWE domain found in HUWE1 is also found in several other E3 ligases, including RNF146, and TRIP12 (Gatti et al., 2020; Wang Z et al., 2012). This domain has been found to interact with PAR and has also been shown to mediate the interaction between the E3 ligases and PARP1 (Aravind, 2001; Gatti et al., 2020; Hunkeler et al., 2021; Wang Z et al., 2012). Given the importance of PARP1 in DNA damage repair pathways, and the observation that HUWE1 depleted cells are more sensitive to PARPi under DNA damage, it was of interest to investigate the potential interaction between HUWE1 and PARP1.

To examine whether HUWE1 interacts with PARP1, 293T cells were subjected to a coimmunoprecipitation experiment with a primary antibody targeting HUWE1. Since the catalytic activity of PARP1 is stimulated by DNA damage, etoposide was used to stimulate PARylation of PARP1 and potentially promote the interaction with HUWE1 (Chaudhuri & Nussenzweig, 2017; Liu C et al., 2017; Shieh et al., 1998). In turn, the PARPi PJ34 was added to inhibit PARylation.

The co-immunoprecipitation showed that PARP1 was readily pulled down by the HUWE1 antibody, and the addition of PJ34 decreased the amount of PARP1 pulled down (**Fig 4-1A)**. This suggests that the interaction between the two proteins is promoted by PAR, since reducing PARylation abrogated the interaction between the two proteins. To examine whether HUWE1 is involved in proteasomal degradation of PARP1, the levels of cellular PARP1 was examined in HUWE1 depleted cells. Importantly, HUWE1 knockout in MEF cells and knockdown in OVCAR3 cells resulted in an increase in cellular PARP1 levels, suggesting that HUWE1 has a role in regulating PARP1 (**Fig 4-1B, C)**. Taken together, these results extend

previous findings and demonstrate that endogenous HUWE1 interacts with PARP1 and regulates its stability (**Fig 4-1D)**. The interaction is likely mediated in part by the PARylation of PARP1.

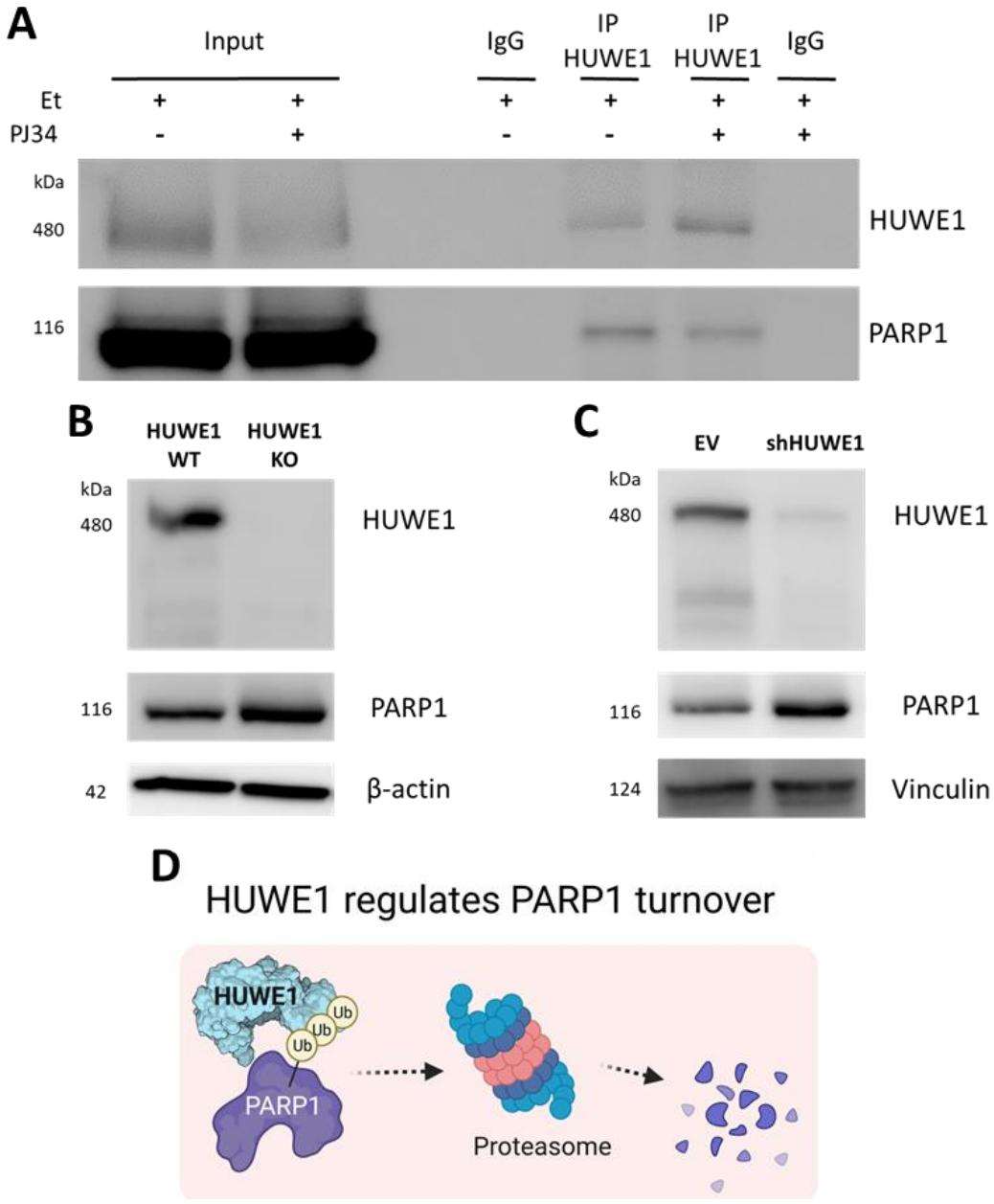

Figure 4-1: HUWE1 knockout can modulate the cellular epigenetic landscape.
A) HEK293T cells were treated with etoposide to stimulate PARP1 activation, or with etoposide and PJ34 to inhibit PARylation. Co-immunoprecipitation was conducted with an antibody against HUWE1 as described. B) Western blot of nuclear fraction from WT and HUWE1 KO MEF cells. C) Western blot of OVCAR3 EV and shHUWE1 cells. D) Graphical model showing the interaction between HUWE1 and PARP1 leading to degradation of PARP1. Created with BioRender.com.

4.2 Chromatin-association of HUWE1 and PARP1 Following PARP Inhibition

Inhibition of the catalytic activity of PARP1 by PARP inhibitors (PARPi) is a relatively recent development that has revolutionized ovarian cancer therapy (Mirza et al. 2020, Zhou et al. 2020). These inhibitors are thought to act via trapping of PARP1 on chromatin, which inhibits repair and subsequently leads to accumulation of DNA damage and cell death, particularly in cells deficient in homologous recombination repair (Chaudhuri & Nussenzweig, 2017; D'Andrea, 2018; Zhou et al., 2020). Since HUWE1 depletion resulted in increased DNA damage after PARPi combination treatments, it was hypothesized that HUWE1 depletion could affect PARP1 trapping. This was investigated by use of two different subcellular fractionation assays.

The effect of HUWE1 depletion on PARP trapping was investigated by use of nuclear fractionation assays. In the first set of experiments, a commercial kit was used to isolate the nuclear soluble and chromatin-associated protein fractions. WT and HUWE1 KO MEF cells were treated with AZD2461 in combination with etoposide to stimulate PARP1 recruitment to the DNA. In the nuclear soluble fraction, HUWE1 knockout cells displayed greater PARP1 levels and PARylation relative to WT, as expected given the role of HUWE1 in regulating PARP1 stability (**Fig 4-2A).** In the chromatin-associated fraction, HUWE1 KO cells treated with etoposide surprisingly showed decreased levels of PARP1 compared to WT cells, despite an elevated PAR signal. This observation could possibly result from a strong initial recruitment of PARP1 that is followed by swift dissociation via electrostatic repulsion resulting from the buildup of PAR chains (Zhou et al. 2020). HUWE1 KO cells treated with both etoposide and AZD2461 displayed a mild increase in chromatin-associated PARP1 relative to WT cells. These findings suggest that HUWE1 depletion can alter the PARP trapping efficiency of PARPi treatments when DNA damage is present.

This method was able to detect chromatin-association of HUWE1. Treatment with etoposide stimulated chromatin recruitment of HUWE1, which was attenuated when cells were co-treated with etoposide and PARPi. Since the WWE domain of HUWE1 interacts with PAR, these findings indicate a possible novel mechanism underlying the function of HUWE1 in DNA repair. They suggest that recruitment of HUWE1 to the chromatin is partially mediated by its interaction with PARylated substrates, such as PARP1 (**Fig 4-2B)**.

In a second set of experiments, a more stringent fractionation method was used to further investigate the effect of HUWE1 KO on cells treated with olaparib and MMS for 4 hours, which is known to cause strong PARP1 activation (Jungmichel et al., 2013; Ovejero et al., 2021). HUWE1 knockout cells co-treated with MMS and olaparib had a clear increase in PARP1 chromatin association compared to WT cells and control treatments (**Fig 4-2C)**. This validates the previous finding that HUWE1 can modulate PARP1 trapping in response to PARPi treatment.

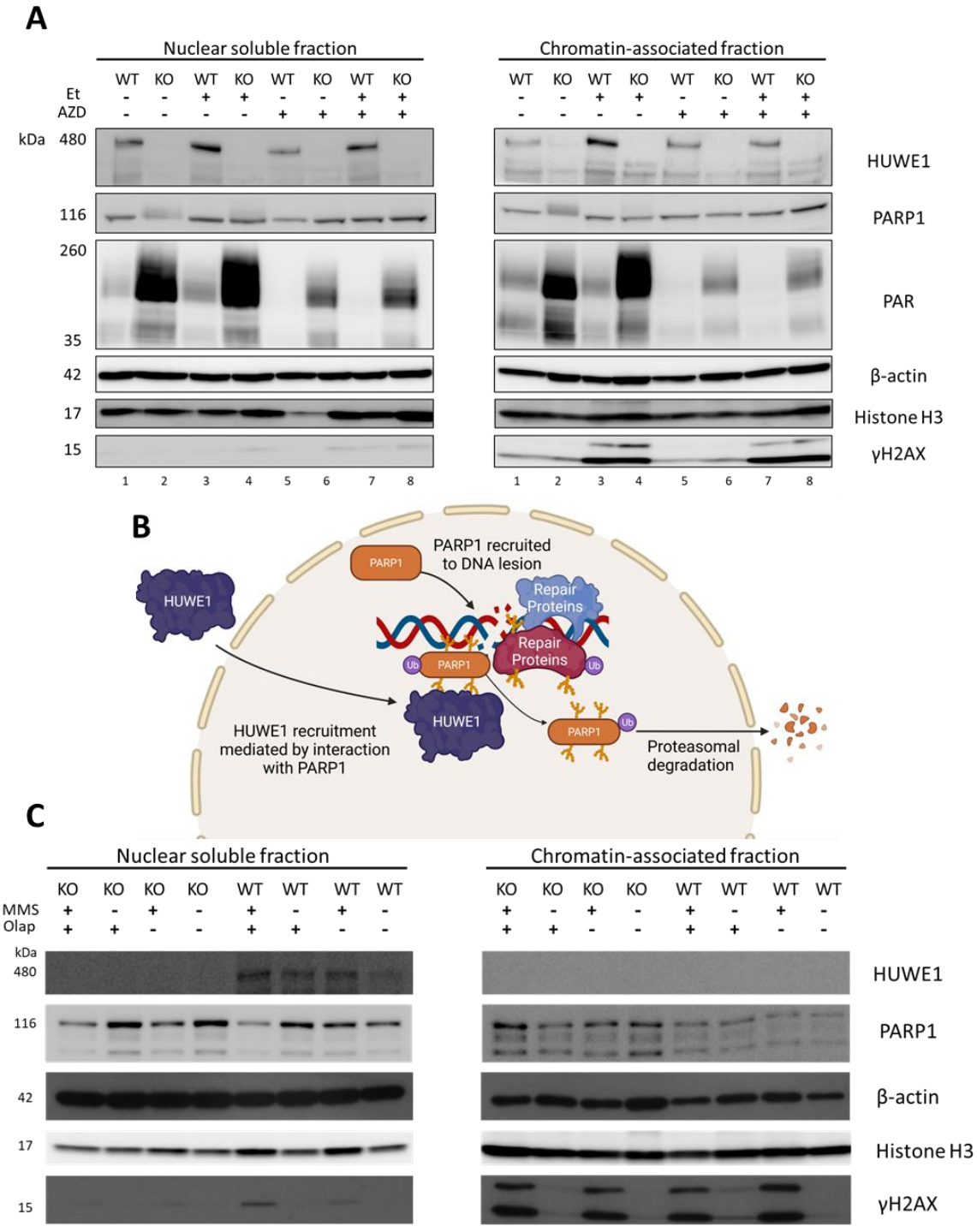

Figure 4-2: Chromatin-association of PARP1 and HUWE1 under DNA damage and PARP inhibition.

A) Western blot of MEF WT and HUWE1 KO cells treated with 10μM etoposide and 1μM AZD2461 for 2 hours. Subcellular fractionation performed with commercial kit as described. B) Model of possible HUWE1 and PAR/PARP1 interaction at sites of DNA damage. C) Western blot of MEF WT and HUWE1 KO cells treated with 0.2mM MMS and 50μM olaparib for 4 hours. Fractionation performed with modified method as described.

Chapter 5: Discussion and Future Directions

5.1 HUWE1's Role in DNA Damage Repair

While HUWE1 is known to play a role in DNA damage repair pathways, its precise function remains enigmatic, and there is conflicting information regarding its function (Fok et al., 2017; Gong et al., 2020; Kunz et al., 2020; Molkentine et al., 2022). Although HUWE1 has substrates associated with DNA repair, such as BRCA1 in HR and polymerase β in BER, the actual impact of HUWE1 loss on DNA damage outcomes in response to DNA damaging treatments remained to be fully explored (Kao et al., 2018; Wang et al., 2014). Therefore, it is imperative to gain a deeper understanding of HUWE1's function by investigating the DNA damage outcomes resulting from HUWE1 perturbation.

This study aimed to assess the impact of HUWE1 depletion on DNA damage repair at the cellular level. Multiple DNA damaging agents were used, with the intent of inducing different kinds of DNA lesions that would in turn necessitate the activation of different DNA damage repair pathways. Etoposide stimulates double strand breaks that are repaired primarily by the HR and NHEJ pathways of double strand break repair (Le et al., 2023; Tammaro et al., 2013). On the other hand, UV radiation causes multiple types of DNA lesions, most frequently pyrimidine dimers which are repaired by NER (Kciuk et al., 2020; Wang et al., 2022). MMS produces alkylated bases that primarily repaired by BER (Lundin et al., 2005; Nikolova et al., 2010). Cisplatin can induce intrastrand adducts that are repaired by NER, though other pathways such as DSB repair are also observed to be involved (Kiss et al., 2021). These treatments were selected to allow for an interrogation of the extent of HUWE1's role in DNA damage repair associated with a range of DNA lesions and repair pathways.

Alkaline comet assays in both MEF and OVCAR3 cells demonstrated that HUWE1 depletion consistently resulted in increased levels of DNA damage, both endogenously and in the

presence of the damaging agents. This implies that perturbing HUWE1 has a clear and significant impact on cellular genomic integrity in response to various exogenous stressors. Therefore, HUWE1 could be a critical factor in multiple DNA repair pathways. HUWE1 loss had previously been shown to result in an increase in endogenous DNA damage in multiple myeloma cells, which was supported by the findings in MEF and OVCAR3 cells presented in this study (Kunz et al., 2020). Furthermore, loss of HUWE1 was found to impede and slow down the repair process. These findings place HUWE1 as a key regulator of cellular DNA damage responses.

It is important to note that there are some reports of HUWE1 having opposing roles in different cellular contexts. For example, increased expression of HUWE1 has been associated with a decrease in HR in squamous cell carcinoma, and HUWE1 knockout was suggested to induce inappropriate or exaggerated activation of DNA repair in mouse spermatogonia cells (Fok et al., 2017; Molkentine et al., 2022). It is therefore likely that having either insufficient or excessive HUWE1 can dysregulate repair, or that the function of HUWE1 in repair is context specific. While the findings presented here were consistent across both MEF and OVCAR3 cell lines, indicating a robust impact of HUWE1 depletion on cellular levels of DNA damage, it remains important for future research to consider that there may be additional factors underlying the effect of HUWE1.

Different damaging agents were selected for this study to induce different kinds of DNA lesions and, by extension, to activate different repair pathways. However, some agents may induce damage that requires multiple pathways to repair. Additionally, the alkaline comet assay output reflects the amount of DNA damage present in the cell at a specific timepoint after treatment and cannot demonstrate the process of repair in a single set of cells. Therefore, to further untangle the role of HUWE1 in specific DNA damage repair pathways, it would be

beneficial for future studies to utilize DNA repair reporter assays in cells with HUWE1 depletion or overexpression (Nagel et al., 2014). In these assays, cells are transfected with a plasmid containing a fluorescent reporter gene with a defect that requires a specific repair pathway to resolve (Nagel et al., 2014). Expression of the reporter is therefore correlated to the ability of the cell to repair a specific type of damage (Nagel et al., 2014). By comparing expression of the fluorescent reporter cassette in these cells to WT cells, these assays would allow for a quantitative assessment of the impact of HUWE1 on various pathways of DNA damage repair and would allow tracking of the repair process at different time points in live cells (Nagel et al., 2014). These experiments would provide further insight into the impact of HUWE1 on the repair capability of specific pathways, and potentially into the importance of HUWE1 for early or prolonged responses to DNA damage.

5.2 HUWE1 Modulates Cellular Responsiveness to PARPi: Implications in Ovarian Cancer

Perturbation of HUWE1 was found to result in an increase in DNA damage in response to a variety of exogenous damaging agents. Some of these agents, such as etoposide and cisplatin, have been used as chemotherapeutics (Dasari & Tchounwou, 2014; Kongsawatvorakul et al., 2022). Cancer cells often have deficiencies in DNA damage repair pathways, resulting in an increased sensitivity to DNA damage that these therapies aim to exploit (Li et al., 2021; Moon et al., 2023; O'Connor 2015). PARPi, a newer class of anti-cancer drugs, also take advantage of these deficiencies by inhibiting PARP mediated DNA repair, along with trapping PARP1 at the site of DNA lesions to induce the accumulation of damage and cell death (Boussios et al., 2019; D'Andrea, 2018; Zhou et al., 2020).

To improve ovarian cancer therapies and combat the rise of resistance, the combination of PARPi with different chemotherapeutics is currently under study, with various studies and

clinical trials showing some benefit for patient outcomes (Beniey et al., 2023; Boussios et al., 2019). There are also ongoing efforts to identify additional factors that can enhance patient responsiveness to PARPi treatments (Beniey et al., 2023, Boussios et al., 2019; Onji & Murai., 2022; Sun et al., 2018). Identifying these factors is crucial for improving patient outcomes, as targeting them may allow for sensitization of cancer cells that would otherwise not respond to PARPi or reduce the risk of adverse events and resistance (Boussios et al., 2019; Sun et al., 2018). Since depletion of HUWE1 increases cellular DNA damage levels after damaging treatments, it was hypothesized that it may be one of these factors and enhance cell sensitivity to combination treatments of PARPi and chemotherapeutics.

Alkaline comet assays revealed that HUWE1 knockout MEF cells treated with etoposide and AZD2461 had significantly greater damage compared to cells treated with etoposide alone and to wild-type cells. Importantly, treatment with AZD2461 alone did not induce DNA damage compared to the vehicle control, indicating that the increase observed with dual treatment was due to a synergistic effect of the two drugs, rather than a simple additive effect. In the cell survival assays, HUWE1 depletion did not significantly alter survival in response to AZD2461 or etoposide alone but resulted in significantly decreased survival to combination treatment with both drugs, in agreement with the DNA damage findings. Since this suggested that HUWE1 depletion could improve PARPi responsiveness, OVCAR3 cells were used to validate the effect of HUWE1 loss in a more clinically relevant cell line. HUWE1 knockdown OVCAR3 cells similarly had increased DNA damage and decreased cell survival in response to treatment with PARPi and various DNA damaging agents. To further confirm the impact of HUWE1 on cell viability, HUWE1 knockout OVCAR3 cells were generated. Once again, these cells were significantly more sensitive to combination treatment with etoposide and AZD2461.

The mechanism underlying the increased susceptibility of cells with HUWE1 depletion to combination treatment with PARPi and damaging agents may be partially explained by the subcellular fractionation experiments. It was found that HUWE1 KO cells treated with both damaging agents and PARPi had greater chromatin association of PARP1, which is indicative of PARP trapping. Trapping is one of the proposed mechanisms underlying the effectiveness of PARPi, as trapping of inactivated PARP1 at the site of DNA lesions interferes with DNA repair and leads to an accumulation of DNA damage (Chaudhuri & Nussenzweig, 2017; D'Andrea, 2018; Zhou et al., 2020). It is important to note that this study also identified that depletion of HUWE1 induced greater levels of DNA damage in response to treatment with damaging agents alone and in combination with PARPi. It is therefore hypothesized that this increased damage in response to the damaging agent provides more damaged sites for PARP1 recruitment, which then results in greater trapping and further accumulation of DNA damage when PARPi are also present (Chaudhuri & Nussenzweig, 2017; Kamaletdinova et al., 2019).

The results of this study have evident implications in ovarian cancer therapies. First and foremost, the decreased survival of HUWE1 depleted cells to combination therapy with PARPi and chemotherapeutics suggests that HUWE1 may be a novel target for improving responsiveness to PARPi therapies. Targeting and inhibiting HUWE1 may improve the efficacy of PARPi treatment, and may also improve the potency of the treatment, lowering the required concentration of PARPi needed to achieve the desired response. Should this be the case, combination therapies could include HUWE1 inhibitors to reduce adverse effects and potentiate the desired effects of the anti-cancer drugs. Additionally, the increased DNA damage in HUWE1 depleted cancers may provide additional sensitivities. Since OVCAR3 cells are HGSOC cells with defective HR, future work should begin by characterizing the impact of HUWE1 depletion

in different cancer cells, to determine the influence of functional HR and other factors. Further, it would be beneficial to investigate the survival of ovarian cancer cells to PARPi in various combinations when HUWE1 is inhibited chemically with small molecule inhibitors (Kunz et al., 2020; Peter et al., 2014).

The second important aspect for ovarian cancer research is that HUWE1 status may be indicative of whether a patient will be responsive to PARPi. Future studies could examine the DNA or RNA sequence of cancer cells from cancer databases or patient-derived cells to determine if there is a correlation between HUWE1 expression and PARPi responsiveness. While the reports that HUWE1 can promote ovarian cancer progression suggest that this correlation may exist, the conflicting roles of HUWE1 demonstrated in other cancers indicate that there are likely additional factors that must be combined with HUWE1 status to accurately predict responsiveness (Podgorska et al., 2015; Yang et al., 2017). Genetic screens for genes that rescue or worsen the PARPi survival of HUWE1 depleted cells can provide some insight into what additional factors should be considered.

5.3 Novel Mechanisms of HUWE1 in DNA Damage Repair

The role of HUWE1 in DNA damage repair has been shown to be a complex and multifaceted one. Much remains to be understood regarding the specific functions of HUWE1 in different repair pathways and genetic contexts. To advance the current understanding of the impact of HUWE1 on DNA repair, this study investigated two possible mechanisms underlying the observed increases of DNA damage when HUWE1 is depleted.

5.3.1 HUWE1 Interacts with and Regulates PARP1

HUWE1 contains a WWE-domain, which is known to mediate interaction with PAR and PARylated proteins (Gatti et al., 2020; Hunkeler et al., 2021; Wang Z et al., 2012). PARP1 is a

key ADP-ribosylation enzyme, responsible for 80-90% of cellular PARylation in response to DNA damage. It also serves as a crucial early sensor of DNA damage repair and plays important roles in several DNA damage repair pathways (Chaudhuri & Nussenzweig, 2017; Kamaletdinova et al., 2019; Matta et al., 2020). Since this enzyme can self-PARylate, it was hypothesized that HUWE1 can interact with PARP1 and mediate its ubiquitination and proteasomal degradation.

Co-immunoprecipitation experiments were conducted in HEK293T cells to show that PARP1 is pulled down with HUWE1, thus confirming that these two proteins can interact. It is important to note that the addition of the PARPi PJ34 partially abrogated the pulldown, suggesting that the interaction between HUWE1 and PARP1 is dependent in part on PARylation, as would be expected from the WWE domain mediated interaction. It was also shown that depletion of HUWE1 resulted in increased PARP1 protein levels, supporting the hypothesis that the interaction of HUWE1 with PARP1 mediates PARP1 ubiquitination and degradation.

Previous work has found that PARylation can direct protein ubiquitination by several other E3 ligases (Ahmed et al., 2020; Gatti et al., 2020; Kang et al., 2011; Pellegrino & Altmeyer, 2016; Vivelo et al., 2019). For example, the E3 ligase RNF146 has been demonstrated to be a PAR-targeted E3 ligase, with various DNA damage repair substrates (Kang et al., 2011; Vivelo et al., 2019). RNF146, as well as the E3 ligases TRIP12 and DELTEX2, have also been shown to bind and interact with PARP1 in a PAR-dependent fashion (Ahmed et al., 2020; Gatti et al., 2020; Kang et al., 2011). The reduced pulldown of PARP1 with HUWE1 in the presence of PARPi suggests that HUWE1 may be another of these PAR-targeted ubiquitin ligases. It is also interesting to note that PARylation by PARP1 in response to DNA damage may promote interactions between HUWE1 and its DNA damage repair substrates, while also promoting negative feedback to dampen PARP1 signalling. It would be of interest for future investigations

to determine whether the interactions between HUWE1 and any of its other known substrates are dependent on PARylation, by assessing whether treatment with PARPi can abrogate their ubiquitination.

The subcellular fractionation experiments showed that HUWE1 KO resulted in increased PARP trapping when cells were treated with damaging agents and PARPi. Additionally, the chromatin association of HUWE1 was reduced in the presence of PARPi, suggesting that PARP1 or PARylation are required for efficient recruitment of HUWE1 to DNA lesions. This indicates that PARylation may be an important mechanism underlying HUWE1 recruitment to the DNA where it can interact with and ubiquitinate other DNA damage repair substrates (Kang et al., 2011). The dynamics of the HUWE1-PARP1 interaction and its impact on chromatin localization of both proteins therefore require further characterization. This could be examined by use of chromatin-immunoprecipitation and sequencing (ChIP-seq) experiments. These experiments could examine the colocalization of HUWE1 and PAR/PARP1 with DNA damage markers such as γH2AX (Seo et al., 2012). The WWE domain of HUWE1 would then be mutated to abolish PAR binding, and ChIP-seq conducted again to look for changes in the HUWE1 and PAR/PARP1 binding profiles. This would demonstrate the role of HUWE1 in PARP1 DNA-binding, as well as the role of PARP1 in HUWE1 localization. Ultimately, these future directions could bring to light another layer of complexity underlying the role of HUWE1 and PARP1/PAR in DNA damage repair.

5.3.2 An Exploration of HUWE1 Depletion and Histone Modifications

The role of HUWE1 in DNA damage repair has been shown to be a complex and multifaceted one. HUWE1 is a known histone ubiquitin ligase and has been demonstrated to have roles in DNA damage repair through its interaction with histones (Atsumi et al., 2015; Kao

et al., 2018; Liu et al., 2005; Mandemaker et al., 2017; Qi et al., 2022; Yang et al., 2017). Histone modification and regulation of chromatin compaction are intrinsically linked to DNA damage repair, and also associated with cancer when dysregulated (Kanherkar et al., 2014; Kaur et al., 2023). It is therefore of interest to further examine how HUWE1 depletion can affect histones and their modifications in response to DNA damaging insults. To accomplish this, an exploratory profiling of histones isolated from WT and HUWE1 KO MEF cells with and without DNA damage induction was conducted. Following 2 hour treatments with etoposide, histones were acid extracted and run on 15% SDS-PAGE gels. These gels were then transferred to membranes for western blot analysis using antibodies specific to a range of histones and histone modifications. Due to the preliminary and exploratory nature of this experiment, the profiling results are presented in the supplementary data.

HUWE1 KO cells were found to have a clear decrease in overall levels of acetyl-lysine (**Fig S-2A)**. This is likely due to the fact that HUWE1 interacts with and downregulates histone deacetylase 2 (HDAC2), one of the major globally expressed HDACs (Kao et al., 2018; Zhang et al., 2011). However, loss of acetylation at histone H3 lysine 9 (H3K9ac) and histone H4 lysine 8 (H4K8ac) were only observed under DNA damage (**Fig S-2A**). Both these modifications are associated with open or active chromatin and have been linked to DNA damage repair pathways (Bergmann et al., 2012; Dhar et al., 2017; Meyer et al., 2016; Switonski et al., 2021; Wang et al., 2008). These findings suggest a DNA-damage specific role for HUWE1 in modulating acetylation of histones H3 and H4.

When profiling core histones, a modified H2A band near 35kDa was lost in HUWE1 KO cells, while a modified H2A band near 25kDa appears to be lost only when DNA damage is induced (**Fig S-2B**). The loss of this 25kDa band is potentially due to the role of HUWE1 in

monoubiquitinating H2A to recruit RNF8 during DSB repair (Mandemaker et al., 2017). Surprisingly, the levels of γH2AX, a known DNA damage marker, appeared to be reduced in HUWE1 KO cells (Seo et al., 2012). This was unexpected, since HUWE1 KO cells have been shown to have increased damage and HUWE1 is known to mediate degradation of H2AX, and thus this observation requires further validation (Atsumi et al., 2015). HUWE1 KO cells also had slight increases in overall histone H3 (**Fig S-2B**).

Interestingly, a clear increase in histone H3 trimethylation at lysine 9 (H3K9me3) in HUWE1 KO cells was observed in a separate chromatin fractionation experiment (**Fig S-2C**). H3K9me3, while typically associated with a repressed chromatin state, acts as a signal for recruitment of factors that initiate double strand break repair (Nicetto & Zaret, 2019; Williamson et al., 2012). As part of this process, histone H3 and H4 get acetylated at various residues (Williamson et al., 2012). The observations presented here thus suggest that HUWE1 depletion could interfere with the normal function of this epigenetic DNA repair mechanism by dysregulating the balance between H3K9me3 and H3K9ac/H4K8ac. This preliminary study has therefore indicated additional roles for HUWE1 in DNA damage repair via modulation of the histone code that require additional investigation.

5.4 Limitations and Final Remarks

The results of this study have provided novel insight into the impact of HUWE1 on DNA repair and cellular DNA damage outcomes, with important implications for ovarian cancer therapy. However, these results have only scratched the surface of the complex systems underlying the functions of HUWE1 and its clinical relevance. Given that HUWE1 has been known to have opposing functions in different contexts, it is of particular importance for future work to clarify what factors determine the switch of HUWE1 from promoting to suppressing

DNA damage repair, or from promoting to suppressing tumorigenesis. This is essential for contextualizing the findings presented here, and for clarifying the clinical viability of targeting HUWE1 for improving cancer therapies.

This study translated results from MEF cells to OVCAR3 cells with the intent of achieving greater clinical relevancy. While OVCAR3 cells are an ovarian cancer cell line that allowed for an interrogation of whether HUWE1 could similarly impact ovarian cancer cells, the fact remains that all the results presented here rely on cell models. This is the basis of much essential preclinical research, but cell models evidently do not capture the full complexity of an organism or even of cancer biology, and thus may not be predictive of clinical outcomes (Maenhoudt et al., 2020). Future work should therefore consider the use of patient-derived xenograft or organoid models to better capture the impact of HUWE1 depletion or inhibition on ovarian cancer responsiveness to PARPi (Liu et al., 2020; Maenhoudt et al., 2020; Witte et al., 2020).

The research presented here has demonstrated that HUWE1 plays a crucial role in the maintenance of genome integrity. It has shown that depletion of HUWE1 leads to impaired DNA repair responses and increases in cellular DNA lesions both endogenously and in response to exogenous induction of DNA damage. Furthermore, the study identified a novel regulatory axis between HUWE1 and PARP1 which may be important for modulation of various DNA damage repair pathways. Moreover, HUWE1 has been identified as a modulator of cellular responsiveness to PARPi in OVCAR3 cells, which has significant implications for ovarian cancer therapy. This study has thus provided early evidence that targeting HUWE1 may be a viable therapeutic approach for ameliorating patient responses to PARPi, and that HUWE1 expression could be indicative of cancer sensitivity to PARPi therapies.

References

Ahmed SF, Buetow L, Gabrielsen M, Lilla S, Chatrin C et al. **2020**. DELTEX2 C-terminal domain recognizes and recruits ADP-ribosylated proteins for ubiquitination *Sci Adv* 6(34): eabc0629. https://doi.org/10.1126/sciadv.abc0629

Alemasova EE & Lavrik OI. **2019**. Poly(ADP-ribosyl)ation by PARP1: reaction mechanism and regulatory proteins. *Nucleic Acids Res* 47(8): 3811-3827. https://doi.org/10.1093/nar/gkz120

Almeida KH & Sobol RW. **2007**. A unified view of base excision repair: lesion-dependent protein complexes regulated by post-translational modification. *DNA Repair* 6(6): 695-711. https://doi.org/10.1016/j.dnarep.2007.01.009

Aravind L. **2001**. The WWE domain: a common interaction module in protein ubiquitination and ADP ribosylation. *Trends Biochem Sci* 26(5): 273-275. https://doi.org/10.1016/s0968-0004(01)01787-x

Atsumi Y, Minakawa Y, Ono M, Dobashi S, Shinohe K et al. **2015**. ATM and SIRT6/SNF2H Mediate Transient H2AX Stabilization When DSBs Form by Blocking HUWE1 to Allow Efficient γH2AX Foci Formation. *Cell Rep* 13(12): 2728-2740. https://doi.org/10.1016/j.celrep.2015.11.054

Bachiller S, Alonso-Bellido IM, Real LM, Pérez-Villegas EM, Venero JL et al. **2020**. The Ubiquitin Proteasome System in Neuromuscular Disorders: Moving Beyond Movement. *Int J Mol Sci* 21(17): 6429. https://doi.org/10.3390/ijms21176429

Bakr A, Oing C, Köcher S, Borgmann K, Dornreiter I et al. **2015**. Involvement of ATM in homologous recombination after end resection and RAD51 nucleofilament formation. *Nucleic Acids Res* 43(6): 3154-3166. https://doi.org/10.1093/nar/gkv160

Beniey M, Hubert A, Haque T, Cotte AK, Béchir N et al. **2023.** Sequential targeting of PARP with carboplatin inhibits primary tumour growth and distant metastasis in triple-negative breast cancer. *Br J Cancer* 128(10): 1964-1975. https://doi.org/10.1038/s41416-023-02226-w

Bergmann JH, Jakubsche JN, Martins NM, Kagansky A, Nakano M et al. **2012**. Epigenetic engineering: histone H3K9 acetylation is compatible with kinetochore structure and function. *J Cell Sci* 125(Pt 2): 411-421. https://doi.org/10.1242/jcs.090639

Boussios S, Karihtala P, Moschetta M, Karathanasi A, Sadauskaite A et al. **2019**. Combined Strategies with Poly (ADP-Ribose) Polymerase (PARP) Inhibitors for the Treatment of Ovarian Cancer: A Literature Review. *Diagnostics* 9(3): 87. https://doi.org/10.3390/diagnostics9030087

Bowtell DD, Böhm S, Ahmed AA, Aspuria P, Bast Jr RC et al. **2015**. Rethinking ovarian cancer II: reducing mortality from high-grade serous ovarian cancer. *Nat Rev Cancer* 15(11): 668-679. https://doi.org/10.1038/nrc4019

Bradbury A, O'Donnell R, Drew Y, Curtin NJ & Saha SS. **2020**. Characterisation of Ovarian Cancer Cell Line NIH-OVCAR3 and Implications of Genomic, Transcriptomic, Proteomic and Functional DNA Damage Response Biomarkers for Therapeutic Targeting. *Cancers* 12(7): 1939. https://doi.org/10.3390/cancers12071939

Bradley D. **2022**. The evolution of post-translational modifications. *Curr Opin Genet Dev* 76: 101956. https://doi.org/10.1016/j.gde.2022.101956

Braithwaite EK, Prasad R, Shock DD, Hou EW, Beard WA et al. **2005**. DNA polymerase lambda mediates a back-up base excision repair activity in extracts of mouse embryonic fibroblasts. *J Biol Chem* 280(18): 18469-18475. https://doi.org/10.1074/jbc.M411864200

Bryant HE, Schultz N, Thomas HD, Parker KM, Flower D et al. **2005**. Specific killing of BRCA2-deficient tumours with inhibitors of poly(ADP-ribose) polymerase. *Nature* 434: 913-917. https://doi.org/10.1038/nature03443

Ceccaldi R, Rondinelli B & D'Andrea AD. **2016**. Repair Pathway Choices and Consequences at the Double-Strand Break. *Trends Cell Biol* 26(1): 52-64. https://doi.org/10.1016/j.tcb.2015.07.009

Chang HHY, Pannunzio NR, Adachi N & Lieber MR. **2017**. Non-homologous DNA end joining and alternative pathways to double-strand break repair. *Nat Rev Mol Cell Biol* 18(8): 495-506. https://doi.org/ 10.1038/nrm.2017.48

Chatterjee N & Walker GC. **2017**. Mechanisms of DNA damage, repair, and mutagenesis. *Environ Mol Mutagen* 58(5): 235-263. https://doi.org/10.1002/em.22087

Chaudhuri AR & Nussenzweig A. **2017**. The multifaceted roles of PARP1 in DNA repair and chromatin remodelling. *Nat Rev Mol Cell Biol* 18(10): 610-621. https://doi.org/10.1038/nrm.2017.53

Choe KN, Nicolae CM, Constantin D, Kawasawa YI, Delgado-Diaz MR et al. **2016**. HUWE1 interacts with PCNA to alleviate replication stress. *EMBO Rep* 17(6): 874-886. https://doi.org/10.15252/embr.201541685

Christie EL & Bowtell DDL. **2017**. Acquired chemotherapy resistance in ovarian cancer. *Ann Oncol* 28 (suppl 8): viii13-viii15. https://doi.org/10.1093/annonc/mdx446

Ciccia A & Elledge SJ. **2010**. The DNA damage response: making it safe to play with knives. *Mol Cell* 40(2): 179-204. https://doi.org/10.1016/j.molcel.2010.09.019

Cokol M, Chua HN, Tasan M, Mutlu B, Weinstein ZB et al. **2011**. Systematic exploration of synergistic drug pairs. *Mol Syst Biol* 7: 544. https://doi.org/10.1038/msb.2011.71

Crawford LJ, Campbell DC, Morgan JJ, Lawson MA, Down JM et al. **2020**. The E3 ligase HUWE1 inhibition as a therapeutic strategy to target MYC in multiple myeloma. *Oncogene* 39(27): 5001-5014. https://doi.org/10.1038/s41388-020-1345-x

Cuijk L, Belle GJ, Turkyilmaz Y, Poulsen SL, Janssens RC et al. **2015**. SUMO and ubiquitin-dependent XPC exchange drives nucleotide excision repair. *Nature Communications* 6: 7499. https://doi.org/10.1038/ncomms8499

Czarny P, Bialek K, Ziolkowska S, Strycharz J & Sliwinski T. **2020**. DNA damage and repair in neuropsychiatric disorders. What do we know and what are the future perspectives? *Mutagenesis* 35(1): 79-106. https://doi.org/10.1093/mutage/gez035

D'Andrea AD. **2018**. Mechanisms of PARP inhibitor sensitivity and resistance. *DNA Repair* 71: 172-176. https://doi.org/10.1016/j.dnarep.2018.08.021

Dantuma NP & van Attikum H. **2016**. Spatiotemporal regulation of posttranslational modifications in the DNA damage response. *EMBO J* 35(1): 6-23. https://doi.org/10.15252/embj.201592595

Dantzer F, de La Rubia G, Murcia JM, Hostomsky Z, de Murcia G et al. **2000**. Base excision repair is impaired in mammalian cells lacking Poly(ADP-ribose) polymerase-1. *Biochemistry* 39(25): 7559-7569. https://doi.org/10.1021/bi0003442

Dasari S & Tchounwou PB. **2014**. Cisplatin in cancer therapy: molecular mechanisms of action. *Eur J Pharmacol* 740: 364-378. https://doi.org/10.1016/j.ejphar.2014.07.025

De Almeida LC, Calil FA, Machado-Neto JA & Costa-Lotufo LV. **2021**. DNA damaging agents and DNA repair: From carcinogenesis to cancer therapy. *Cancer Genet* 252-253: 6-24. https://doi.org/10.1016/j.cancergen.2020.12.002

Dhar S, Gursoy-Yuzugullu O, Parasuram R & Price BD. **2017**. The tale of a tail: histone H4

acetylation and the repair of DNA breaks. *Philos Trans R Soc Lond Biol Sci* 371(1731): 20160284. https://doi.org/10.1098/rstb.2016.0284

Dianov GL & Hübscher U. **2013**. Mammalian base excision repair: the forgotten archangel. *Nucleic Acids Res* 41(6): 3483-3490. https://doi.org/10.1093/nar/gkt076

Farmer H, McCabe N, Lord CJ, Tutt ANJ, Johnson DA et al. **2005**. Targeting the DNA repair defect in BRCA mutant cells as a therapeutic strategy. *Nature* 434: 917-921. https://doi.org/10.1038/nature03445

Ferlay J, Soerjomataram I, Dikshit R, Eser S, Mathers C et al. **2015**. Cancer incidence and mortality worldwide: sources, methods and major patterns in GLOBOCAN 2012. *Int J Cancer* 136(5): E359-386. https://doi.org/10.1002/ijc.29210

Fishel R. **2015**. Mismatch repair. *J Biol Chem* 290(44): 26395-26403. https://doi.org/10.1074/jbc.R115.660142

Fok KL, Bose R, Sheng K, Chang C, Katz-Egorov M et al. **2017**. Huwe1 Regulates the Establishment and Maintenance of Spermatogonia by Suppressing DNA Damage Response. *Endocrinology* 158(11): 4000-4016. https://doi.org/10.1210/en.2017-00396

Foo T, George A & Banerjee S. **2021**. PARP inhibitors in ovarian cancer: An overview of the practice-changing trials. *Genes Chromosomes Cancer* 60(5): 385-397. https://doi.org/10.1002/gcc.22935

Gatti M, Imhof R, Huang Q, Baudis M, & Altmeyer M. **2020**. The Ubiquitin Ligase TRIP12 Limits PARP1 Trapping and Constrains PARP Inhibitor Efficiency. *Cell Rep* 32(5): 107985. https://doi.org/10.1016/j.celrep.2020.107985

Gatti M, Pinato S, Maiolica A, Rocchio F, Prato MG et al. **2015**. RNF168 promotes noncanonical

K27 ubiquitination to signal DNA damage. *Cell Rep* 10(2) : 226-238. https://doi.org/10.1016/j.celrep.2014.12.021

Gong X, Du D, Deng Y, Zhou Y, Sun L et al. **2020**. The structure and regulation of the E3 ubiquitin ligase HUWE1 and its biological functions in cancer. *Invest New Drugs* 38(2): 515-524. https://doi.org/10.1007/s10637-020-00894-6

Graham TGW, Walter JC & Loparo JJ. **2016**. Two-Stage Synapsis of DNA Ends during Non-homologous End Joining. *Mol Cell* 61(6): 850-858. https://doi.org/10.1016/j.molcel.2016.02.010

Groslambert J, Prokhorova E & Ahel I. **2021**. ADP-ribosylation of DNA and RNA. *DNA Repair* 105 : 103144. https://doi.org/10.1016/j.dnarep.2021.103144

Guibbal F, Hopkins SL, Pacelli A, Isenegger PG, Mosley M et al. **2020**. [^{18}F]AZD2461, an Insight on Difference in PARP Binding Profiles for DNA Damage Response PET Imaging. *Mol Imaging Biol* 22(5): 1226-1234. https://doi.org/10.1007/s11307-020-01497-6

Guirouilh-Barbat J, Lambert S, Bertrand P & Lopez BS. **2014**. Is homologous recombination really an error-free process? *Front Genet* 5: 175. https://doi.org/10.3389/fgene.2014.00175

Guo Z, Wang S, Xie Y, Han Y, Hu S et al. **2020**. HUWE1-dependent DNA-PKcs neddylation modulates its autophosphorylation in DNA damage response. *Cell Death Discov* 11(5): 400. https://doi.org/10.1038/s41419-020-2611-0

Gyori BM, Venkatachalam G, Thiagarajan PS, Hsu D & Clement M. **2014**. OpenComet: an automated tool for comet assay image analysis. *Redox Biol* 2: 457-465. https://doi.org/10.1016/j.redox.2013.12.020

Haince J, McDonald D, Rodrigue A, Déry U, Masson J et al. **2008**. PARP1-dependent kinetics of recruitment of MRE11 and NBS1 proteins to multiple DNA damage sites. *J Biol Chem* 283(2): 1197-1208. https://doi.org/10.1074/jbc.M706734200

Hakem R. **2008**. DNA-damage repair; the good, the bad, and the ugly. *EMBO J* 27(4): 589-605. https://doi.org/10.1038/emboj.2008.15

Hanzlikova H, Gittens W, Krejcikova K, Zeng Z & Caldecott KW. **2017**. Overlapping roles for PARP1 and PARP2 in the recruitment of endogenous XRCC1 and PNKP into oxidized chromatin. *Nucleic Acids Res* 45(5): 2546-2557https://doi.org/10.1093/nar/gkw1246

Hochegger H, Dejsuphong D, Fukushima T, Morrison C, Sonoda E et al. **2006**. Parp-1 promotes homologous recombination from interference by Ku and Ligase IV in vertebrate cells. *EMBO J* 25(6): 1305-1314. https://doi.org/10.1038/sj.emboj.7601015

Hopkins TA, Shi Y, Rodriguez LE, Solomon LR, Donawho CK et al. **2015**. Mechanistic Dissection of PARP1 Trapping and the Impact on In Vivo Tolerability and Efficacy of PARP Inhibitors. *Mol Cancer Res* 13(11): 1465-1477. https://doi.org/10.1158/1541-7786.MCR-15-0191-T

Hosoya N & Miyagawa K. **2014**. Targeting DNA damage response in cancer therapy. *Cancer Sci* 105(4): 370-388. https://doi.org/ 10.1111/cas.12366

Hu Y, Petit SA, Ficarro SB, Toomire KJ, Xie A et al. **2014**. PARP1-driven poly-ADP-ribosylation regulates BRCA1 function in homologous recombination-mediated DNA repair. *Cancer Discov* 4(12): 1430-1447. https://doi.org/10.1158/2159-8290.CD-13-0891

Huang D & Kraus WL. **2022**. The expanding universe of PARP1-mediated molecular and therapeutic mechanisms. *Mol Cell* 82(12): 2315-2334. https://doi.org/10.1016/j.molcel.2022.02.021

Huang R & Zhou P. **2021**. DNA damage repair: historical perspectives, mechanistic pathways and clinical translation for targeted cancer therapy. *Signal Transduct Target Ther* 6(1): 254. https://doi.org/10.1038/s41392-021-00648-7

Huang TT & D'Andrea AD. **2006**. Regulation of DNA repair by ubiquitylation. *Nat Rev Mol Cell Biol* 7(5) : 323-334. https://doi.org/10.1038/nrm1908

Hunkeler M, Jin CY, Ma MW, Monda JK, Overwijn D et al. **2021**. Solenoid architecture of HUWE1 contributes to ligase activity and substrate recognition. *Mol Cell* 81(17): 3468-3480.e7. https://doi.org/10.1016/j.molcel.2021.06.032

Ianevski A, Giri AK & Tero Aittokallio. **2020**. SynergyFinder 2.0: visual analytics of multi-drug combination synergies. *Nucleic Acids Res* 48(W1): W488-W493. https://doi.org/10.1093/nar/gkaa216

Ianevski A, He L, Aittokallio T & Tang J. **2017**. SynergyFinder: a web application for analyzing drug combination dose-response matrix data. *Bioinformatics* 33(15): 2413-2415. https://doi.org/10.1093/bioinformatics/btx162

Ignatov AV, Bondarenko KA & Makarova AV. **2017**. Non-bulky Lesions in Human DNA: the Ways of Formation, Repair, and Replication. *Acta Naturae* 9(3): 12-26.

Inoue S, Hao Z, Elia AJ, Cescon D, Zhou L et al. **2013**. Mule/Huwe1/Arf-BP1 suppresses Ras-driven tumorigenesis by preventing c-Myc/Miz1-mediated down-regulation of p21 and p15. *Genes Dev* 27(10): 1101-1114. https://doi.org/10.1101/gad.214577.113

Jackson SP & Bartek J. **2009**. The DNA-damage response in human biology and disease. *Nature* 461(7267): 1071-1078. https://doi.org/10.1038/nature08467

Ji Y, Karbaschi M, Abdulwahed A, Quinete NS, Evans MD et al. **2022**. A High-Throughput

Comet Assay Approach for Assessing Cellular DNA Damage. *J Vis Exp* (183): 10.3791/63559. https://doi.org/10.3791/63559

Jungmichel S, Rosenthal F, Altmeyer M, Lukas J, Hottiger MO et al. **2013**. Proteome-wide identification of poly(ADP-Ribosyl)ation targets in different genotoxic stress responses. *Mol Cell* 52(2): 272-285. https://doi.org/10.1016/j.molcel.2013.08.026

Kamaletdinova T, Fanaei-Kahrani Z & Wang Z. **2019**. The Enigmatic Function of PARP1: From PARylation Activity to PAR Readers. *Cells* 8(12): 1625. https://doi.org/10.3390/cells8121625

Kang HC, Lee Y, Shin J, Andrabi SA, Chi Z et al. **2011**. Iduna is a poly(ADP-ribose) (PAR)-dependent E3 ubiquitin ligase that regulates DNA damage. *Proc Natl Acad Sci USA* 108(34): 14103-14108. https://doi.org/10.1073/pnas.1108799108

Kang M, Park S, Park S, Lee HG & Park JH. **2022**. A Double-Edged Sword: The Two Faces of PARylation. *Int J Mol Sci* 23(17): 9826. https://doi.org/10.3390/ijms23179826

Kanherkar RR, Bhatia-Dey N & Csoka AB. **2014**. Epigenetics across the human lifespan. *Front Cell Dev Biol* 2: 49. https://doi.org/10.3389/fcell.2014.00049

Kao S, Wu H & Wu K. **2018**. Ubiquitination by HUWE1 in tumorigenesis and beyond. *J Biomed Sci* 25(1): 67. https://doi.org/10.1186/s12929-018-0470-0

Kaur P, Verma S, Kushwaha PP & Gupta S. **2023**. EZH2 and NF-κB: A context-dependent crosstalk and transcriptional regulation in cancer. *Cancer Lett* 560: 216143. https://doi.org/10.1016/j.canlet.2023.216143

Kciuk M, Marciniak B, Mojzych M & Kontek R. **2020**. Focus on UV-Induced DNA Damage and Repair-Disease Relevance and Protective Strategies. *Int J Mol Sci* 21(19): 7264. https://doi.org/10.3390/ijms21197264

Keung MYT, Wu Y & Vadgama JV. **2019**. PARP Inhibitors as a Therapeutic Agent for Homologous Recombination Deficiency in Breast Cancers. *J Clin Med* 8(4): 435. https://doi.org/10.3390/jcm8040435

Khan KA, Ng MK & Cheung, P. **2020**. The Use of Mononucleosome Immunoprecipitation for Analysis of Combinatorial Histone Post-translational Modifications and Purification of Nucleosome-Interacting Proteins. *Front Cell Dev Biol* 8 : 331. https://doi.org/10.3389/fcell.2020.00331

Kim S, Han Y, Kim SI, Kim H, Kim SJ et al. **2018**. Tumor evolution and chemoresistance in ovarian cancer. *NPJ Precis Oncol* 2: 20. https://doi.org/10.1038/s41698-018-0063-0

Kiss RC, Xia F & Acklin S. **2021**. Targeting DNA Damage Response and Repair to Enhance Therapeutic Index in Cisplatin-Based Cancer Treatment. *Int J Mol Sci* 22(15): 8199. https://doi.org/10.3390/ijms22158199

Kongsawatvorakul C, Charakorn C, Chittithaworn S & Lertkhachonsuk A. **2022**. Effectiveness of oral etoposide in recurrent or refractory epithelial ovarian cancer, primary peritoneal cancer and fallopian tube cancer. *J Obstet Gynaecol* 42(6): 2331-2335. https://doi.org/10.1080/01443615.2022.2049724

Koo S, Park E, Noh H, Jo S, Ko B et al. **2023**. Ubiquitination Links DNA Damage and Repair Signaling to Cancer Metabolism. *Int J Mol Sci* 24(9): 8441. https://doi.org/10.3390/ijms24098441

Kunz V, Bommert KS, Kruk J, Schwimming D, Chatterjee M et al. **2020**. Targeting of the E3 ubiquitin-protein ligase HUWE1 impairs DNA repair capacity and tumor growth in preclinical multiple myeloma models. *Sci Rep* 10(1): 18419. https://doi.org/10.1038/s41598-020-75499-3

Kwon YT & Ciechanover A. **2017**. The Ubiquitin Code in the Ubiquitin-Proteasome System and Autophagy. *Trends Biochem Sci* 42(11): 873-886. https://doi.org/10.1016/j.tibs.2017.09.002

Le TT, Wu M, Lee JH, Bhatt N, Inman JT et al. **2023**. Etoposide promotes DNA loop trapping and barrier formation by topoisomerase II. *Nat Chem Biol* 19(5): 641-650. https://doi.org/10.1038/s41589-022-01235-9

Lee BL, Anamika, Glover JNM, Hendzel MJ & Spyracopoulos L. **2017**. Molecular basis for K63-linked ubiquitination processes in double-strand DNA break repair: A focus on kinetics and dynamics. *J Mol Biol* 429(22): 3409-3429. https://doi.org/ 10.1016/j.jmb.2017.05.029

Lheureux S, Gourley C, Vergote I, Oza AM. **2019**. Epithelial ovarian cancer. *Lancet* 393(10177): 1240-1253. https://doi.org/10.1016/S0140-6736(18)32552-2

Li J, Sun H, Huang Y, Wang Y, Liu Y et al. **2019**. Pathways and assays for DNA double-strand break repair by homologous recombination. *Acta Biochim Biophys Sin (Shanghai)* 51(9): 879-889. https://doi.org/10.1093/abbs/gmz076

Li L, Guan Y, Chen X, Yang J & Cheng Y. **2021**. DNA Repair Pathways in Cancer Therapy and Resistance. *Front Pharmacol* 11: 629266. https://doi.org/10.3389/fphar.2020.629266

Li M & Yu X. **2013**. Function of BRCA1 in the DNA damage response is mediated by ADP-ribosylation. *Cancer Cell* 23(5): 693-704. https://doi.org/10.1016/j.ccr.2013.03.025

Lisio M, Fu L, Goyeneche A, Gao Z & Telleria C. **2019**. High-Grade Serous Ovarian Cancer: Basic Sciences, Clinical and Therapeutic Standpoints. *Int J Mol Sci* 20(4): 952. https://doi.org/10.3390/ijms20040952

Liu C, Vyas A, Kassab MA, Singh AK & Yu X. **2017**. The role of poly ADP-ribosylation in the

first wave of DNA damage response. *Nucleic Acids Res* 45(14): 8129-8141. https://doi.org/10.1093/nar/gkx565

Liu D, Keijzers G & Rasmussen LJ. **2017**. DNA mismatch repair and its many roles in eukaryotic cells. *Mutat Res Rev Mutat Res* 773 : 174-187. https://doi.org/10.1016/j.mrrev.2017.07.001

Liu HD, Xia BR, Jin MZ & Lou G. **2020**. Organoid of ovarian cancer: genomic analysis and drug screening. *Clin Transl Oncol* 22(8): 1240-1251. https://doi.org/10.1007/s12094-019-02276-8

Liu Z, Oughtred R & Wing SS. **2005**. Characterization of $E3^{histone}$, a Novel Testis Ubiquitin Protein Ligase Which Ubiquitinates Histones. *Mol Cell Biol* 25(7): 2819-2831. https://doi.org/10.1128/MCB.25.7.2819-2831.2005

Lord CJ & Ashworth A. **2017**. PARP inhibitors: Synthetic lethality in the clinic. *Science* 355(6330): 1152-1158. https://doi.org/10.1126/science.aam7344

Lundin C, North M, Erixon K, Walters K, Jenssen D et al. **2005**. Methyl methanesulfonate (MMS) produces heat-labile DNA damage but no detectable in vivo DNA double-strand breaks. *Nucleic Acids Res* 33(12): 3799-3811. https://doi.org/10.1093/nar/gki681

Maenhoudt N, Defraye C, Boretto M, Jan Z, Heremans R et al. **2020**. Developing Organoids from Ovarian Cancer as Experimental and Preclinical Models. *Stem Cell Rep* 14(4): 717-729. https://doi.org/10.1016/j.stemcr.2020.03.004

Mandemaker IK, van Cuijk L, Janssens RC, Lans H, Bezstarosti et al. **2017**. DNA damage-induced histone H1 ubiquitylation is mediated by HUWE1 and stimulates the RNF8-RNF168 pathway. *Sci Rep* 7(1): 15353. https://doi.org/10.1038/s41598-017-15194-y

Markkanen E, van Loon B, Ferrari E, Parsons JL, Dianov GL et al. **2012**. Regulation of oxidative

DNA damage repair by DNA polymerase λ and MutYH by cross-talk of phosphorylation and ubiquitination. *Proc Natl Acad Sci USA* 109(2): 437-442. https://doi.org/10.1073/pnas.1110449109

Marteijn JA, Lans H, Vermeulen W & Hoeijmakers JH. **2014**. Understanding nucleotide excision repair and its roles in cancer and ageing. *Nat Rev Mol Cell Biol* 15(7): 465-481. https://doi.org/10.1038/nrm3822

Matta E, Kiribayeva A, Khassenov B, Matkarimov BT & Ishchenko AA. **2020**. Insight into DNA substrate specificity of PARP1-catalysed DNA poly(ADP-ribosyl)ation. *Sci Rep* 10(1): 3699. https://doi.org/10.1038/s41598-020-60631-0

Matulonis UA, Sood AK, Fallowfield L, Howitt BE, Sehouli J et al. **2016**. Ovarian cancer. *Nat Rev Dis Primers* 2: 16061. https://doi.org/10.1038/nrdp.2016.61

Meyer B, Fabbrizi MR, Raj S, Zobel CL, Hallahan DE et al. **2016**. Histone H3 Lysine 9 Acetylation Obstructs ATM Activation and Promotes Ionizing Radiation Sensitivity in Normal Stem Cells. *Stem Cell Rep* 7(6): 1013-1022. https://doi.org/10.1016/j.stemcr.2016.11.004

Mikolaskova B, Jurcik M, Cipakova I, Kretova M, Chovanec M et al. **2018**. Maintenance of genome stability: the unifying role of interconnections between the DNA damage response and RNA-processing pathways. *Curr Genet* 64(5): 971-983. https://doi.org/10.1007/s00294-018-0819-7

Miller RE, El-Shakankery KH & Lee J. **2022**. PARP inhibitors in ovarian cancer: overcoming resistance with combination strategies. *J Gynecol Oncol* 33(3): e44. https://doi.org/10.3802/jgo.2022.33.e44

Mirza MR, Coleman RL, González-Martin A, Moore KN, Colombo N et al. **2020**. The forefront

of ovarian cancer therapy: update on PARP inhibitors. *Ann Oncol* 31(9):1148-1159. https://doi.org/10.1016/j.annonc.2020.06.004

Molkentine DP, Molkentine JM, Bridges KA, Valdecanas DR, Dhawan A et al. **2022**. p16 Represses DNA Damage Repair via a Novel Ubiquitin-Dependent Signaling Cascade. *Cancer Res* 82(5): 916-928. https://doi.org/10.1158/0008-5472.CAN-21-2101

Moon J, Kitty I, Renata K, Qin S, Zhao F et al. **2023**. DNA Damage and Its Role in Cancer Therapeutics. *Int J Mol Sci* 24(5): 4741. https://doi.org/10.3390/ijms24054741

Moortgat S, Berland S, Aukrust I, Maystadt I, Baker L. **2018**. HUWE1 variants cause dominant X-linked intellectual disability: a clinical study of 21 patients. *Eur J Hum Genet* 26(1): 64-74. https://doi.org/10.1038/s41431-017-0038-6

Muthurajan UM, Hepler MRD, Hieb AR, Clark NJ, Kramer M et al. **2014**. Automodification switches PARP-1 function from chromatin architectural protein to histone chaperone. *Proc Natl Acad Sci USA* 111(35) : 12752-12757. https://doi.org/10.1073/pnas.1405005111

Murai J, Huang SN, Das BB, Renaud A, Zhang Y et al. **2012**. Trapping of PARP1 and PARP2 by Clinical PARP Inhibitors. *Cancer Res* 72(21): 5588-5599. https://doi.org/10.1158/0008-5472.CAN-12-2753

Myant KB, Cammareri P, Hodder MC, Wills J, Kriegsheim AV et al. **2017**. HUWE1 is a critical colonic tumour suppressor gene that prevents MYC signalling, DNA damage accumulation and tumour initiation. *EMBO Mol Med* 9(2): 181-197. https://doi.org/10.15252/emmm.201606684

Nagel ZD, Margulies CM, Chaim IA, McRee SK, Mazzucato P et al. **2014**. Multiplexed DNA

repair assays for multiple lesions and multiple doses via transcription inhibition and transcriptional mutagenesis. *Proc Natl Acad Sci USA* 111(18): E1823-1832. https://doi.org/10.1073/pnas.1401182111

Nandhakumar S, Parasuraman S, Shanmugam MM, Ramachandra RK, Chand P & Bhat BV. **2011**. Evaluation of DNA damage using single-cell gel electrophoresis (Comet Assay). *J Pharmacol Pharmacotherm* 2(2): 107-111. https://doi.org/10.4103/0976-500X.81903

Ngo LP, Owiti NA, Swartz C, Winters J, Su Y et al. **2020**. Sensitive CometChip assay for screening potentially carcinogenic DNA adducts by trapping DNA repair intermediates. Nucleic Acids Res 48(3): e13. https://doi.org/10.1093/nar/gkz1077

Nicetto D & Zaret K. **2019**. Role of H3K9me3 Heterochromatin in Cell Identity Establishment and Maintenance. *Curr Opin Genet Dev* 55: 1-10. https://doi.org/10.1016/j.gde.2019.04.013

Nikolova T, Ensminger M, Löbrich M & Kaina B. **2010**. Homologous recombination protects mammalian cells from replication-associated DNA double-strand breaks arising in response to methyl methanesulfonate. *DNA Repair* 9(10): 1050-1063. https://doi.org/10.1016/j.dnarep.2010.07.005

O'Connor LO, Rulten SL, Cranston AN, Odedra R, Brown H et al. **2016**. The PARP Inhibitor AZD2461 Provides Insights into the Role of PARP3 Inhibition for Both Synthetic Lethality and Tolerability with Chemotherapy in Preclinical Models. *Cancer Res* 76(20): 6084-6094. https://doi.org/10.1158/0008-5472.CAN-15-3240

O'Connor MJ. **2015**. Targeting the DNA Damage Response in Cancer. *Mol Cell* 60(4): 547-560. https://doi.org/10.1016/j.molcel.2015.10.040

Odell ID, Wallace SS & Pederson DS. **2013**. Rules of engagement for base excision repair in

chromatin. *J Cell Physiol* 228(2): 258-266. https://doi.org/10.1002/jcp.24134

Olave MC & Graham RP. **2022**. Mismatch repair deficiency: The what, how and why it is important. *Genes Chromosomes Cancer* 61(6): 314-321. https://doi.org/10.1002/gcc.23015

Onji H & Murai J. **2022**. Reconsidering the mechanisms of action of PARP inhibitors based on clinical outcomes. *Cancer Sci* 113(9): 2943-2951. https://doi.org/10.1111/cas.15477

Ovejero S, Soulet C & Moriel-Carretero. 2021. The Alkylating Agent Methyl Methanesulfonate Triggers Lipid Alterations at the Inner Nuclear Membrane That Are Independent from Its DNA-Damaging Ability. Int J Mol Sci 22(14): 7461. https://doi.org/10.3390/ijms22147461

Parsons JL, Tait PS, Finch D, Dianova II, Edelmann MJ et al. **2009**. Ubiquitin ligase ARF-BP1/Mule modulates base excision repair. *EMBO J* 28(20) : 3207-3215. https://doi.org/10.1038/emboj.2009.243

Pellegrino S & Altmeyer M. **2016**. Interplay between Ubiquitin, SUMO, and Poly(ADP-Ribose) in the Cellular Response to Genotoxic Stress. *Front Genet* 7:63. https://doi.org/10.3389/fgene.2016.00063

Peter S, Bultinck J, Myant K, Jaenicke LA, Walz S et al. **2014**. Tumor cell-specific inhibition of MYC function using small molecule inhibitors of the HUWE1 ubiquitin ligase. *EMBO Mol Med* 6(12): 1525-1541. https://doi.org/10.15252/emmm.201403927

Pines A, Vrouwe MG, Marteijn JA, Typas D, Luijsterburg MS et al. **2012**. PARP1 promotes nucleotide excision repair through DDB2 stabilization and recruitment of ALC1. *J Cell Biol* 199(2): 235-249. https://doi.org/10.1083/jcb.201112132

Podgorska A, Rembiszewska A, Szafron L, Konopka B, Lukasik M et al. **2015**. Clinical

significance of HUWE1 expression in ovarian cancer. *Eur J Cancer* 51: suppl 3, S94 https://doi.org/10.1016/S0959-8049(16)30282-9

Qi L, Xu X & Qi X. **2022**. The giant E3 ligase HUWE1 is linked to tumorigenesis, spermatogenesis, intellectual disability, and inflammatory diseases. *Front Cell Infect Microbiol* 12 : 905906. https://doi.org/10.3389/fcimb.2022.905906

Ramsden DA, Carvajal-Garcia J & Gupta GP. **2022**. Mechanism, cellular functions and cancer roles of polymerase-theta-mediated DNA end joining. *Nat Rev Mol Cell Biol* 23(2): 125-140. https://doi.org/ 10.1038/s41580-021-00405-2

Rastogi RP, Richa, Kumar A, Tyagi MB & Sinha RP. **2010**. Molecular mechanisms of ultraviolet radiation-induced DNA damage and repair. *J Nucleic Acids* 2010: 592980. https://doi.org/10.4061/2010/592980

Reuvers TGA, Kanaar R & Nonnekens J. **2020**. DNA Damage-Inducing Anticancer Therapies: From Global to Precision Damage. *Cancer* 12(8): 2098. https://doi.org/10.3390/cancers12082098

Rudolph J, Mahadevan J, Dyer P & Luger K. **2018**. Poly(ADP-ribose) polymerase 1 searches DNA via a 'monkey bar' mechanism. *eLife* 7: e37818. https://doi.org/10.7554/eLife.37818

Rudolph J, Muthurajan UM, Palacio M, Mahadevan J, Roberts G et al. **2021**. The BRCT domain of PARP1 binds intact DNA and mediates intrastrand transfer. *Mol Cell* 81(24): 4994-5006.e5. https://doi.org/10.1016/j.molcel.2021.11.014

Ruscetti T, Lehnert BE, Halbrook J, Trong HL, Hoekstra MF et al. **1998**. Stimulation of the DNA-dependent protein kinase by poly(ADP-ribose) polymerase. *J Biol Chem* 273(23): 14461-14467. https://doi.org/10.1074/jbc.273.23.14461

Satoh MS & Lindahl T. **1992**. Role of poly(ADP-ribose) formation in DNA repair. *Nature* 356(6367): 356-358. https://doi.org/10.1038/356356a0

Schreiber V, Amé J, Dollé P, Schultz I, Rinaldi B et al. **2002**. Poly(ADP-ribose) polymerase-2 (PARP-2) is required for efficient base excision DNA repair in association with PARP-1 and XRCC1. *J Biol Chem* 277(25): 23028-23036. https://doi.org/10.1074/jbc.M202390200

Schwerman P, Bekker-Jensen S & Mailand N. **2016**. Regulation of DNA double-strand break repair by ubiquitin and ubiquitin-like modifiers. *Nat Rev Mol Cell Biol* 17(6): 379-394. https://doi.org/10.1038/nrm.2016.58

Scully R, Panday A, Elango R & Willis NA. **2019**. DNA double-strand break repair-pathway choice in somatic mammalian cells. *Nat Rev Mol Cell Biol* 20(11): 698-714. https://doi.org/10.1038/s41580-019-0152-0

Sekiguchi M & Matsushita N. **2022**. DNA Damage Response Regulation by Histone Ubiquitination. *Int J Mol Sci* 23(15): 8187. https://doi.org/10.3390/ijms23158187

Seluanov A, Mao Z & Gorbunova V. **2010**. Analysis of DNA double-strand break (DSB) repair in mammalian cells. *J Vis Exp* (43): 2002. https://doi.org/10.3791/2002

Seo J, Kim SC, Lee H, Kim JK, Shon HJ et al. **2012**. Genome-wide profiles of H2AX and γ-H2AX differentiate endogenous and exogenous DNA damage hotspots in human cells. *Nucleic Acids Res* 40(13): 5965-5974. https://doi.org/10.1093/nar/gks287

Shieh WM, Amé JC, Wilson MV, Wang ZQ, Koh DW et al. **1998**. Poly(ADP-ribose) polymerase null mouse cells synthesize ADP-ribose polymers. *J Biol Chem* 273(46): 30069-30072. https://doi.org/10.1074/jbc.273.46.30069

Singh JK, Smith R, Rother MB, de Groot AJL, Wiegant WW et al. **2021**. Zinc finger protein

ZNF384 is an adaptor of Ku to DNA during classical non-homologous end-joining. *Nat Commun* 12(1): 6560. https://doi.org/10.1038/s41467-021-26691-0

Smeenk G & Mailand N. **2016**. Writers, Readers, and Erasers of Histone Ubiquitylation in DNA Double-Strand Break Repair. *Front Genet* 7: 122. https://doi.org/10.3389/fgene.2016.00122

Spivak G. **2015**. Nucleotide excision repair in humans. *DNA Repair* 36: 13-18. https://doi.org/10.1016/j.dnarep.2015.09.003

Su C, Wang T, Zhao J, Cheng J & Hou J. **2019**. Meta-analysis of gene expression alterations and clinical significance of the HECT domain-containing ubiquitin ligase HUWE1 in cancer. *Oncol Lett* 18(3): 2292-2303. https://doi.org/10.3892/ol.2019.10579

Sugasawa K, Okuda Y, Saijo M, Nishi R, Matsuda N et al. **2005**. UV-induced ubiquitylation of XPC protein mediated by UV-DDB-ubiquitin ligase complex. *Cell* 121(3): 387-400. https://doi.org/10.1016/j.cell.2005.02.035

Sun C, Yin J, Fang Y, Chen J, Jeong KJ et al. **2018**. BRD4 Inhibition Is Synthetic Lethal with PARP Inhibitors through the Induction of Homologous Recombination Deficiency. *Cancer Cell* 33(3): 401-416.e8. https://doi.org/10.1016/j.ccell.2018.01.019

Switonski PM, Delaney JR, Bartelt LC, Niu C, Ramos-Zapatero M et al. **2021**. Altered H3 histone acetylation impairs high-fidelity DNA repair to promote cerebellar degeneration in spinocerebellar ataxia type 7. *Cell Rep* 37(9): 110062. https://doi.org/10.1016/j.celrep.2021.110062

Tallarida RJ. **2011**. Quantitative Methods for Assessing Drug Synergism. *Genes Cancer* 2(11): 1003-1008. https://doi.org/10.1177/1947601912440575

Tammaro M, Barr P, Ricci B & Yan H. **2013**. Replication-dependent and transcription-dependent

mechanisms of DNA double-strand break induction by the topoisomerase 2-targeting drug etoposide. *PLoS One* 8(11): e79202. https://doi.org/10.1371/journal.pone.0079202

Uryga A, Gray K & Bennett M. **2016**. DNA Damage and Repair in Vascular Disease. *Annu Rev Physiol* 78: 45-66. https://doi.org/10.1146/annurev-physiol-021115-105127

Vivelo CA, Ayyappan V & Leung AKL. **2019**. Poly(ADP-ribose)-dependent ubiquitination and its clinical implications. *Biochem Pharmacol* 167: 3-12. https://doi.org/10.1016/j.bcp.2019.05.006

Wang G, Gao Y, Li L, Jin G, Cai Z et al. **2012**. K63-linked ubiquitination in kinase activation and cancer. *Front Oncol* 2:5. https://doi.org/10.3389/fonc.2012.00005

Wang M, Wu W, Wu W, Rosidi B, Zhang L et al. **2006**. PARP-1 and Ku compete for repair of DNA double strand breaks by distinct NHEJ pathways. *Nucleic Acids Res* 34(21): 6170-6182. https://doi.org/10.1093/nar/gkl840

Wang Y, Xie H, Chang X, Hu W, Li M et al. **2022**. Single-Cell Dissection of the Multiomic Landscape of High-Grade Serous Ovarian Cancer. *Cancer Res* 82(21): 3903-3916. https://doi.org/10.1158/0008-5472.CAN-21-3819

Wang X, Lu G, Li L, Yi J, Yan K et al. **2014**. HUWE1 interacts with BRCA1 and promotes its degradation in the ubiquitin-proteasome pathway. *Biochem Biophys Res Commun* 444(3): 290-295. https://doi.org/10.1016/j.bbrc.2013.12.053

Wang Z, Michaud GA, Cheng Z, Zhang Y, Hinds TR et al. **2012**. Recognition of the iso-ADP-ribose moiety in poly(ADP-ribose) by WWE domains suggests a general mechanism for poly(ADP-ribosyl)ation-dependent ubiquitination. *Genes Dev* 26(3): 234-240. https://doi.org/10.1101/gad.182618.111

Wang Z, Zang C, Rosenfeld JA, Schones DE, Barski A et al. **2008**. Combinatorial patterns of

histone acetylations and methylations in the human genome. *Nat Genet* 40(7): 897-903. https://doi.org/10.1038/ng.154

Wei H & Yu X. **2016.** Functions of PARylation in DNA Damage Repair Pathways. *Genom Proteom Bioinform* 14(3): 131-139. https://doi.org/10.1016/j.gpb.2016.05.001

Williamson EA, Wray JW, Bansal P & Hromas R. **2012**. Overview for the histone codes for DNA repair. *Prog Mol Biol Transl Sci* 110: 207-227. https://doi.org/10.1016/B978-0-12-387665-2.00008-0

Witte CJD, Valle-Inclan JE, Hami N, Lõhmussaar K, Kopper O et al. **2020**. Patient-Derived Ovarian Cancer Organoids Mimic Clinical Response and Exhibit Heterogeneous Inter- and Intrapatient Drug Responses. *Cell Rep* 31(11): 107762. https://doi.org/10.1016/j.celrep.2020.107762

Yadav B, Wennerberg K, Aittokallio T & Jing Tang. Searching for Drug Synergy in Complex Dose-Response Landscapes Using an Interaction Potency Model. *Comput Struct Biotechnol J* 13: 504-513. https://doi.org/10.1016/j.csbj.2015.09.001

Yajima H, Lee K, Zhang S, Kobayashi J & Chen BPC. **2009**. DNA double-strand break formation upon UV-induced replication stress activates ATM and DNA-PKcs kinases. *J Mol Biol* 385(3): 800-810. https://doi.org/10.1016/j.jmb.2008.11.036

Yang D, Sun B, Zhang X, Cheng D, Yu X et al. **2017.** Huwe1 Sustains Normal Ovarian Epithelial Cell Transformation and Tumor Growth through the Histone H1.3- H19 Cascade. *Cancer Res* 77(18): 4773-4784. https://doi.org/10.1158/0008-5472.CAN-16-2597

Yang K, Guo R & Xu D. **2016**. Non-homologous end joining: advances and frontiers. *Acta Biochim Biophys Sin (Shanghai)* 48(7): 632-640. https://doi.org/10.1093/abbs/gmw046

Zhang F, Shi J, Chen S, Bian C & Yu X. **2015**. The PIN domain of EXO1 recognizes poly(ADP-

ribose) in DNA damage response. *Nucleic Acids Res* 43(22): 10782-10794. https://doi.org/10.1093/nar/gkv939

Zhang J, Li Y, Liu H, Zhang J, Wang J et al. **2022**. Genome-wide CRISPR/Cas9 library screen identifies PCMT1 as a critical driver of ovarian cancer metastasis. *J Exp Clin Cancer Res* 41(1): 24. https://doi.org/10.1186/s13046-022-02242-3

Zhang X, Yin M & Hu J. **2022**. Nucleotide excision repair: a versatile and smart toolkit. *Acta Biochim Biophys Sin (Shanghai)* 54(6): 807-819. https://doi.org/10.3724/abbs.2022054

Zhang Y, Liu S, Mickanin C, Feng Y, Charlat O et al. **2011**. RNF146 is a poly(ADP-ribose)-directed E3 ligase that regulates axin degradation and Wnt signalling. *Nat Cell Biol* 13(5): 623-629. https://doi.org/10.1038/ncb2222

Zhong G, Gao W, Du F & Wang X. **2005**. Mule/ARF-BP1, a BH3-only E3 ubiquitin ligase, catalyzes the polyubiquitination of Mcl-1 and regulates apoptosis. *Cell* 121(7): 1085-1095. https://doi.org/10.1016/j.cell.2005.06.009

Zhou P, Wang J, Mishail D & Wang C. **2020**. Recent advancements in PARP inhibitors-based targeted cancer therapy. *Precis Clin Med* 3(3): 187-201. https://doi.org/10.1093/pcmedi/pbaa030

Appendix

Appendix A: Supplementary Data

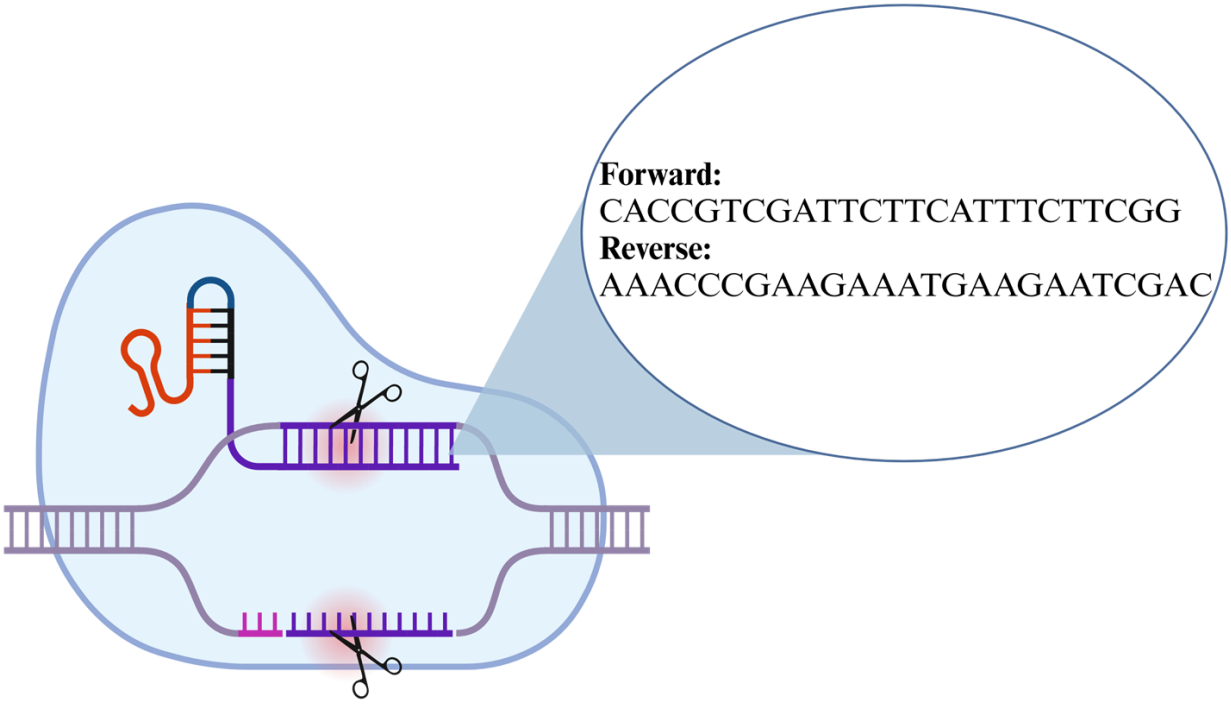

Figure S-1: CRISPR gRNA Sequence for HUWE1 Knockout
Diagram demonstrating the CRISPR-Cas9 system used to generate OVCAR3 HUWE1 KO cells. The lentiCRISPR vector with the shown gRNA sequence was obtained from Dr. Yi Sheng.

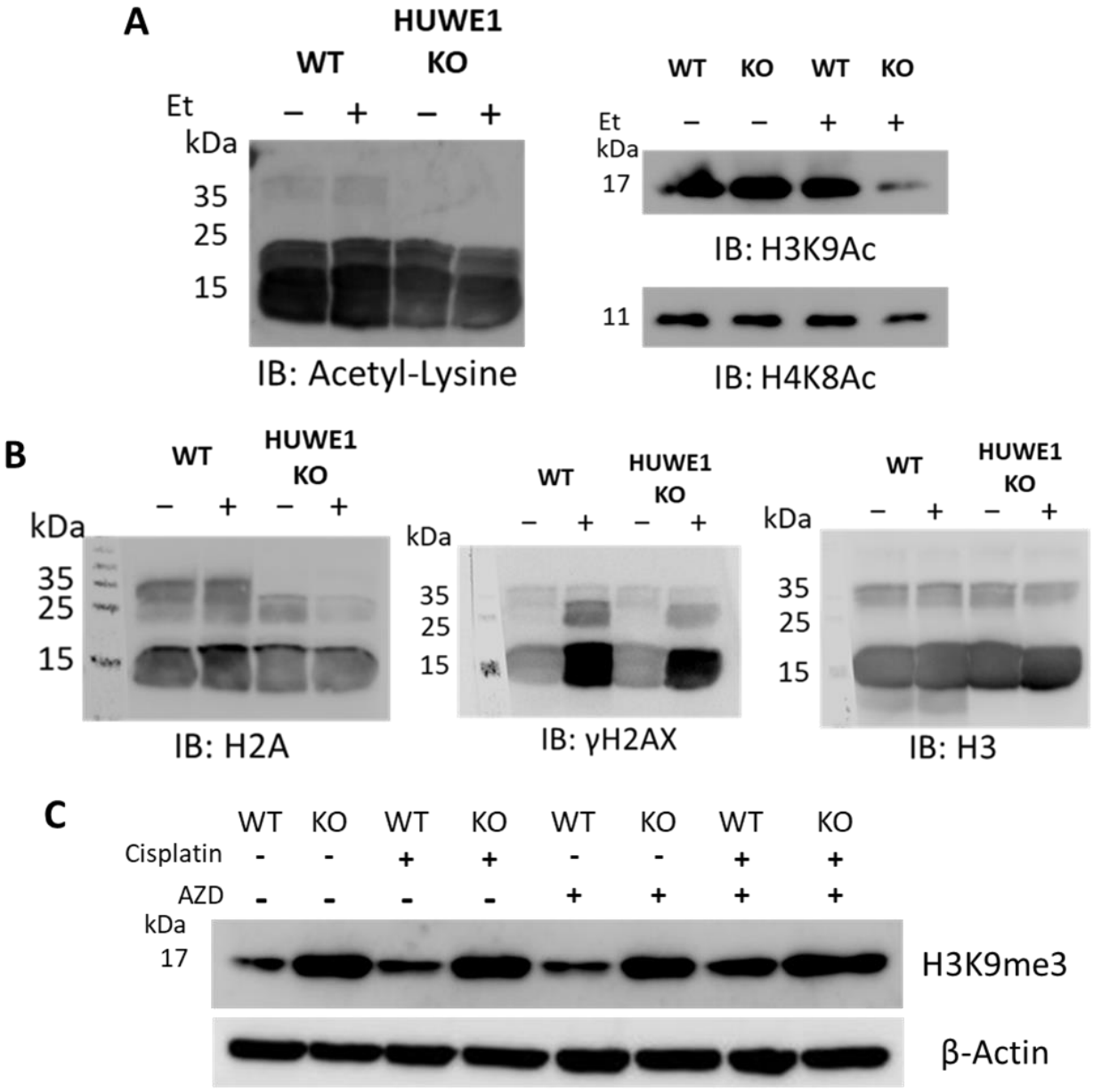

Figure S-2: HUWE1 knockout can modulate the cellular epigenetic landscape.
A) B) MEF WT and HUWE1 KO cells were treated with 10μM etoposide where indicated and subjected to acid extraction of histones. Western blotting was then used to profile various histones and associated epigenetic modifications. C) Western blot showing chromatin-associated fraction isolated during subcellular fractionation. Cells were treated with 3μM cisplatin or 1μM AZD.

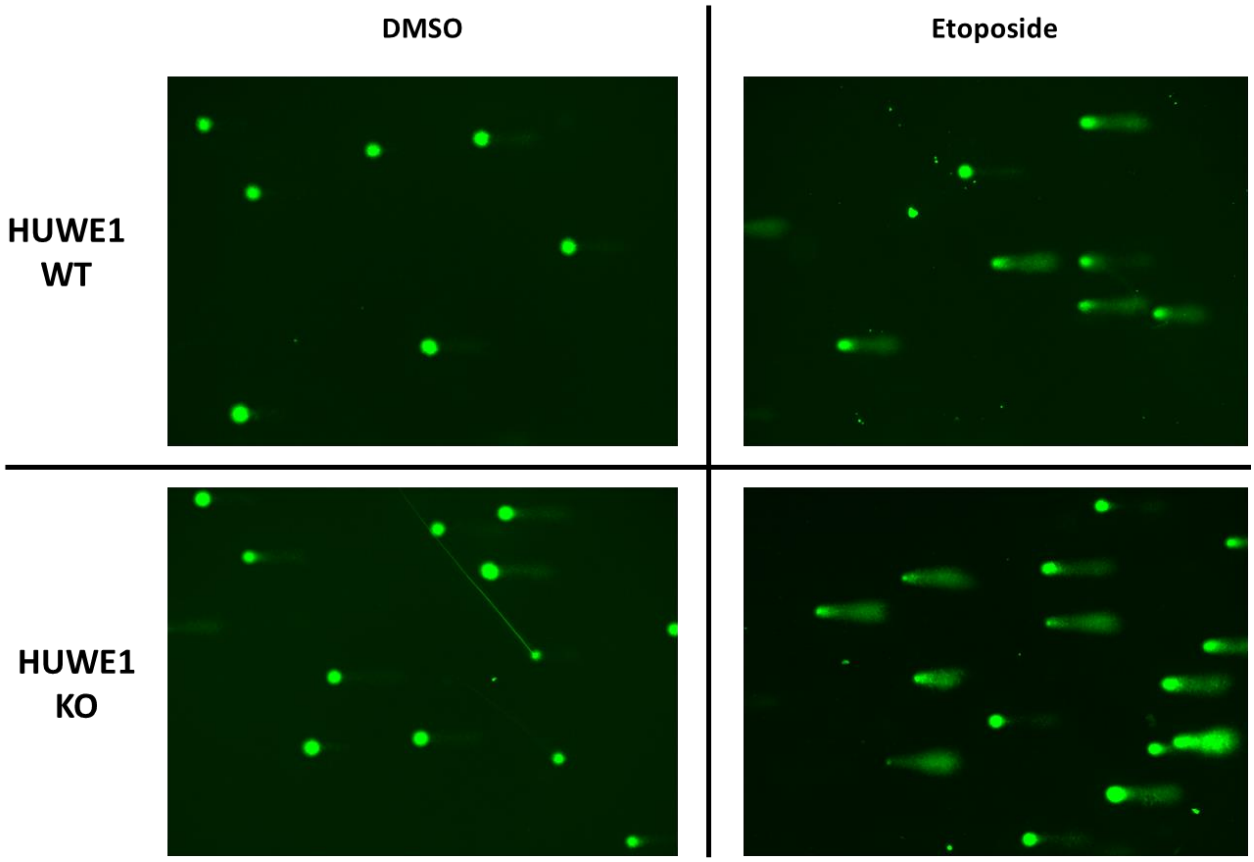

Figure S-3: HUWE1 knockout results in increased DNA damage in MEF cells.
Etoposide comet assay representative images from Figure 3-1, showing wider field of view with multiple cells. Over 50 comets were quantified per treatment group with OpenComet, with the middle 50 values being extracted and used for analysis.

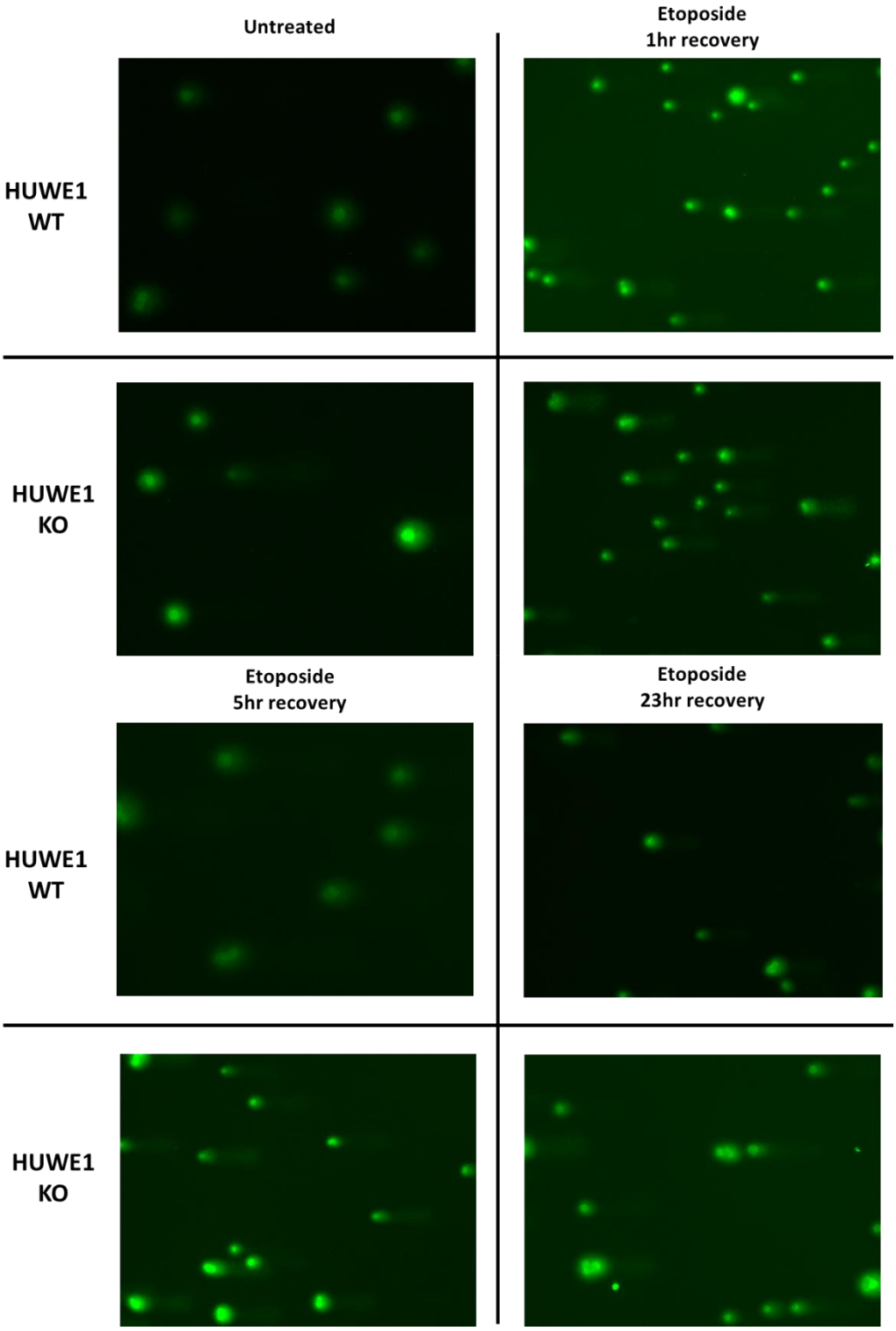

Figure S-4: HUWE1 knockout MEFs experience increased and prolonged DNA damage: etoposide
Representative images from etoposide timecourse assay in Figure 3-2A, showing wider field of view with multiple cells. Over 150 comets were quantified per treatment group with OpenComet, with the middle 150 values being extracted and used for analysis.

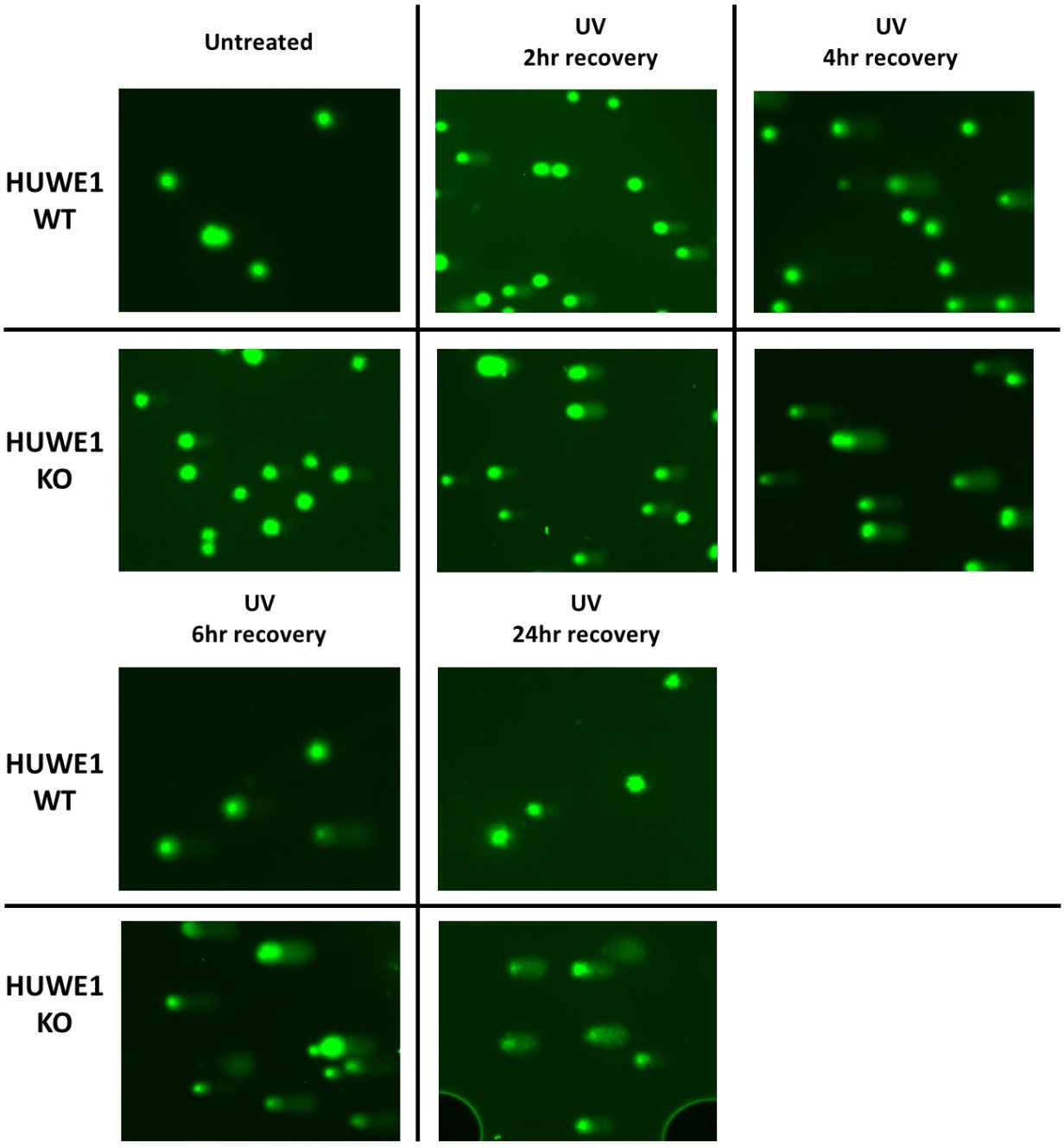

Figure S-5: HUWE1 knockout MEFs experience increased and prolonged DNA damage: UV
Representative images from UV timecourse assay in Figure 3-2B, showing wider field of view with multiple cells. Over 150 comets were quantified per treatment group with OpenComet, with the middle 150 values being extracted and used for analysis.

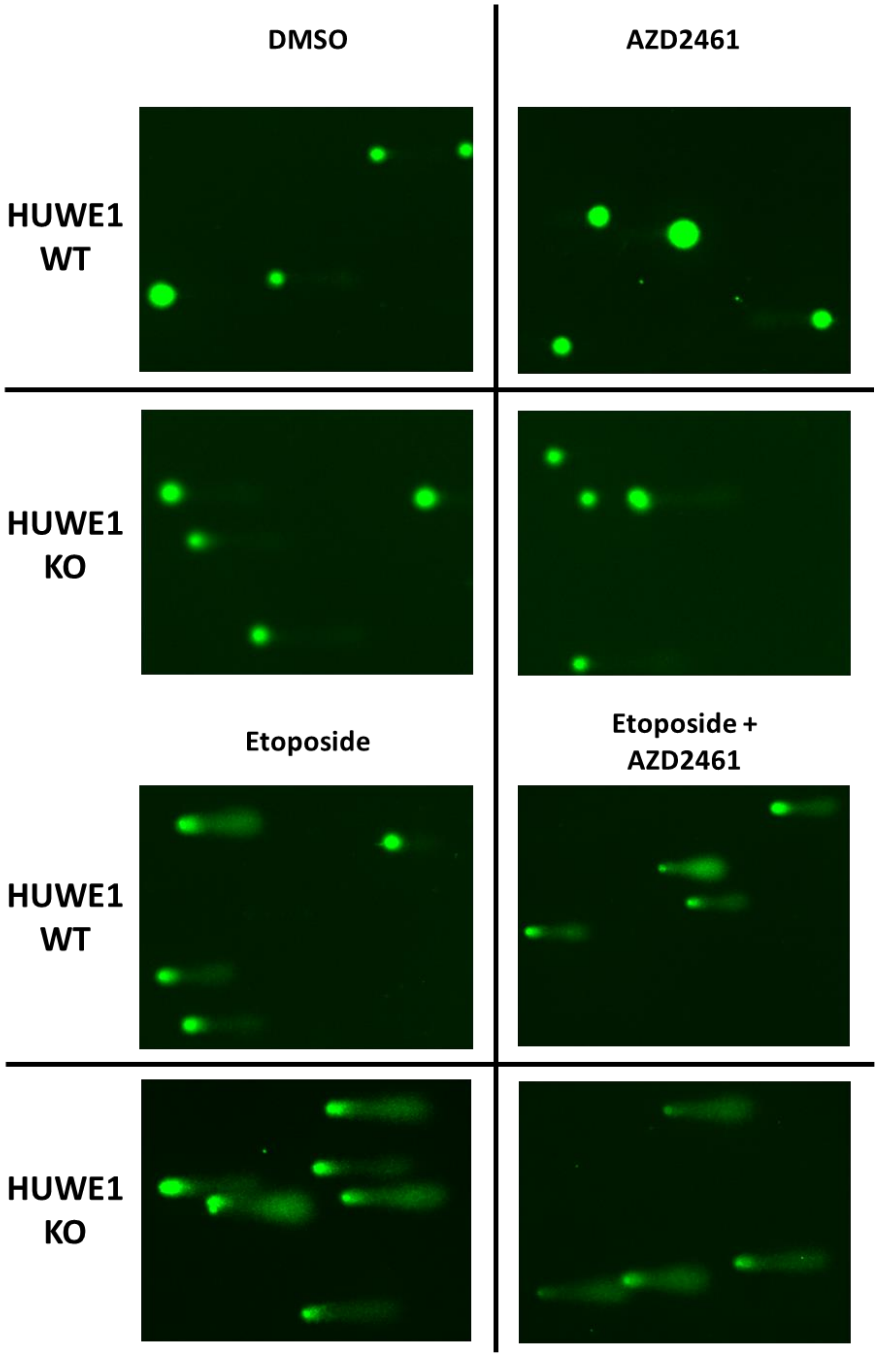

Figure S-6: HUWE1 knockout MEFs exhibit increased DNA damage in response to DNA damage and PARP inhibition.
Representative images from the etoposide and AZD2461 comet assay in MEF cells from Figure 3-3. Over 50 comets were quantified per treatment group, with the middle 50 values being extracted and used for

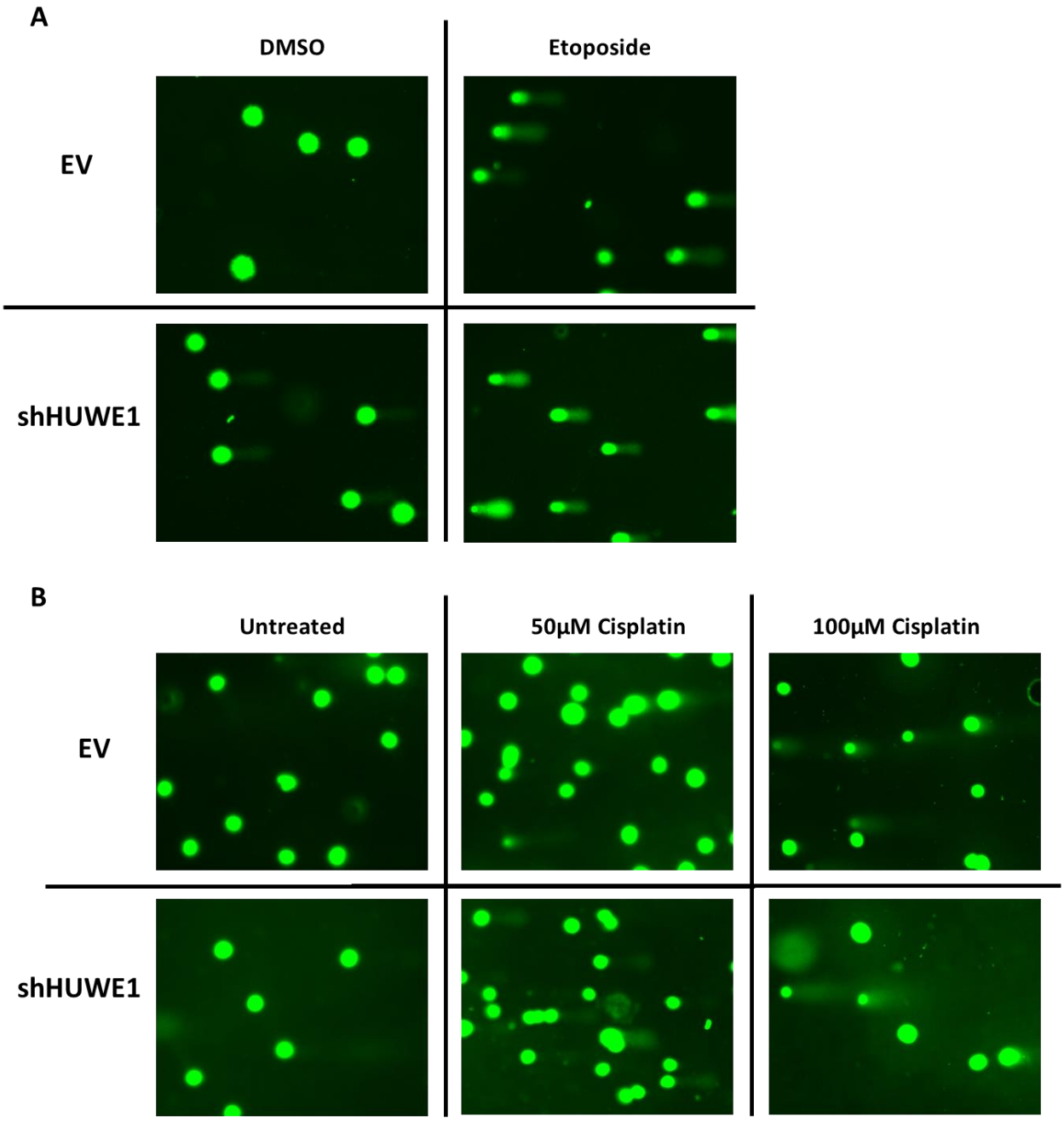

Figure S-7: HUWE1 knockdown increased DNA damage in response to different damaging agents in OVCAR3 cells.
Representative images from the A) etoposide and B) cisplatin comets performed in OVCAR3 cells from Figure 3-6. More than 80 comets were quantified per treatment group in the etoposide experiment, and over 100 comets in the cisplatin experiment. The middle 80 and 100 values, respectively, were extracted and used for analysis.

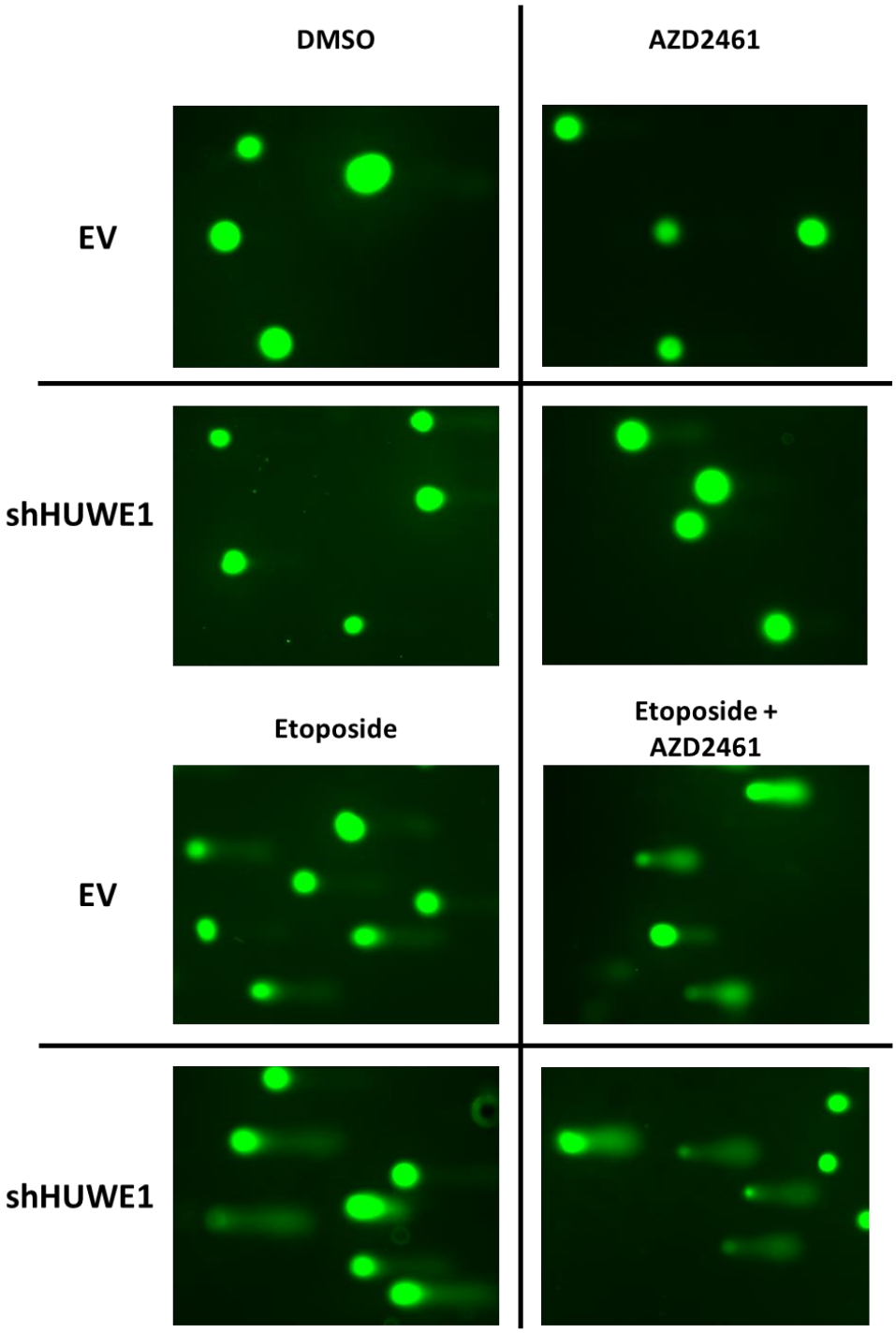

Figure S-8: HUWE1 knockdown increased DNA lesions after treatment with etoposide and AZD2461 in OVCAR3 cells.
Representative images from the etoposide and AZD2461 comet carried out in OVCAR3 cells from Figure 3-7A. Over 100 comets were quantified per treatment group, with the middle 100 values being extracted for analysis.

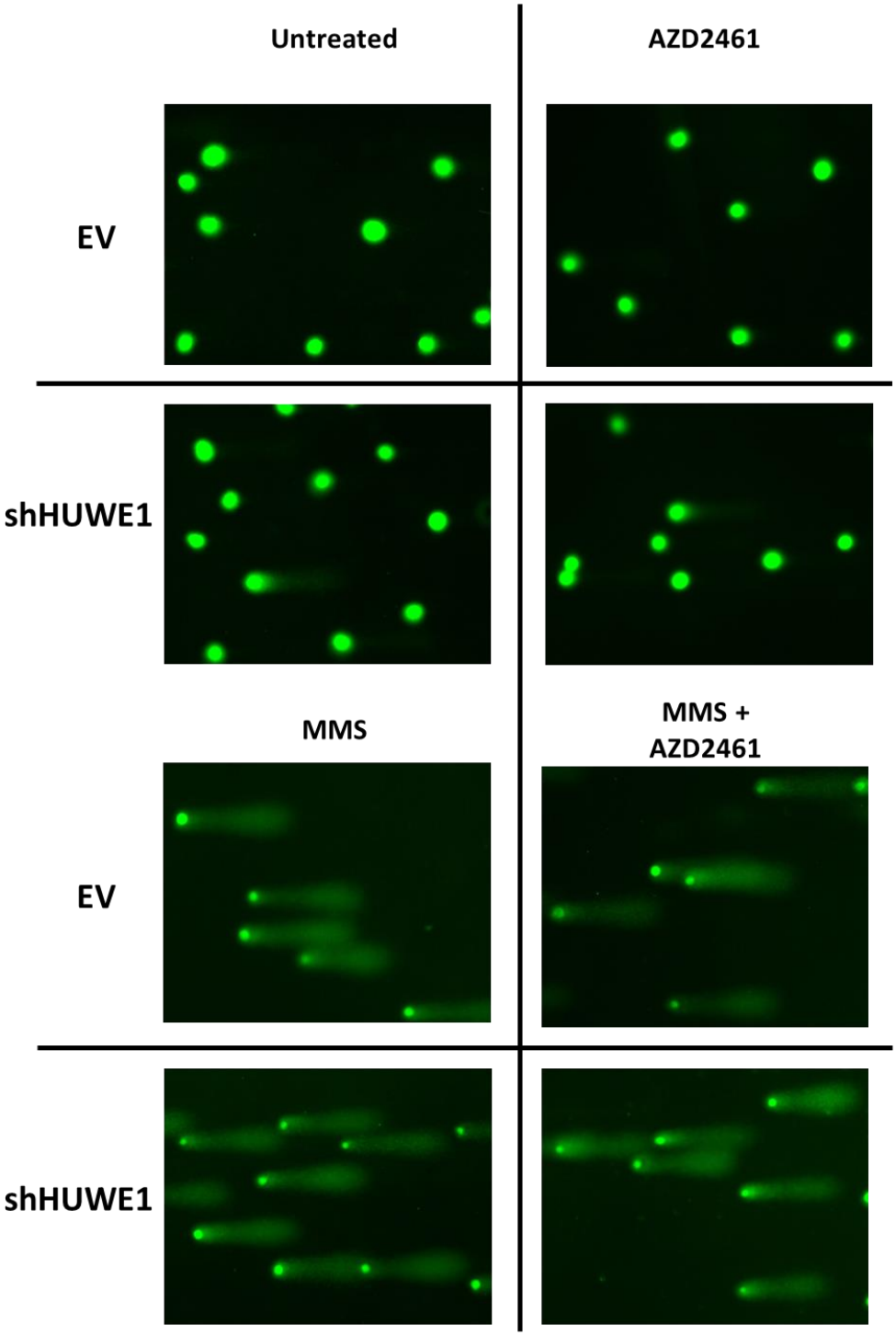

Figure S-9: HUWE1 knockdown increased DNA lesions after treatment with MMS and AZD2461 in OVCAR3 cells.
Representative images from the MMS and AZD2461 comet assay carried out in OVCAR3 cells from Figure 3-7B. Over 100 comets were quantified per treatment group, with the middle 100 values being extracted for analysis.